Application of Liquid Chromatography Tandem Mass Spectrometry (LC-MS/MS) for Lipid-based Nanomedicine Development

by

Ben Nie

A dissertation submitted to the Graduate Faculty of
Auburn University
in partial fulfillment of the
requirements for the Degree of
Doctor of Philosophy

Auburn, Alabama
May 6, 2017

Keywords: Nanomedicine, Secretory phospholipase A_2 ($sPLA_2$), LC-MS/MS, Deuterated phospholipids, Intracellular uptake, $sPLA_2$ responsive liposomes

Approved by

Robert D. Arnold, Chair, Associate Professor of Drug Discovery and Development
Randall Clark, Professor of Drug Discovery and Development
Jayachandra Babu Ramapuram, Professor of Drug Discovery and Development
Daniel L. Parsons, Emeritus Professor of Drug Discovery and Development
William R. Ravis, Emeritus Professor of Drug Discovery and Development

Abstract

Secretory phospholipase A_2 ($sPLA_2$) are increased in various cancers. The lipid specificity and reactivity of $sPLA_2$ and its ability to interact with PLA2 receptors (PLA2R) are potential targets for development of liposome drug delivery systems. However, many phospholipids used to prepare liposomal formulations can be found endogenously and have biological isomers that complicate quantitative analysis. Thus, the challenges associated with the development and optimization of liposome nanoparticles are the difficulty to extract them from biological milieu and to distinguish liposome formulations and their metabolites from endogenous phospholipids. The purpose of this work is to establish a quantitative method that is capable to distinguish and quantify liposomes and their metabolites in biological samples. To achieve this purpose, we incorporated deuterated lipids in our $sPLA_2$ responsive liposomes (SPRL) and developed an acidified Bligh-Dyer extraction method in combination with liquid chromatography tandem mass spectrometry (LC-MS/MS) to evaluate their intracellular uptake and degradation in prostate cancer.

Chapter 1 is an overview of the technical challenges to evaluate intracellular uptake and disposition of lipid-based Nano-carriers. The challenges are stated in two aspects of developing a quantitative method: extraction and differentiation. The current available methods that researchers use to overcome these challenges are described as well.

Chapter 2 addresses the extraction challenge. We tested the extraction efficiency of 6 commonly used phospholipids for lipid-based nanomedicine using Bligh-Dyer (BD) extraction

method, and proposed two different acidification procedures for certain anionic phospholipids with a poor extraction efficiency using conventional BD extraction: DSPA, one-step acidification in aqueous solution before extraction; DSPE, two step-acidification before and after extraction.

Chapter 3 introduces the development of LC-MS/MS method for differentiation and quantification of liposome. Deuterated (d70)-1,2-distearoyl-*sn*-glycero-3-phosphocholine (d70-DSPC) was used as a substitute for DSPC to increase the uniqueness of SPRL formulations, which has no changes on the physiochemical or biochemical properties of the formulations. Both deuterated parent phospholipid (d70-DSPC) and one of its metabolites (d35-LysoPC) were able to be distinguished and quantified. The method was validated for its specificity, linearity, sensitivity (LOD and LLOQ), accuracy and precision.

Chapter 4 is the application of the newly developed LC-MS/MS method for *in vitro* and *in vivo* evaluation of intracellular uptake and disposition of SPRL. The experiments were carried out on human prostate adenocarcinoma (PC-3) cells and mouse xenograft model of PC-3 cells implanted subcutaneously in athymic NCr (*nu*/*nu*) mice. The method provided detailed uptake and disposition information that pre-existing methods weren't able to, which is critical for understanding uptake mechanisms and further optimizing the formulation.

The establishment of this new LC-MS/MS method fills in the technical gap for evaluating *in vivo* performance of lipid-based nanomedicine. This method strengthens the ability to evaluate and optimize lipid-based drug carriers such as liposomes. Such tools are critical to gaining mechanistic insights into the distribution and intracellular fate of nanomedicines.

Acknowledgments

I would like, at first to express my appreciation to Dr. Robert D. Arnold for his willingness to accept me as a student for my PhD study, and for his continuous guidance and support throughout the whole time. I am also extremely grateful for my committee members, Dr. Randall Clark, Dr. Jayachandra Babu Ramapuram, Dr. Daniel L. Parsons and Dr. William R. Ravis, for the lessons and discussions I had with them. The ideas and feedback from them have been invaluable. I would to thank Dr. Dawn M. Boothe for being my dissertation reader and for the suggestions she gave to me.

My sincere appreciation is extended to all faculty, staff and students in the Department of Drug Discovery and Development for their support and help. Thank you for your efforts to make DDD a wonderful place to study and pursue a higher degree. Special thanks goes to Ms. Jennifer Johnston for her generous help whenever I needed it. I would like to express my gratitude specifically to my laboratory mates, Matthew Eggert, Shanese Jasper, Joshua Davis, Connor Dobson, Anna Burcham, Audrey McCandless and Christinga Pickering. Thank you for your support and unconditional friendship.

Last, but not least, I dedicate this dissertation to my family, especially to my parents, Yueying Han and Chengxiang Nie. Without their continuous motivation, constant support and unconditional love through all these years away from home I would not be able to complete my PhD successfully.

Table of Contents

List of Tables

List of Figures

List of Abbreviations

RES	Reticulo-endothelial system
DTPA	Diethylenne-triamine pentaacetic acid
NTA	Nitrilotriacetic acid
BD	Bligh-Dyer
PC	Phosphatidylcholine
PG	Phosphatidylglycerol
PE	Phosphatidylethanolamine
PA	Phosphatidic acid
PS	Phosphatidylserine
C31PC	1-O-hexadecyl-2-pentadenoyl-sn-glycero-3- phosphatidylcholine
DPPC	1,2-dipalmitoyl-sn-glycero-3-phosphatidylcholine
d62-DPPC	1,2-dipalmitoyl-d62-*sn*-glycero-3-phosphatidylcholine
DPPA	1,2-dipalmitoyl-*sn*-glycero-3-phosphatidic acid
DPPS	1,2-dipalmitoyl-*sn*-glycero-3-phosphatidylserine
DPPG	1,2-dipalmitoyl-*sn*-glycero-3-phosphatidylglycerol
DSPA	1,2-distearoyl-sn-glycero-3-phosphatidic acid
DSPC	1,2-distearoyl-sn-glycero-3-phosphatidylcholine
d70-DSPC	1,2-distearoyl-d70-*sn*-glycero-3-phosphatidylcholine

DSPE	1,2-distearoyl-sn-glycero-3-phosphatidylethanolamine
DSPG	1,2-distearoyl-sn-glycero-3-phosphatidylglycerol
DSPS	1,2-distearoyl-sn-glycero-3-phosphatidylserine
d35-Lyso PC	1-distearoyl-d35-*sn*-glycero-3-phosphatidylcholine
d31-Lyso PC	1-dipalmitoyl-d31-*sn*-glycero-3-phosphatidylcholine
ESI-MS	Electrospray ionization - mass spectrometry
LC-MS/MS	Liquid chromatography tandem mass spectrometry
FA	Fatty acid
LP	Lysophospholipid
$sPLA_2$	Secretory phospholipase A_2
PLA2R	Phospholipase A_2 receptor
SSL	Sterically-stabilized liposome
SPRL	$sPLA_2$ responsive liposome
TRIS	Tris (hydroxymethyl) aminomethane
DXR	Doxorubicin
DAR	Daunorubicin
SEM	Standard error of the mean
SD	Standard deviation

Chapter 1. Introduction: Technical Challenges for Evaluation of Intracellular Uptake and Disposition of Lipid-based Nanomedicine

1.1 Introduction

Lipid-based nanomedicine has been applied widely in modern health care due to the effectiveness in drug delivery and its biocompatibility. Liposomes, for example, can be functionalized as carriers for diagnostic and therapeutic agents, providing diagnosis and for treatment of disease. Ever since Gregoriadis in 1981 (Gregoriadis 1981) proposed the use of liposomes as carriers for chemotherapeutic agents, liposomes have become a major focus for manipulating drug distribution to improve antitumor efficacy and reduce toxicity. Many liposomal formulations have been developed during the past decades, from conventional plain liposomes to PEGylated sterically stabilized liposome in order to bypass reticulo-endothelial system (RES) (Juliano and Stamp 1975, Poste, Bucana et al. 1982) and increase circulation time (Allen and Hansen 1991, Lasic, Martin et al. 1991, Papahadjopoulos, Allen et al. 1991, Woodle and Lasic 1992), to ligand-targeted liposomes developed by conjugating with peptides or mAbs recognized by cell receptors to enhance the selective targeting of tumors (Sapra and Allen 2003, Ruoslahti 2012, Suga, Fuchigami et al. 2017), to enzymatic triggered (Davidsen, Jørgensen et al. 2003, Zhu, Mock et al. 2011), thermal sensitive (Yatvin, Weinstein et al. 1978, Gaber, Hong et al. 1995, Needham, Anyarambhatla et al. 2000, de Smet, Hijnen et al. 2013), pH sensitive (Simões, Moreira et al. 2004, Giansanti, Mauceri et al. 2016, Fan, Chen et al. 2017) and ultrasound mediated (Evjen, Nilssen et al. 2011, de Smet, Hijnen et al. 2013, Crasto, Kartner et

al. 2016, Elkhodiry, Momah et al. 2016, Yu, Chen et al. 2016) release liposomes in order to better control drug release in targeted tumors or tissue regions.

Despite the popularity of liposomes for drug delivery and the countless formulations that have been developed, the techniques for evaluation of their *in vivo* distribution and disposition are inadequate. Thus, the physiological fate of liposomes is unclear and formulation optimization is restricted. There are two challenges every researcher has to face for developing such a technique. These are the difficulty to extract liposomal formulations from biological milieu and the difficulty to distinguish them and their metabolites from endogenous phospholipids due to the fact that many phospholipids used to prepare liposomal formulations can be found endogenously and/or have biological isomers that complicate the analysis. To overcome these challenges, the available assays and techniques heavily rely on labeling. The most commonly used labels include radioactive labels (^{3}H, ^{111}In, ^{67}Ga) (Gabizon, Pappo et al. 1993, Harrington, Mohammadtaghi et al. 2001), fluorescence labels (DiO, DiI, DiR) (Huth, Wieschollek et al. 2004, Sengupta, Holowka et al. 2007), MR imaging contrast agents (Gd, Dy, Mn Fe) (Schwendener, Wuthrich et al. 1990), and encapsulated therapeutic agents (DXR, cisplatin) (Gabizon, Pappo et al. 1993, Kieler-Ferguson, Chan et al. 2017). Those labeling techniques have achieved a tremendous success on visually localizing the destination of liposomes. However, they are problematic from a quantitative point of view. First, the signals from the labels are not directly associated with liposomes but labels themselves. Therefore, the labeling technique needs to be repeatedly validated. Even so, the label/lipid ratio could still be questionable. Second, label signals could be easily interfered with by tissues and endogenous molecules. Tissue auto-fluorescence is a major source of interference for fluorescence labels. Also, encapsulated drugs, such as doxorubicin, fluorescence are partially quenched when they bind DNA (Gabizon,

Shmeeda et al. 2003), resulting in an underestimated evaluation. Last, but not least, potential free labels could interfere with the assay. The integrity of labeled liposomes are heavily challenged in blood circulation. Any potentially leaked label could result a false positive result.

Extraction and differentiation are two essential steps to develop a quantitative analysis method. The challenges involved in both extraction and differentiation of liposomal formulation from biological samples are the reasons why rarely an adequate quantitative method has been developed. This chapter will focus on the challenges and some of the current available techniques.

1.2 Challenge 1: Extraction

The complexity of biological samples, such as tissues, cells and body fluids, often require optimization of techniques for sample preparation. For the extraction and analysis of lipids, there are two major challenges to overcome. These are extraction efficiency and complete removal of non-lipid contents. By optimizing sample preparation, it is possible to increase throughput and analyses reproducibility. The key for selecting an optimized extraction method for quantifying liposomal formulations from biological samples is the understanding of the biochemical and physiochemical properties of each individual lipid component employed in the formulations, and the matrixes that they are in. However, no method has been evaluated for this purpose. This section will discuss organic solvent extraction and solid-phase extraction (SPE), which have been used extensively for lipid sample preparation. Figure 1.1 provides a summary of these extraction techniques (Pati, Nie et al. 2016).

1.2.1 Organic Solvent Extraction

Proper organic solvent extraction relies heavily on the selection of lipid-soluble solvents. For polar lipids containing both hydrophilic and hydrophobic groups, appropriate organic solvents include chloroform and methanol. Alkane solvents are well suited for extraction of nonpolar lipids lacking hydrophilic groups, such as triacyglycerols and sterols. Lipid solubility can be quantified directly using pure lipid standards; however, predicting or measuring extraction efficiencies is often a challenge when extracting lipids from biological samples. This is due mainly to the strong interactions between lipids and cell biopolymers such as proteins and polysaccharides. Extraction solvents should be selected carefully in order to disrupt these molecular associations, with a balance of both polar and nonpolar characteristics. Polar solvents, such as methanol, have high dielectric constants that are able to access regions of ion-dipole interactions and hydrogen bonds, and can interrupt such associations.

The Folch method, published in 1957, is the most commonly used lipid extraction technique (Folch, Lees et al. 1957). It uses a mixture of chloroform and methanol in a 2:1 ratio, which can simultaneously overcome both hydrophobic and polar interactions between lipids and biopolymers. A wash step is incorporated following extraction to remove non-lipid components using small volumes of water. It is critical that the ratio of chloroform-methanol-water is maintained at 8:4:3 to prevent the loss of polar lipids as a result of excess water. This method yields a higher lipid extraction efficiency than other single solvent methods.

The Bligh and Dyer method was introduced as a variation of the Folch method (Bligh and Dyer 1959), which incorporated water present within samples into the solvent system and made the extraction procedure convenient and economical. Generally, the Folch method is used for the

extraction of lipids from solid tissue whereas the Bligh-Dyer method is advantageous for biological fluids (Schiller, Suss et al. 2004).

Charged, polar lipids such as glycerophospholipids bind to various biopolymers through ionic interactions that cannot be disrupted easily by polar organic solvents. In such cases, pH adjustments to the aqueous medium prior to extraction can be beneficial for achieving quantitative extraction. Acidification is an effective way to increase extraction efficiency. The addition of acid can convert negatively charged ionized molecules (lipids or biopolymers) to non-ionized forms, interrupting ionic interactions along with increasing lipid hydrophobicity. This was demonstrated in a study where the extraction of polar lipids from *M. thermoautotrophicum* cells were six times greater by replacing the water in the Bligh-Dyer solvent system with 5% (w/v) trichloroacetic acid (Nishihara and Koga 1987). We also determined that acidified extraction is not only beneficial for maximal recovery, but can also increase the ionization efficiency of lipids in mass spectrometric analysis (Figure 1.2). However, acidification of extraction procedures must be used cautiously, where the pH range is maintained at 2-4. Ester bonds are vulnerable to acid, and hydrolysis can take place after long exposures to concentrated acid, resulting in the loss of lipids. To overcome this phenomenon, Nishihara and Yosuke (Nishihara and Koga 1987) used 5% trichloroacetic acid in the place of hydrochloric acid (2 M).

Temperature is another feature that should be controlled. Low temperatures are essential for large sample sizes undergoing acidified extraction and quantitation. Our laboratory, along with many others, showed that reduced temperatures reduce degradation and improve lipid stability (Figure 1.3). The control of both pH and temperature can prevent the occurrence or reduce the rate of hydrolysis. It is important to note that acidified extraction methods are not

suitable for the long-term storage of samples, thus requiring analysis immediately following extraction.

A liquid-liquid extraction method utilizing methyl *tert*-butyl ether (MTBE)/methanol was developed recently and simplified the handling of samples in comparison to the Folch and Bligh–Dyer methods (Matyash, Liebisch et al. 2008). In this method, the low density of MTBE causes the lipid-containing organic phase to form the upper layer during liquid-phase extraction. In the Folch and Bligh-Dyer methods, the lipid-containing phase forms the lower layer due to the high density of chloroform, which can make lipid layer collection difficult. Also, non-extractable matrices such as denatured proteins can be removed by centrifugation easily since they form a dense pellet at the bottom of the extraction tube instead of in between the upper and lower phases as observed with the Folch and Bligh–Dyer methods. This suggests that the MTBE method yields similar or better recoveries of most major lipid classes compared with Folch or Bligh–Dyer. It can also be used for the simultaneous extraction of lipids and metabolites for metabolic profiling and lipidomic analysis. MTBE extractions can be performed on limited amounts of tissue samples (i.e. 2.5 mg) and are suitable for the handling of clinical specimens (Chen, Hoene et al. 2013).

Organic solvent extraction, such as chloroform and methanol, has been used widely for lipid research and while there are various advantages, limitations persist. Some of these include labor intensive and time-consuming procedures such as multiple extractions per sample for optimal recovery. Extraction efficiencies can be inconsistent, especially in the presence of emulsifiers, a common occurrence in complex biological samples. Emulsions can result in the partial or complete loss of complex glycolipids and polar prostaglandins in the aqueous layers

(Chen, Hoene et al. 2013). Further, the need for high volumes of toxic organic solvents requires researchers to utilize extra preparative measures for safety.

It is important to point out that methanol, mentioned in the methods above, does not typically serve as an extraction reagent for lipids since it is miscible with water. Rather, it is used as a reagent that disrupts the interaction between lipids and biopolymers. Similar solvents would be ethanol, 1-propanol, 2-propanol and n-butanol. While ethanol may offer a similar disruption effect as methanol, 1- and 2-propanol may be weaker owing to the larger hydrophobic moiety. *n*-Butanol is the weakest in disruption among these four solvents, but it is only partially miscible with water and can sometimes be used to extract lipids without the aid of other organic solvents. Altering solvents with the goal of providing a cleaner matrix is usually more applicable when the analyte is fully understood. In this case, the solvents can be chosen accordingly to inhibit the extraction of undesirable lipids and non-lipid content. However, this is not always the case in most lipid research, especially in lipidomics where hundreds, if not thousands, of lipids are extracted at once. Generally, a recommended approach would be to extract total lipids as much as possible, then further clean the sample using SPE if necessary. In such a scenario, methanol is usually the best choice.

1.2.2 Solid Phase Extraction

Solid-phase extraction was first introduced in the mid-1970s as a method for quick and efficient sample preparation for lipid analysis (Thurman and Mills 1998). This technique uses principles similar to those in liquid chromatography where lipids in hydrophilic media are retained on the SPE column, while the non-lipid impurities are allowed to pass through. Lipids are then eluted and collected using organic solvents with lower polarities. SPE is a useful method

for the isolation and purification of targeted lipids along with the enrichment of minor lipid species. The cartridges come in a variety of formats for the handling of different lipids, matrices, volumes and sample concentrations. Some of these include the syringe barrel, large volume capacity barrel, 96-well format and pipette tip format. SPE cartridges, like columns used in high-performance liquid chromatography (HPLC), can be classified as reversed phase, normal phase and ion exchange. SPE is powerful for a broad range of applications and when combined with a variety of elution procedures, is useful for total lipid purification as well as class separation.

With reversed-phase SPE (C18) cartridges, crude lipid extracts obtained from the Folch or Bligh-Dyer method can be diluted with water/methanol, and then loaded on the activated SPE cartridge. As the polarity of the solvent is increased, lipids remain bound to the column through hydrophobic interactions while water-soluble impurities can pass through. The remaining lipids can be collected by elution using chloroform-methanol (1:2, v/v). Alternatively, a two-step elution can permit two fractions to be collected. This would require the first elution to be performed with methanol-water (12:1, v/v), and the second elution using chloroform-methanol (1:2, v/v). In doing so, the first fraction contains gangliosides, phosphatidylserine, phosphatidylinositol, phosphatidic acid and sulfatides, while the second fraction contains all phospholipids, cerebrosides and cholesterol (Kyrklund 1987).

Normal-phase SPE binds lipids via polar interactions, such as hydrogen-bonding and ion-dipole forces, and can be used to separate polar lipids from nonpolar lipids that lack polar functional groups. The cartridges available for normal-phase SPE include amino- (NH_2), cyano- (CN) and silica- (Si) phases. Kaluzny et al. (Kaluzny, Duncan et al. 1985) demonstrated that aminopropyl (NH_2) normal-phase SPE can serve as an effective technique to separate different lipid classes including cholesterol, cholesteryl esters, triglycerides, diglycerides, monoglycerides,

fatty acids and phospholipids. For example, Kaluzny et al. (Kaluzny, Duncan et al. 1985) reported the performance of three NH2-SPE cartridges loaded with crude lipid extracts. The first elution was performed with chloroform-isopropanol (2:1, v/v), ethanol-acetic acid (98:2, v/v) and methanol, which sequentially produced three fractions. The first contained cholesterol, cholesteryl esters, tryglycerides, diglycerides and monoglycerides, which were then loaded onto a second cartridge. The second and third fractions contained fatty acids and phospholipids, respectively. Additional elution steps were carried out sequentially with hexane (100%), hexane-dichloromethane-ethanol (89:10:1, v/v/v), hexane-ethyl acetate (95:5, v/v), hexane-ethyl acetate (85:15, v/v) and chloroform-methanol (2:1, v/v). This yielded five fractions: (1) cholesterol esters, and later fractions with (3) 90% of cholesterol, (4) diglycerides and (5) monoglycerides. A third cartridge was then able to separate the second fraction (2) into triglycerides and 10% cholesterol. A modified procedure was also developed for separating chlorinated fatty acid methyl esters from the unchlorinated counterparts (Akesson-Nilsson 2003).

Ion-exchange SPE, another useful technique for the isolation and separation of lipid species, can be classified into weak or strong cation and anion exchangers. Strong cation exchangers typically contain negatively charged benzenesulfonic acids or propylsulfonic acids, while weak cation exchangers have carboxylic acids that are charged at high pH ranges and neutral at low pH ranges. Strong anion exchangers possess positively charged quaternary amines, while weak anion exchangers have primary, secondary or tertiary amines that are positively charged at low pH but neutral at high pH. An earlier method used silver ion-exchangers (Christie 1989) that have silica-based benzenesulfonic acid SPE cartridges, which can be loaded with a solution of silver nitrate in acetonitrile-water (10:1, v/v) for conversion to the ionic form of silver. The elution scheme for isolating fractions from these ion-exchange cartridges uses

varying ratios of dichloromethane, acetone and acetonitrile to separate saturated monoenes, dienes, trienes, tetraenes, pentaenes, hexaenes-fatty acid methyl ester derivatives. A similar study was performed to achieve separation of saturated, unsaturated and trans-unsaturated fatty acids (Goto, Shionoya et al. 2012). Ion-exchange SPE cartridges are used widely for the removal of lipids from analytes of interest (Shen, Motyka et al. 2005, Yoon, Kim et al. 2015). Method development can be optimized easily for separating positively or negatively charged lipids and is especially appropriate for phospholipids. Anionic phospholipids, such as phosphatidic acid and phosphatidylserine, are negatively charged at high pH, permitting them to be retained on strong anion-exchange SPE cartridges, allowing cationic phospholipids (neutral at high pH) to pass through. Eluting solvent pH can be easily adjusted to <3, where anionic phospholipids are neutral and can be easily collected from the SPE cartridge. Similar procedures can be performed for cationic phospholipids using strong cation exchange SPE. Zwitterionic phospholipids are negatively charged at high pH and positively charged at low pH, which makes them good candidates for either strong anion or cation exchange SPE with pH adjustments. Mixed mode ion-exchange SPE is a combination of reversed-phase and ion-exchange modes and provides an additional dimension of separation for charged and neutral lipids using proper strengths of organic solvents.

SPE is not only an effective tool for analysis of crude lipid extracts, but can also be applied directly to some bio-fluid samples such as serum, urine and cerebrospinal fluid. It is important to note that acidification is an essential step prior to sample loading onto SPE cartridges in order to increase lipid retention. Further, low loading and reduced flow rates should be employed for maximal retention. Online SPE liquid chromatography (SPC-LC) is the preferred method when compared with manual SPE (offline). It is highly reproducible, less time

consuming and labor intensive, and reduces the potential of exposure to potentially hazardous biological samples. Although online SPE has several advantages including high-throughput features for large sample sizes, clinical research, and diagnostics, it has higher instrumentation costs (de Jong, Graham et al. 2007).

1.2.3 Summary

Extracting lipids from biological samples is the first step of establishing a quantitative assay for liposomal formulations. It is crucial to know the chemical properties of each individual lipid component in the formulations, and to evaluate their extraction efficiency separately using the selected extraction method. However, all the lipid extraction techniques mentioned above were only evaluated by the extraction efficiency of total lipids or a certain class of lipids. The performance of the extraction methods on extracting a specifically designed liposome is unclear. Therefore, in **Chapter 2**, the extraction efficiencies of 6 phospholipids that are commonly used for liposomal formulations, including zwitterionic lipids (DPPC, DSPC, DSPE) and anionic lipids (DSPA, DSPG, DSPS) are evaluated using the Bligh-Dye method. An acidified procedure is proposed to increase the extraction efficiencies of certain anionic lipids (DSPA and DSPS).

1.3 Challenge 2: Differentiation

Differentiating liposomal formulations from endogenous lipids is extremely challenging due to the nature of the formulation components and the complicity of the sample matrixes. Phospholipids share many common molecular features but few differences, which increase the difficulty to distinguish them among each other. No extraction method was developed for extracting a sole lipid. A subsequent separation is essential for quantification. But the presence of

regional isomers and isobars highly complicate the analysis. Figure 1.4 shows that even using a powerful instrument like LC-MS/MS, the endogenous lipid interference still cannot be eliminated. For these reasons, many researchers have been using labeling techniques bypassing the extraction and separation steps to detect or visually localize the *in vitro* and *in vivo* destination of liposomes. This section will discuss some of the labeling techniques that have been widely applied.

1.3.1 Radioactive Labeling

Radioactive labeling is one of the earliest used labeling techniques for tracking liposome distribution. Many studies have shown that this technique is adequate to provide definitive evidence on uptake of liposomes in various organs and tissues. Radioactive elements are usually bond with metal chelators such as diethylene-triamine pentaacetic acid (DTPA) (Tilcock, Unger et al. 1989), then encapsulated in liposomes. Metal chelators usually have fast renal excretion (Hauser, Atkins et al. 1970), thus, the leaked radiolabels will be cleared by kidneys quickly and minimize the radioactivity background. The *in vivo* stability of the metal-chelator complex becomes critical for this manner. For a weak chelator such as nitrilotriacetic acid (NTA), radioactive metals will partially translocate to transferrin and other metal-binding plasma or tissue proteins (Moerlein and Welch 1981) if the complex leaks from liposomes. Subsequently, the radioactivity background will increase. Gallium 67-Deferoxamine complex (^{67}Ga-DF) is a radiotracer for liposomes developed by Gabizon et al in 1988 (Gabizon, Hliberty et al. 1988). The ^{67}Ga labeled liposome was produced by the incubation of DF-mesylate encapsulated liposomes with 1-2 µCi of ^{67}Ga-oxine/µmol phospholipid at 4 ºC overnight. The excessive ^{67}Ga-oxine was removed by passing the liposome suspension through an anion-exchange resin

(AG1X2, acetate from, 200-400 mesh size). The mechanism of achieving ^{67}Ga-DF forming into aqueous interior of liposome was using a lipophilic chelator, oxine. Oxine carried ^{67}Ga across the liposome bilayer. ^{67}Ga then bound to a stronger hydrophilic chelator, DF, within the aqueous interior of the liposomes and was trapped in the liposome aqueous phase. A distribution comparison of ^{67}Ga-DF encapsulated liposomes and free ^{67}Ga-DF showed a significant difference in distribution patterns. Also, the results showed that free ^{67}Ga-DF had an extremely fast excretion (less than 5% of the injected dose remained in the body 1 hr after injection), while the majority (> 85%) of the ^{67}Ga-DF encapsulated liposomes were still able to be detected. Based on their results, the authors claimed that ^{67}Ga-DF complex had significant advantages for *in vivo* tracing of liposomes: high stability of ^{67}Ga-DF complex, avoiding metal translocation to plasma proteins; rapid renal clearance of free ^{67}Ga-DF complex, minimizing the background of radioactivity. ^{67}Ga-DF encapsulated liposomes were used for both quantitative pharmacokinetic study and imaging.

[^{3}H]Chol-hexadecyl ether (Gabizon, Pappo et al. 1993) is a non-exchangeable radiotracer. A pharmacokinetic study was conducted using [^{3}H]Chol-hexadecyl ether to quantify the PEGylated liposome plasma concentrations compared to the concentrations of encapsulated doxorubicin. The results, presented as percentages of injected Dose (Figure 1.5), showed that the initial clearances were the same for both DXR and ^{3}H labeled PEGylated liposomes, however, a faster clearance for DXR was observed after 24 hours. These results indicated that some leakage from circulating liposomes took place.

A clinical application of radioactive labeling worth mentioning was reported in 2001 (Harrington, Mohammadtaghi et al. 2001). In 17 patients with a variety of locally advanced solid tumors, human whole body γ-camera imaging (Figure 1.6) were captured by using ^{111}In-DTPA

labeled PEGylate liposomes. Liposome uptake in tumors was observed as well as in the RES of the liver, spleen and bone marrow. Another important clinical relevant observation in the same study was the smaller sized tumors tended to have higher concentrations of liposome uptake.

1.3.2 Fluorescence Labeling

While radioactive labels are predominately used *in vivo*, some fluorescence labels are suitable for *in vitro* study. Quenchable fluorescent probes, such as calcein and 6-carboxyfluorescein, have low levels of fluorescence when encapsulated in liposomes, higher levels in free form (Weinstein, Yoshikami et al. 1977, Gregoriadis and Davis 1979, Bajoria, Sooranna et al. 1997, Kokkona, Kallinteri et al. 2000). This property is perfect for liposomal formulation *in vitro* stability and drug release evaluation. Our group published a study in 2011 (Zhu, Mock et al. 2011) on the development of a new enzymatic triggered liposomal formulation, $sPLA_2$ responsive liposome (SPRL). In this study, we used 6-carboxyfluorescein as an indicator to evaluate the enzymatic responsiveness and *in vitro* stability of SPRL, as well as the selectivity of different $sPLA_2$ groups (Group III vs Group IIA) to SPRL.

Doxorubicin, as an antitumor agent with fluorescence property, has demonstrated many preclinical and clinical successes in *in vivo* tracing of liposomes. The pharmacokinetic studies, including single dose (Gabizon, Pappo et al. 1993) and multiple dose (Arnold, Mager et al. 2005) studies, clearly showed alternation in circulation time between DXR encapsulated liposomes and free DXR. Tissue distribution results showed a higher accumulation of DXR encapsulated liposomes than free DXR as well (Gabizon, Pappo et al. 1993). Similar results were found in clinical studies. During the phase I clinical study of Doxil®, a 4- to 16-fold increase in malignant pleural effusion drug concentrations was achieved with Doxil® when compared with free DXR

administered in the same patient 3 weeks apart (Gabizon, Catane et al. 1994). A 5- to 11-fold drug concentration in skin tumor lesions was also observed in AIDS related Kaposi's sarcoma (ARKS) patients using Doxil® (Northfelt, Martin et al. 1996).

Fluorescence microscopy in combination with florescence dyes is a useful tool for visually observing the *in vitro* intracellular uptake of lipid-based carriers. A study was conducted on immunomicelles (Torchilin, Lukyanov et al. 2003) which was engineered by conjugating (Torchilin, Levchenko et al. 2001, Torchilin, Rammohan et al. 2001) a monoclonal antibody 2C5 that are processing nucleosome restricted specificity and reactive towards a variety of different cancer cells (Iakoubov, Rokhlin et al. 1995, Iakoubov and Torchilin 1997, Iakoubov and Torchilin 1998). The immunemicelles were labeled using a lipophilic fluorescence dye, rhodamine-phosphatidylethanolamine (Rh-PE). Fluorescence imaging showed clear binding of Rh-PE labeled 2C5-immunomicelles to all 4 cancer cell lines tested (murine LLC and EL4 cells, human BT-20 and MCF-7 cells), while the plain micelles only showed background level of fluorescence. Spectral imaging microscopy equipped with a triple bandpass filter set enabled researchers to use multiple fluorescence dyes to generate multi-color fluorescence imaging to study the fate of liposomes. A study (Huth, Wieschollek et al. 2004) used hydrophilic dye fluorescein lisothiocyanate-dextran (FITC-dextran) or lipophilic membrane marker Rh-PE to label pH sensitive liposomes. The liposomes were then incubated with DOS-7 cells. Further, the cell membranes were stained with DiO, lysosomes were stained with LysoTracker Red, and nuclei were counterstained with 4',6 diamidino-2-phenylindole dihydrochloride (DAPI). All 5 dyes were used simultaneously and were spectrally distinguished by the system. The results showed that liposomes labeled with two different dyes (lipophilic vs hydrophilic), respectively, demonstrated two different cellular distribution patterns. This experiment raised another concern

of using labeling techniques that the labels could potentially change the physiochemical or biochemical properties of the native liposomal formulation.

The next application is not a typical fluorescence imagining technique, but it eliminated such concern. Raman microspectroscopy is an imaging technique that reconstructs molecular vibrations excited either by infrared radiation or nonelastic scattering of photons (Raman Effect) into images. This technique offers the possibility to image cellular structures, such as nucleus or chromatin (Uzunbajakava, Lenferink et al. 2003, Matthaus, Boydston-White et al. 2006), mitochondria (Matthaus, Chernenko et al. 2007) and lipid bodies (van Manen, Kraan et al. 2005, Krafft, Knetschke et al. 2006), based on their vibrational properties of their chemical composition, without using any staining chemicals. A research group from Northeastern University (Matthaus, Kale et al. 2008) used Raman microspectroscopy to track the intracellular uptake of liposomes containing 1,2-distearoyl-d70-*sn*-glycero-3-phosphatidylcholine (d70-DSPC). The C-D stretching vibration has different wavelengths compared to C-H bound (Figure 1.7), and can be reconstruct into two different images. The overlay of two images can be used to localize d70-DSPC contained liposomes (Figure 1.8). d70-DSPC is an synthetic isotopic molecule of DSPC which is one of the formulation components. Their physiochemical and biochemical properties are identical. The major advantage of using d70-DSPC is that it will not alter the native liposomal formulations, it is part of the formulation. Also, problems such as premature leakage, translocation or lipid exchange will not occur with d70-DSPC as observed with other labeling techniques.

1.3.3 MR Imaging Contrast Agents

The preparation of MRI contrast agents for liposome tracing is similar to radioactive labeling. In brief, the contrast agent contains reporter metals (Gd, Dy, Mn, Fe) and chelators, either encapsulated in the aqueous interior of liposomes (Gabizon, Hliberty et al. 1988, Tilcock, Unger et al. 1989) or anchored on the surface of the liposome (Kabalka, Davis et al. 1991). For a better MR signal, all reporter atoms should be freely exposed for interaction with water. In such case, anchoring the metal-chelator complex on the surface of the liposomes will be a better option. Membranotropic chelating agents such as DTPA-stearylamine (DTPA-SA) (Kabalka, Davis et al. 1991) or DTPA-phosphatidyl ethanolamine (DTPA-PE) (Schwendener, Wuthrich et al. 1990) consists of a polar head containing a chelator which can bind with paramagnetic atom, and the lipid moiety that anchors the metal-chelator complex in the liposome membrane.

Although MRI is a powerful technique to trace *in vivo* localization of liposomes, many researchers have been using liposomes as carriers for MRI diagnostic agents (Huh, Jun et al. 2005, Elbayoumi, Pabba et al. 2007) due to the better pharmacokinetic characteristics and quick accumulation in RES of the liver, lung, and spleen. One practical example of such application is using Gd-loaded liposomes for MRI of the lymphatic system. This is important for discovering metastases in lymph nodes (Trubetskoy and Torchilin 1996).

1.3.4 Summary

Differentiation of liposomes from biological milieu are extremely difficult. Labeling is the most commonly used method to achieve this purpose. However, labeling methodology is problematic in quantification. Premature leakage, translocation and altering the native formulations, compromise the use of labeling methods. In **Chapter 3**, we developed a new

quantitative method using deuterated phospholipids (d70-DSPC, d35-LysoPC) in combination of LC-MS/MS. With this method, we are able to directly quantify liposomes and their metabolites simultaneously from biological matrix, and conduct *in vitro* and *in vivo* studies in **Chapter 4**.

1.4 Conclusion

Due to the complexity of biological samples, liposomes are difficult to trace and quantify. This is why so many labeling techniques have been developed. Some techniques are adequate for localization and visualization, but problematic in quantification. Doxorubicin is the most used indicator for liposome pharmacokinetics and tumor accumulation. However, a study has shown (Gabizon, Pappo et al. 1993) that DXR leakage occurred during circulation, which could lead to underestimated pharmacokinetic parameters of liposomes. Furthermore, the unknown concentrations of the liposomes accumulated in tumor is the missing information for understanding the drug accumulation mechanism. [^{3}H]Chol-hexadecyl ether is a non-exchangeable radioactive label that has no translocation and leaking problems like other labels. Incorporation into liposomal formulation can be used to quantify liposome concentration *in vivo*. But radioactive tracers with a long half-live (^{3}H: 12.3years) requires special handling. Not many laboratories are certified for using radioactive material. The ability to directly examine the metabolism of liposome composition is not possible using [^{3}H]Chol-hexadecyl ether. Raman microspectroscopy provided an example of using deuterated phospholipids to overcome almost all the labeling disadvantages. Unfortunately, counting optical density is not an accurate quantitative analysis.

Therefore, a fully quantitative method for liposomes is very much needed in this field. The purpose of this project is to establish a new method using LC-MS/MS for liposome *in vitro*

and *in vivo* quantification to enhance our ability for optimizing formulations and understanding intracellular mechanisms.

1.5 Acknowledgement

Part of this chapter (1.2 Challenge 1: Extraction) has been published in our review paper in 2016 (Pati, S., B. Nie, R. D. Arnold and B. S. Cummings. "Extraction, chromatographic and mass spectrometric methods for lipid analysis." Biomed Chromatogr **30**(5): 695-709).

1.6 References

Akesson-Nilsson, G. (2003). "Isolation of chlorinated fatty acid methyl esters derived from cell-culture medium and from fish lipids by using an aminopropyl solid-phase extraction column." J Chromatogr A **996**(1-2): 173-180.

Allen, T. M. and C. Hansen (1991). "Pharmacokinetics of stealth versus conventional liposomes: effect of dose." Biochim Biophys Acta **1068**(2): 133-141.

Arnold, R. D., D. E. Mager, J. E. Slack and R. M. Straubinger (2005). "Effect of repetitive administration of Doxorubicin-containing liposomes on plasma pharmacokinetics and drug biodistribution in a rat brain tumor model." Clin Cancer Res **11**(24 Pt 1): 8856-8865.

Bajoria, R., S. R. Sooranna and S. F. Contractor (1997). "Endocytotic uptake of small unilamellar liposomes by human trophoblast cells in culture." Hum Reprod **12**(6): 1343-1348.

Bligh, E. G. and W. J. Dyer (1959). "A rapid method of total lipid extraction and purification." Can J Biochem Physiol **37**(8): 911-917.

Chen, S., M. Hoene, J. Li, Y. Li, X. Zhao, H. U. Haring, E. D. Schleicher, C. Weigert, G. Xu and R. Lehmann (2013). "Simultaneous extraction of metabolome and lipidome with methyl tert-butyl ether from a single small tissue sample for ultra-high performance liquid chromatography/mass spectrometry." J Chromatogr A **1298**: 9-16.

Christie, W. W. (1989). "Silver ion chromatography using solid-phase extraction columns packed with a bonded-sulfonic acid phase." J Lipid Res **30**(9): 1471-1473.

Crasto, G. J., N. Kartner, N. Reznik, M. V. Spatafora, H. Chen, R. Williams, P. N. Burns, C. Clokie, M. F. Manolson and S. A. Peel (2016). "Controlled bone formation using ultrasound-triggered release of BMP-2 from liposomes." J Control Release **243**: 99-108.

Davidsen, J., K. Jørgensen, T. L. Andresen and O. G. Mouritsen (2003). "Secreted phospholipase A2 as a new enzymatic trigger mechanism for localised liposomal drug release and absorption in diseased tissue." Biochim Biophys Acta (BBA) - Biomembranes **1609**(1): 95-101.

de Jong, W. H., K. S. Graham, J. C. van der Molen, T. P. Links, M. R. Morris, H. A. Ross, E. G. de Vries and I. P. Kema (2007). "Plasma free metanephrine measurement using automated online solid-phase extraction HPLC tandem mass spectrometry." Clin Chem **53**(9): 1684-1693.

de Smet, M., N. M. Hijnen, S. Langereis, A. Elevelt, E. Heijman, L. Dubois, P. Lambin and H. Grull (2013). "Magnetic resonance guided high-intensity focused ultrasound mediated hyperthermia improves the intratumoral distribution of temperature-sensitive liposomal doxorubicin." Invest Radiol **48**(6): 395-405.

Elbayoumi, T. A., S. Pabba, A. Roby and V. P. Torchilin (2007). "Antinucleosome antibody-modified liposomes and lipid-core micelles for tumor-targeted delivery of therapeutic and diagnostic agents." J Liposome Res **17**(1): 1-14.

Elkhodiry, M. A., C. C. Momah, S. R. Suwaidi, D. Gadalla, A. M. Martins, R. F. Vitor and G. A. Husseini (2016). "Synergistic Nanomedicine: Passive, Active, and Ultrasound-Triggered Drug Delivery in Cancer Treatment." J Nanosci Nanotechnol **16**(1): 1-18.

Evjen, T. J., E. A. Nilssen, S. Barnert, R. Schubert, M. Brandl and S. L. Fossheim (2011). "Ultrasound-mediated destabilization and drug release from liposomes comprising dioleoylphosphatidylethanolamine." Eur J Pharm Sci **42**(4): 380-386.

Fan, Y., C. Chen, Y. Huang, F. Zhang and G. Lin (2017). "Study of the pH-sensitive mechanism of tumor-targeting liposomes." Colloids Surf B **151**: 19-25.

Folch, J., M. Lees and G. H. Sloane Stanley (1957). "A simple method for the isolation and purification of total lipids from animal tissues." J Biol Chem **226**(1): 497-509.

Gaber, M. H., K. Hong, S. K. Huang and D. Papahadjopoulos (1995). "Thermosensitive sterically stabilized liposomes: formulation and in vitro studies on mechanism of doxorubicin release by bovine serum and human plasma." Pharm Res **12**(10): 1407-1416.

Gabizon, A., R. Catane, B. Uziely, B. Kaufman, T. Safra, R. Cohen, F. Martin, A. Huang and Y. Barenholz (1994). "Prolonged circulation time and enhanced accumulation in malignant exudates of doxorubicin encapsulated in polyethylene-glycol coated liposomes." Cancer Res **54**(4): 987-992.

Gabizon, A., J. Hliberty, R. M. Straubinger, D. C. Price and D. Papahadjopoulos (1988). "An Improved Method for in Vivo Tracing and Imaging of Liposomes Using a Gallium 67-Deferoxamine Complex." J Liposome Res **1**(1): 123-135.

Gabizon, A., H. Shmeeda and Y. Barenholz (2003). "Pharmacokinetics of Pegylated Liposomal Doxorubicin." Clin Pharmacokinet **42**(5): 419-436.

Gabizon, A. A., O. Pappo, D. Goren, M. Chemla, D. Tzemach and A. T. Horowitz (1993). "Preclinical Studies with Doxorubicin Encapsulated in Polyethyleneglycol-Coated Liposomes." J Liposome Res **3**(3): 517-528.

Giansanti, L., A. Mauceri, L. Galantini, B. Altieri, A. Piozzi and G. Mancini (2016). "Glucosylated pH-sensitive liposomes as potential drug delivery systems." Chem Phys Lipids **200**: 113-119.

Goto, H., N. Shionoya, M. Sugie, M. Tominaga, O. Shimelis, M. Taniguchi, T. Igarashi and Y. Hirata (2012). "Novel pre-fractionation method of trans fatty acids by gas chromatography with silver-ion cartridge column." J Oleo Sci **61**(2): 49-56.

Gregoriadis, G. (1981). "Targeting of drugs: implications in medicine." Lancet **2**(8240): 241-246.

Gregoriadis, G. and C. Davis (1979). "Stability of liposomes in vivo and in vitro is promoted by their cholesterol content and the presence of blood cells." Biochem Biophys Res Commun **89**(4): 1287-1293.

Harrington, K. J., S. Mohammadtaghi, P. S. Uster, D. Glass, A. M. Peters, R. G. Vile and J. S. Stewart (2001). "Effective targeting of solid tumors in patients with locally advanced cancers by radiolabeled pegylated liposomes." Clin Cancer Res **7**(2): 243-254.

Hauser, W., H. L. Atkins, K. G. Nelson and P. Richards (1970). "Technetium-99m DTPA: a new radiopharmaceutical for brain and kidney scanning." Radiology **94**(3): 679-684.

Huh, Y. M., Y. W. Jun, H. T. Song, S. Kim, J. S. Choi, J. H. Lee, S. Yoon, K. S. Kim, J. S. Shin, J. S. Suh and J. Cheon (2005). "In vivo magnetic resonance detection of cancer by using multifunctional magnetic nanocrystals." J Am Chem Soc **127**(35): 12387-12391.

Huth, U., A. Wieschollek, Y. Garini, R. Schubert and R. Peschka-Suss (2004). "Fourier transformed spectral bio-imaging for studying the intracellular fate of liposomes." Cytometry A **57**(1): 10-21.

Iakoubov, L., O. Rokhlin and V. Torchilin (1995). "Anti-nuclear autoantibodies of the aged reactive against the surface of tumor but not normal cells." Immunol Lett **47**(1): 147-149.

Iakoubov, L. Z. and V. P. Torchilin (1997). "A Novel Class of Antitumor Antibodies: Nucleosome-Restricted Antinuclear Autoantibodies (ANA) From Healthy Aged Nonautoimmune Mice." Oncol Res **9**(8): 439-446.

Iakoubov, L. Z. and V. P. Torchilin (1998). "Nucleosome-releasing treatment makes surviving tumor cells better targets for nucleosome-specific anticancer antibodies." Cancer Detect Prev **22**(5): 470-475.

Juliano, R. L. and D. Stamp (1975). "The effect of particle size and charge on the clearance rates of liposomes and liposome encapsulated drugs." Biochem Biophys Res Commun **63**(3): 651-658.

Kabalka, G. W., M. A. Davis, E. Holmberg, K. Maruyama and L. Huang (1991). "Gadolinium-labeled liposomes containing amphiphilic Gd-DTPA derivatives of varying chain length: Targeted MRI contrast enhancement agents for the liver." Magn Reson Imaging **9**(3): 373-377.

Kaluzny, M. A., L. A. Duncan, M. V. Merritt and D. E. Epps (1985). "Rapid separation of lipid classes in high yield and purity using bonded phase columns." J Lipid Res **26**(1): 135-140.

Kieler-Ferguson, H. M., D. Chan, J. Sockolosky, L. Finney, E. Maxey, S. Vogt and F. C. Szoka Jr (2017). "Encapsulation, controlled release, and antitumor efficacy of cisplatin delivered in liposomes composed of sterol-modified phospholipids." Eur J Pharm Sci.

Kokkona, M., P. Kallinteri, D. Fatouros and S. G. Antimisiaris (2000). "Stability of SUV liposomes in the presence of cholate salts and pancreatic lipases: effect of lipid composition." Eur J Pharm Sci **9**(3): 245-252.

Krafft, C., T. Knetschke, R. H. Funk and R. Salzer (2006). "Studies on stress-induced changes at the subcellular level by Raman microspectroscopic mapping." Anal Chem **78**(13): 4424-4429.

Kyrklund, T. (1987). "Two procedures to remove polar contaminants from a crude brain lipid extract by using prepacked reversed-phase columns." Lipids **22**(4): 274-277.

Lasic, D. D., F. J. Martin, A. Gabizon, S. K. Huang and D. Papahadjopoulos (1991). "Sterically stabilized liposomes: a hypothesis on the molecular origin of the extended circulation times." Biochim Biophys Acta **1070**(1): 187-192.

Matthaus, C., S. Boydston-White, M. Miljkovic, M. Romeo and M. Diem (2006). "Raman and infrared microspectral imaging of mitotic cells." Appl Spectrosc **60**(1): 1-8.

Matthaus, C., T. Chernenko, J. A. Newmark, C. M. Warner and M. Diem (2007). "Label-free detection of mitochondrial distribution in cells by nonresonant Raman microspectroscopy." Biophys J **93**(2): 668-673.

Matthaus, C., A. Kale, T. Chernenko, V. Torchilin and M. Diem (2008). "New ways of imaging uptake and intracellular fate of liposomal drug carrier systems inside individual cells, based on Raman microscopy." Mol Pharm **5**(2): 287-293.

Matyash, V., G. Liebisch, T. V. Kurzchalia, A. Shevchenko and D. Schwudke (2008). "Lipid extraction by methyl-tert-butyl ether for high-throughput lipidomics." J Lipid Res **49**(5): 1137-1146.

Moerlein, S. M. and M. J. Welch (1981). "The chemistry of gallium and indium as related to radiopharmaceutical production." Int J Nucl Med Biol **8**(4): 277-287.

Needham, D., G. Anyarambhatla, G. Kong and M. W. Dewhirst (2000). "A new temperature-sensitive liposome for use with mild hyperthermia: characterization and testing in a human tumor xenograft model." Cancer Res **60**(5): 1197-1201.

Nishihara, M. and Y. Koga (1987). "Extraction and composition of polar lipids from the archaebacterium, Methanobacterium thermoautotrophicum: effective extraction of tetraether lipids by an acidified solvent." J Biochem **101**(4): 997-1005.

Northfelt, D. W., F. J. Martin, P. Working, P. A. Volberding, J. Russell, M. Newman, M. A. Amantea and L. D. Kaplan (1996). "Doxorubicin encapsulated in liposomes containing surface-bound polyethylene glycol: pharmacokinetics, tumor localization, and safety in patients with AIDS-related Kaposi's sarcoma." J Clin Pharmacol **36**(1): 55-63.

Papahadjopoulos, D., T. M. Allen, A. Gabizon, E. Mayhew, K. Matthay, S. K. Huang, K. D. Lee, M. C. Woodle, D. D. Lasic, C. Redemann and et al. (1991). "Sterically stabilized liposomes: improvements in pharmacokinetics and antitumor therapeutic efficacy." Proc Natl Acad Sci U S A **88**(24): 11460-11464.

Pati, S., B. Nie, R. D. Arnold and B. S. Cummings (2016). "Extraction, chromatographic and mass spectrometric methods for lipid analysis." Biomed Chromatogr **30**(5): 695-709.

Poste, G., C. Bucana, A. Raz, P. Bugelski, R. Kirsh and I. J. Fidler (1982). "Analysis of the fate of systemically administered liposomes and implications for their use in drug delivery." Cancer Res **42**(4): 1412-1422.

Ruoslahti, E. (2012). "Peptides as targeting elements and tissue penetration devices for nanoparticles." Adv Mater **24**(28): 3747-3756.

Sapra, P. and T. M. Allen (2003). "Ligand-targeted liposomal anticancer drugs." Prog Lipid Res **42**(5): 439-462.

Schiller, J., R. Suss, J. Arnhold, B. Fuchs, J. Lessig, M. Muller, M. Petkovic, H. Spalteholz, O. Zschornig and K. Arnold (2004). "Matrix-assisted laser desorption and ionization time-of-flight

(MALDI-TOF) mass spectrometry in lipid and phospholipid research." Prog Lipid Res **43**(5): 449-488.

Schwendener, R. A., R. Wuthrich, S. Duewell, E. Wehrli and G. K. von Schulthess (1990). "A pharmacokinetic and MRI study of unilamellar gadolinium-, manganese-, and iron-DTPA-stearate liposomes as organ-specific contrast agents." Invest Radiol **25**(8): 922-932.

Sengupta, P., D. Holowka and B. Baird (2007). "Fluorescence resonance energy transfer between lipid probes detects nanoscopic heterogeneity in the plasma membrane of live cells." Biophys J **92**(10): 3564-3574.

Shen, J. X., R. J. Motyka, J. P. Roach and R. N. Hayes (2005). "Minimization of ion suppression in LC-MS/MS analysis through the application of strong cation exchange solid-phase extraction (SCX-SPE)." J Pharm Biomed Anal **37**(2): 359-367.

Simões, S., J. N. Moreira, C. Fonseca, N. Düzgüneş and M. C. Pedroso de Lima (2004). "On the formulation of pH-sensitive liposomes with long circulation times." Adv Drug Deliv Rev **56**(7): 947-965.

Suga, T., Y. Fuchigami, M. Hagimori and S. Kawakami (2017). "Ligand peptide-grafted PEGylated liposomes using HER2 targeted peptide-lipid derivatives for targeted delivery in breast cancer cells: The effect of serine-glycine repeated peptides as a spacer." Int J Pharm **521**(1-2): 361-364.

Thurman, E. M. and M. S. Mills (1998). Solid-phase extraction : principles and practice. New York, Wiley.

Tilcock, C., E. Unger, P. Cullis and P. MacDougall (1989). "Liposomal Gd-DTPA: preparation and characterization of relaxivity." Radiology **171**(1): 77-80.

Torchilin, V. P., T. S. Levchenko, A. N. Lukyanov, B. A. Khaw, A. L. Klibanov, R. Rammohan, G. P. Samokhin and K. R. Whiteman (2001). "p-Nitrophenylcarbonyl-PEG-PE-liposomes: fast and simple attachment of specific ligands, including monoclonal antibodies, to distal ends of PEG chains via p-nitrophenylcarbonyl groups." Biochim Biophys Acta **1511**(2): 397-411.

Torchilin, V. P., A. N. Lukyanov, Z. Gao and B. Papahadjopoulos-Sternberg (2003). "Immunomicelles: targeted pharmaceutical carriers for poorly soluble drugs." Proc Natl Acad Sci **100**(10): 6039-6044.

Torchilin, V. P., R. Rammohan, V. Weissig and T. S. Levchenko (2001). "TAT peptide on the surface of liposomes affords their efficient intracellular delivery even at low temperature and in the presence of metabolic inhibitors." Proc Natl Acad Sci U S A **98**(15): 8786-8791.

Trubetskoy, V. and V. Torchilin (1996). "Polyethyleneglycol based micelles as carriers of therapeutic and diagnostic agents." STP pharma sciences **6**(1): 79-86.

Uzunbajakava, N., A. Lenferink, Y. Kraan, E. Volokhina, G. Vrensen, J. Greve and C. Otto (2003). "Nonresonant confocal Raman imaging of DNA and protein distribution in apoptotic cells." Biophys J **84**(6): 3968-3981.

van Manen, H. J., Y. M. Kraan, D. Roos and C. Otto (2005). "Single-cell Raman and fluorescence microscopy reveal the association of lipid bodies with phagosomes in leukocytes." Proc Natl Acad Sci U S A **102**(29): 10159-10164.

Weinstein, J. N., S. Yoshikami, P. Henkart, R. Blumenthal and W. A. Hagins (1977). "Liposome-cell interaction: transfer and intracellular release of a trapped fluorescent marker." Science **195**(4277): 489-492.

Woodle, M. C. and D. D. Lasic (1992). "Sterically stabilized liposomes." Biochim Biophys Acta **1113**(2): 171-199.

Yatvin, M. B., J. N. Weinstein, W. H. Dennis and R. Blumenthal (1978). "Design of liposomes for enhanced local release of drugs by hyperthermia." Science **202**(4374): 1290-1293.

Yoon, S. H., M. S. Kim, S. H. Kim, H. M. Park, H. Pyo, Y. M. Lee, K. T. Lee and J. Hong (2015). "Effective application of freezing lipid precipitation and SCX-SPE for determination of pyrrolizidine alkaloids in high lipid foodstuffs by LC-ESI-MS/MS." J Chromatogr B Analyt Technol Biomed Life Sci **992**: 56-66.

Yu, F. T., X. Chen, J. Wang, B. Qin and F. S. Villanueva (2016). "Low Intensity Ultrasound Mediated Liposomal Doxorubicin Delivery Using Polymer Microbubbles." Mol Pharm **13**(1): 55-64.

Zhu, G., J. N. Mock, I. Aljuffali, B. S. Cummings and R. D. Arnold (2011). "Secretory phospholipase A(2) responsive liposomes." J Pharm Sci **100**(8): 3146-3159.

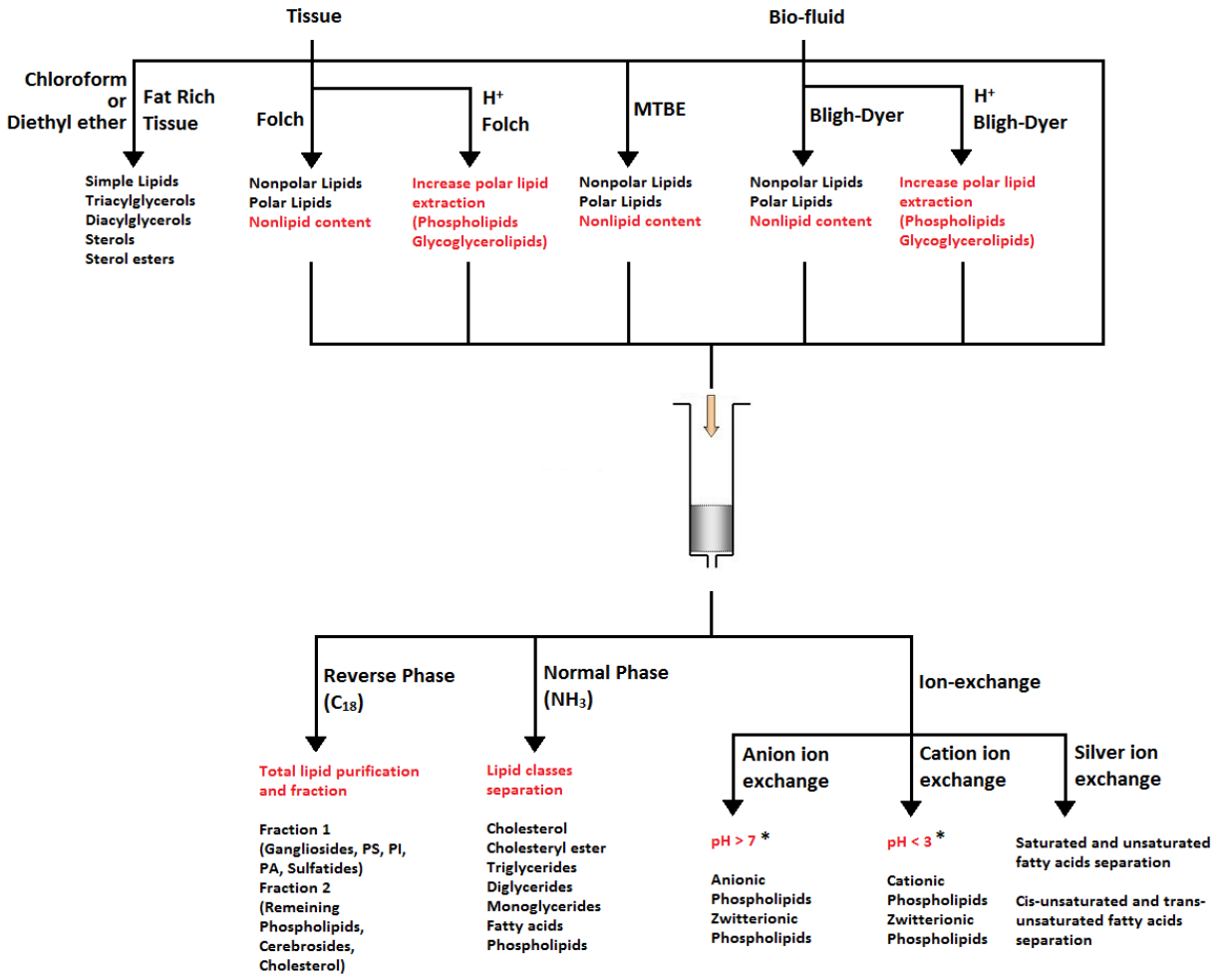

Figure 1.1 Overall Applications of Extraction Techniques on Lipids Research. *pH values are approximated, pH adjustment depends on analytes (Pati, Nie et al. 2016).

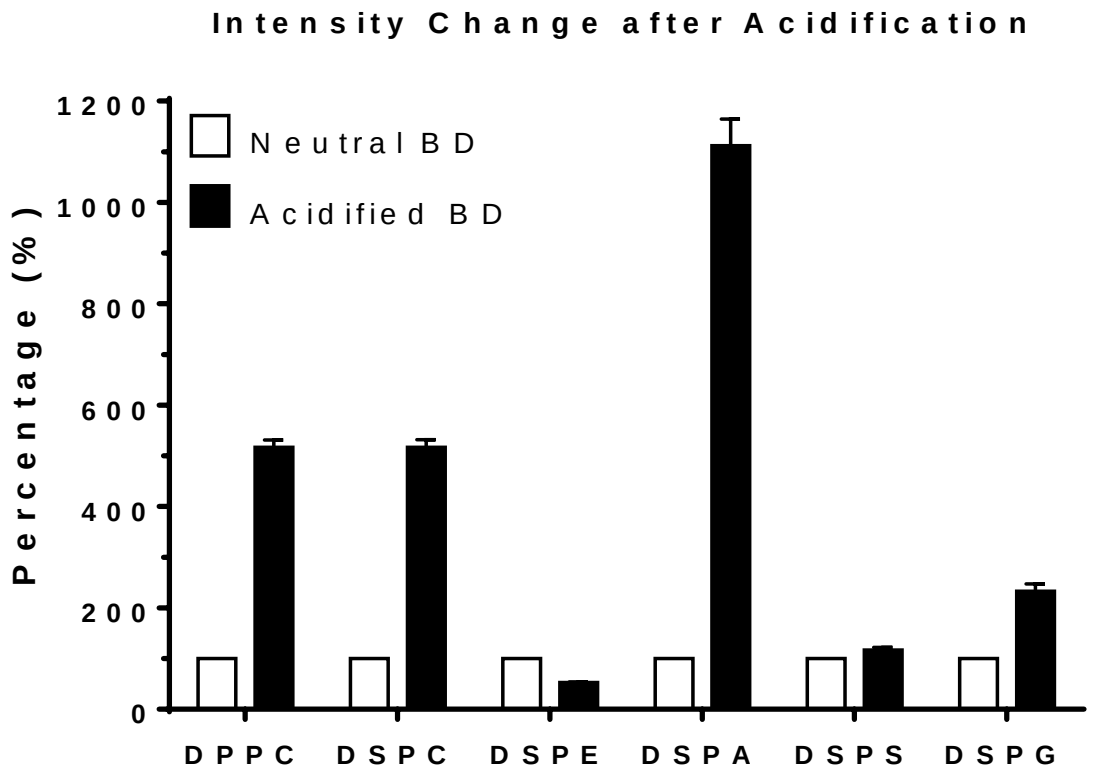

Figure 1.2 Effect of Acidification on the Signal Intensity of DPPC, DSPC, DSPE, DSPA, DSPS, and DSPG after Acidified Bligh-Dyer (BD) Extraction. Six different phospholipids were prepared, extracted using neutral or acidified BD extraction, then analyzed using ESI-MS. The intensity changes after acidification were shown via comparing to control. The conventional BD extraction was set as control and made 100%. Data are presented as mean ± SEM (n = 3) (Pati, Nie et al. 2016).

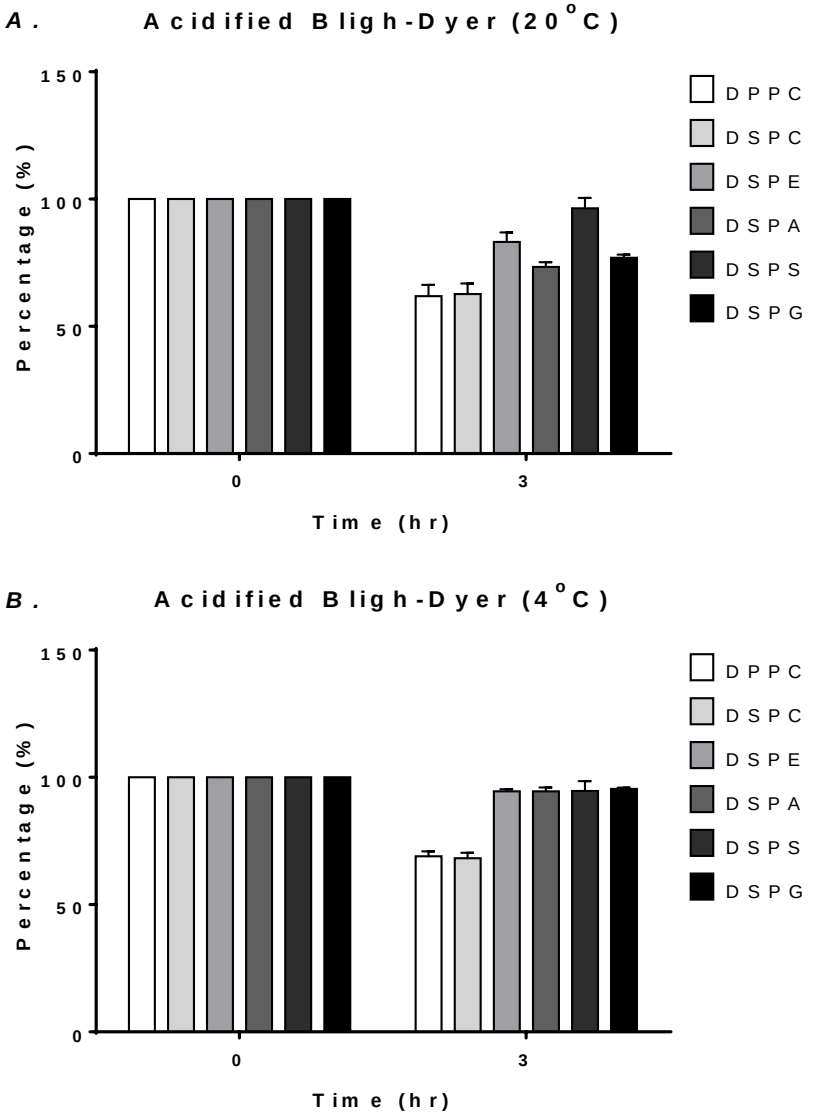

Figure 1.3 Effect of Acidification on Stability of Phospholipids after Acidified BD Extraction. Six different phospholipids were prepared, extracted using neutral or acidified BD extraction. The extracts were allowed to incubate at either 20 or 4 °C for 0 or 20 h prior to analysis using ESI-MS. With acidified BD extraction, a varying extent of degradation was observed with all phospholipids except DSPS at 20 °C (A). At 4 °C (B), only phosphatidylcholines (PCs) show significant degradation. No significant degradation was observed in samples extracted using conventional BD extraction. The time point of 0 h was set as a control with the value being set at 100%. Data are presented as mean ± SEM (n = 3) (Pati, Nie et al. 2016).

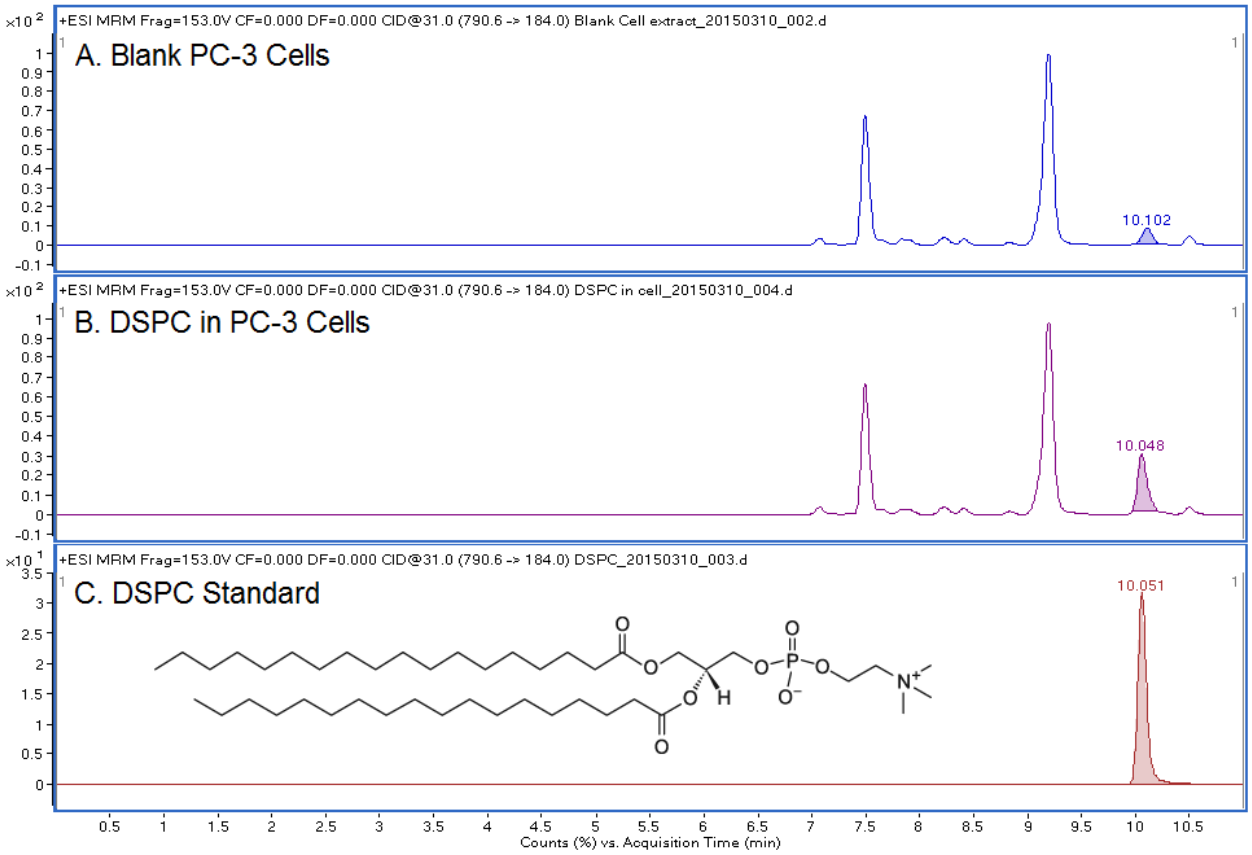

Figure 1.4 Comparison of LC-MS/MS Chromatography of DSPC Standard, Sample and Background. The retention time of DSPC was indicated by standard at 10.051 min (C), PC-3 blank cells showed an interference peak very close to target peak at 10.102 min (A), PC-3 cells incubated with SPRL showed an asymmetric peak due to the co-elute interference peak at 10.048 min (B).

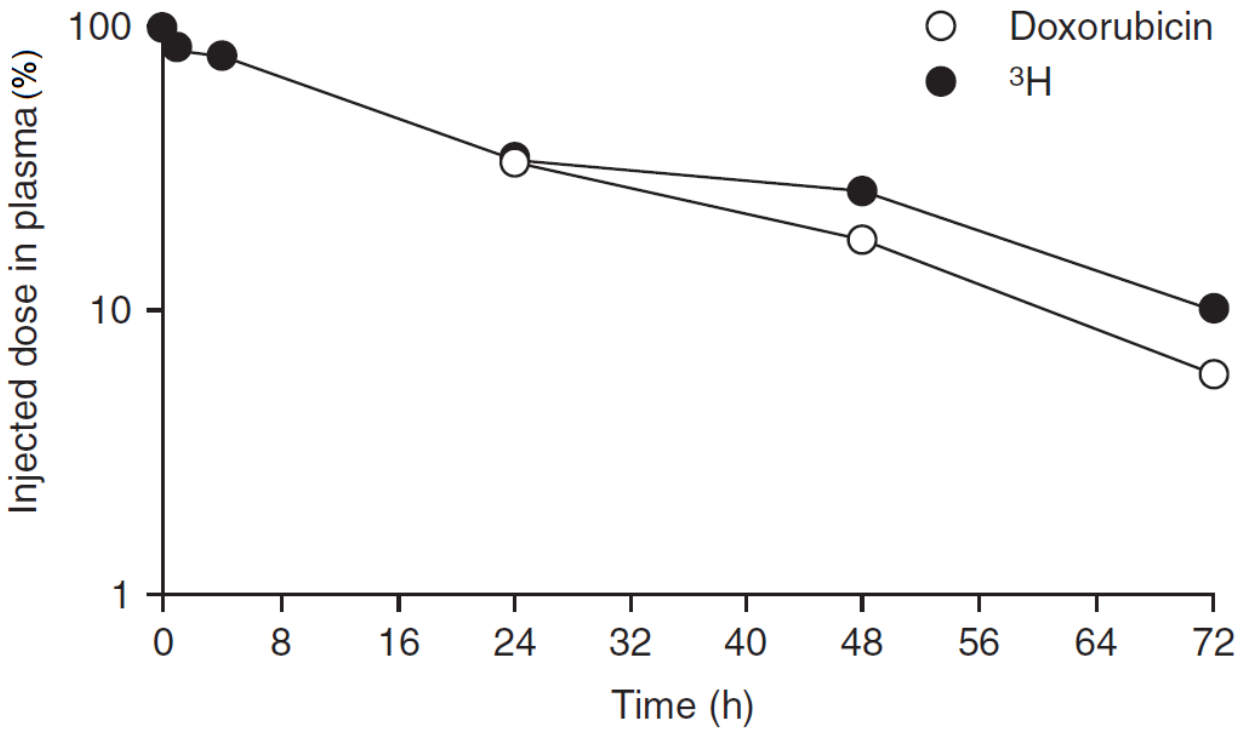

Figure 1.5 Clearance of [^{3}H]cholesterol-labelled PEGylated liposomal doxorubicin from plasma in mice. The curves depict percentage of injected dose in plasma of liposome-associated doxorubicin and [^{3}H]cholesterol hexadecyl ether, a non-exchangeable liposome radioactive tracer. Note that up to 24 hours after injection the curves are superimposable, indicating that at least two-thirds of the liposome dose has been cleared with an intact drug payload. At 48 and 72 hours the curves diverge, indicating that a detectable amount of drug has leaked from the liposomes (Gabizon, Pappo et al. 1993).

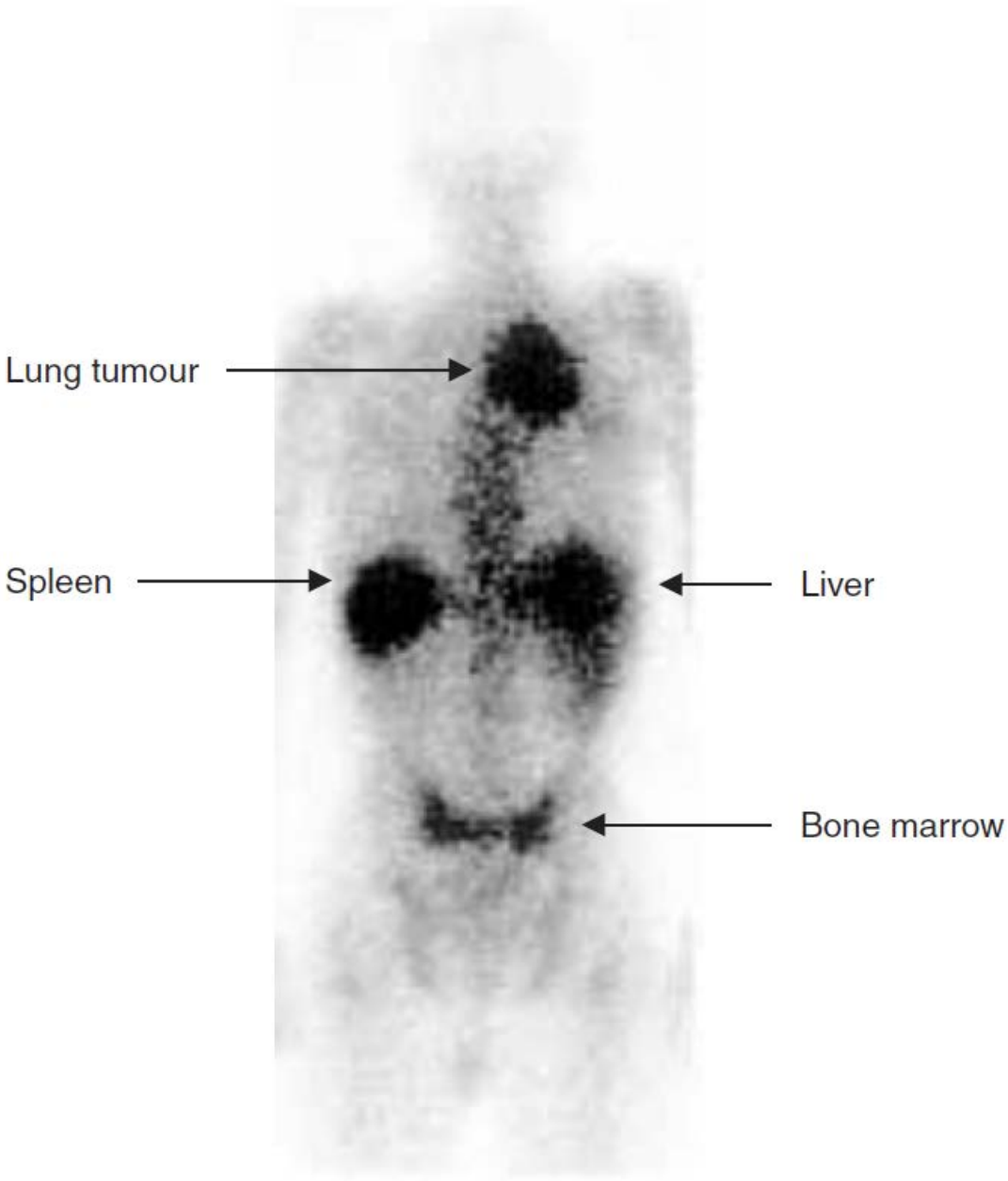

Figure 1.6 Gamma scintigraphy (posterior view) of patient with lung cancer 48 hours after injection of ^{111}In-radiolabelled STEALTH® (PEGylated) liposomes. The liposomes are taken up by a large tumor in the right upper lung. Prominent uptake can also be seen in the liver, spleen, and bone marrow (Harrington, Mohammadtaghi et al. 2001).

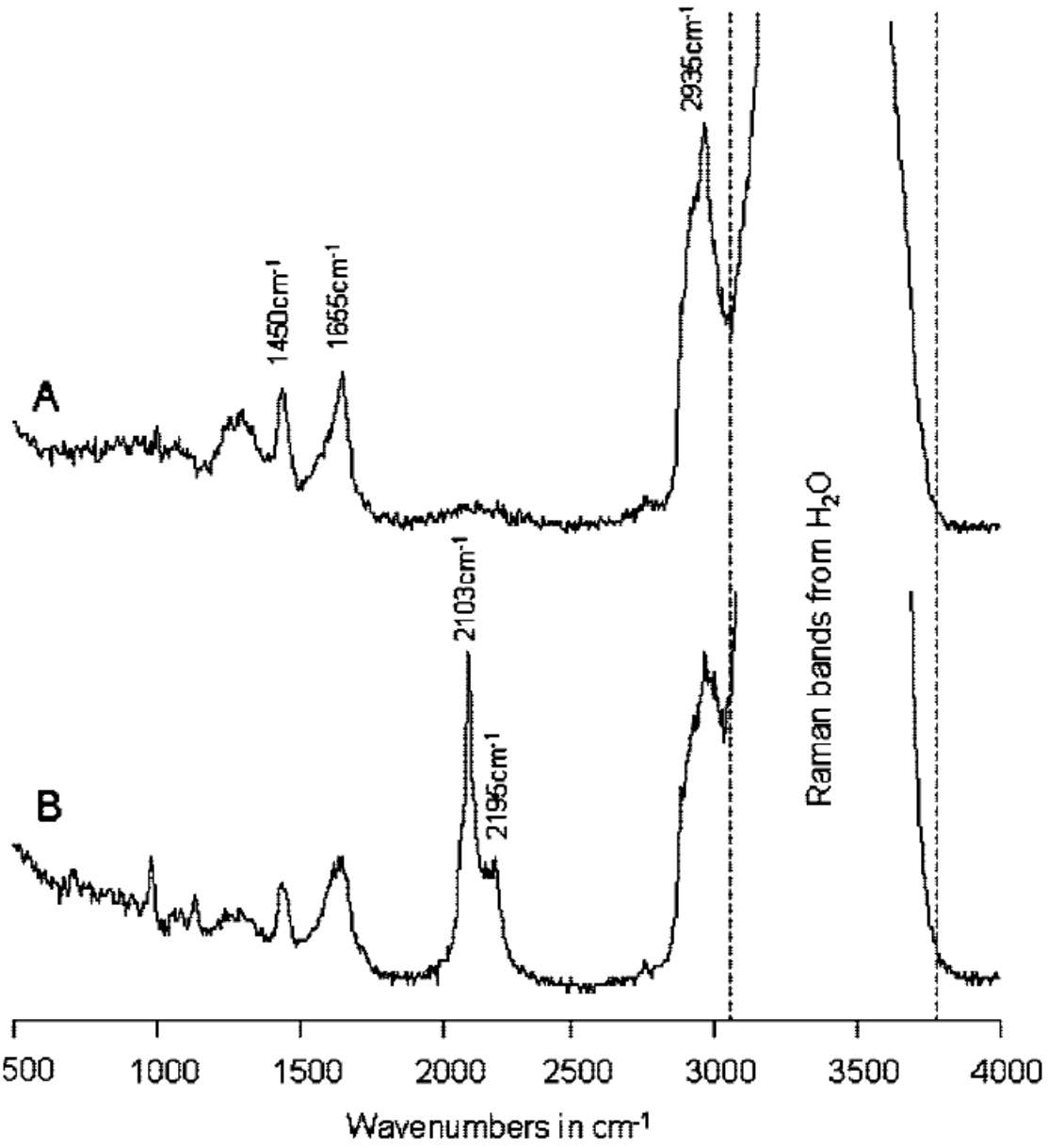

Figure 1.7 Raman Spectrum. Typical Raman spectrum from within the cytoplasm (A) with characteristic protein bands, and a spectrum from DSPC-*d*70 liposomes inside the cell with strong C-D stretching intensities (B) (Matthaus, Chernenko et al. 2007).

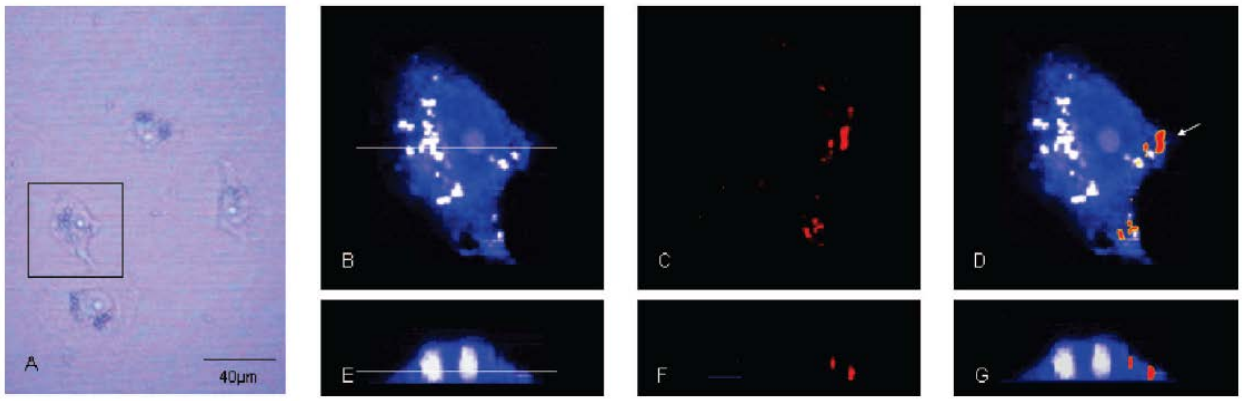

Figure 1.8 MCF-7 cells treated with d70-DSPC liposomes. Raman images of one cell reconstructed from the C-H (B) and C-D stretching intensities (C). The image (D) represents an overlay of panels (B) and (C). A depth profile was collected for the same cell (E-G). Scanning positions are indicated by the white bar (Matthaus, Chernenko et al. 2007).

Chapter 2. Extraction and Quantification of Individual Glycerophospholipids Using Bligh-Dyer Method with ESI-MS: Effective Quantitative Extraction by an Acidified Protocol

2.1 Introduction

Robust methods of extracting glycerophospholipids sufficiently from media and quantifying them accurately are critical for many studies. Glycerophospholipids are basic constituents of plasma and organelle membranes and have roles in signal transduction (Chaurio, Janko et al. 2009). Changes in individual glycerophospholipids in membranes can modulate biological functions, such as increased expression of phosphatidic acid (PAs) in platelet activation (Broekman, Ward et al. 1980) or externalization of phosphatidylserines (PSs) in apoptosis (Fadok, Voelker et al. 1992). More importantly, changes in individual glycerophospholipids and lipid profiles in cell membranes may indicate the occurrence of specific diseases like prostate cancer (Zhou, Mao et al. 2012). In most studies mentioned above, specific glycerophospholipids need to be extracted and quantified, which requires a sensitive and reproducible method for targeted glycerophosopholipids.

The combination of the Bligh-Dyer (BD) extraction method and electrospray ionization-mass spectrometry (ESI-MS) techniques is one of the most popular strategies to study glycerophospholipids. The BD extraction method (Bligh and Dyer 1959), in which chloroform and methanol mixtures are used for extracting total lipids from biological samples, is reported to extract more than 95% of the total lipids from biological samples (Iverson, Lang et al. 2001). Electrospray ionization-mass spectrometry (ESI-MS) has significantly advanced the study of

lipids in biological samples. Compared to traditional lipid detection techniques, ESI-MS has increased sensitivity, specificity, and speed of analysis (Peterson and Cummings 2006, Pati, Nie et al. 2016). A combination of BD extraction protocols with ESI-MS is used widely for phospholipid profiling (lipidomics) (Kim, Wang et al. 1994, Zhang, Peterson et al. 2005, Peterson and Cummings 2006, Pati, Nie et al. 2016), determination of lipid degradation (Zhu, Mock et al. 2011) and tracking specific lipid probes in biological samples (Zhu, Alhamhoom et al. 2011).

Even though the BD extraction methods have been employed for more than five decades, its ability to recover individual glycerophospholipids and their metabolites such as fatty acids (FAs) and lysophoslipids (LPs) from aqueous media has rarely been investigated. Traditionally, many studies using the BD method were focused not on the extraction efficiency of a single lipid, but rather of the total lipid mixture (Smedes and Thomasen 1996, Iverson, Lang et al. 2001, Manirakiza, Covaci et al. 2001, Singh, Sinha et al. 2014). Further, the BD extraction method was developed at the time when techniques like gravimetric methods, thin-layer chromatography and phosphorus analysis made it difficult to accurately track individual lipids. Thus, as mentioned above, only a few studies have addressed the extraction efficiency of the BD method for individual phosphatidic acids (PAs) or certain lysophoslipids(LPs) (Daae and Bremer 1970, Bjerve, Daae et al. 1974, Gerrard and Robinson 1989). No studies assessing the extraction efficiencies of the BD extraction method on a wide spectrum of individual phospholipids with different functional “head” groups were found. Thus, a further investigation using high sensitivity and high specificity ESI-MS was needed.

Recently, we used BD extraction methods in combination with ESI-MS to study the degradation of glycerophospholipids by different secretory phospholipase A_2 ($sPLA_2$) isoforms,

and used this knowledge to study the degradation of lipid-based nanoparticles (liposome) (Zhu, Mock et al. 2011). This approach allowed for the rapid and accurate analysis of multiple formulations composed of diverse phospholipids. However, a drawback was found that for some anionic lipids, such as DSPA and DSPS, the loss of the parent-ion was not proportional to formation of the metabolite-ion. Further, the extent of degradation of zwitterionic lipids like DSPC in the presence of $sPLA_2$ could be monitored by the loss of the parent-ion or the formation of the metabolite-ions. This suggests that conventional BD extraction methods were not sufficient to examine all glycerophospholipids.

The data presented in this chapter demonstrated that the extraction yields of the BD method fell short for two anionic lipids, DSPA and DSPS. A simple and quick acidification procedure increased the efficiencies of the BD extraction method for these lipids and increased the ionization of all glycerophospholipids (except DSPE) using ESI-MS. Furthermore, this modified BD extraction method, in combination with ESI-MS, can be used for accurate measurement of different lipid components in liposome formulation.

2.2 Materials and Methods

2.2.1 Chemical and Reagents

Phospholipids, DPPC (1,2-dipalmitoyl-*sn*-glycero-3-phosphatidylcholine), DPPA (1,2-dipalmitoyl-*sn*-glycero-3-phosphatidic acid), DPPS (1,2-dipalmitoyl-*sn*-glycero-3-phosphatidylserine), DPPG (1,2-dipalmitoyl-*sn*-glycero-3-phosphatidylglycerol), DSPC (1,2-distearoyl-*sn*-glycero-3-phosphatidylcholine), DSPG (1,2-distearoyl-*sn*-glycero-3-phosphatidylglycerol), DSPS (1,2-distearoyl-*sn*-glycero-3-phosphatidylserine), DSPE (1,2-distearoyl-*sn*-glycero-3-phosphatidylethanolamine), and DSPA (1,2-distearoyl-*sn*-glycero-3-

phosphatidic acid), were purchased from Avanti Polar Lipids, Inc. (Alabaster, AL). C31PC (1-*O*-hexadecyl-2-pentadenoyl-*sn*-glycero-3- phosphatidylcholine) was synthetized in the Department of Pharmaceutical and Biomedical Sciences at the University of Georgia (Zhu, Alhamhoom et al. 2011). Group III $sPLA_2$ was purchased from Cayman Chemical Company (Ann Arbor, MI) and Genway Biotech Inc (San Diego, CA). Acetonitrile and methanol of HPLC grade were from Fisher Scientific (Pittsburgh, PA). All other chemicals and solvents were of analytical grade, obtained from commercial sources and used without further purification. All experiments used ultrapure water (> 18.3 MΩ) obtained from a Millipore Milli-Q synthesis system (Billerica, MA).

2.2.2 Conventional Bligh-Dyer Extraction of Phospholipids and Their Metabolites after $sPLA_2$-mediated Degradation Studies

Phospholipid degradation was induced by combining each lipid sample (1 µmol/mL) with Group III $sPLA_2$ (2.5 µg/mL) (Zhu, Mock et al. 2011), $CaCl_2$ (1 mM) in TRIS buffer (total volume: 200 µL) , followed by incubation at 37°C for 24 hrs. Phospholipids and their metabolites were extracted using the BD method for ESI-MS analysis (Bligh and Dyer 1959). Briefly, following incubation, 400 µL solution of chloroform and methanol (3:1 v/v) were added and mixed using a vortex, followed by centrifugation at 2500 × g for 5 min. The organic layer was taken out and separated into a new glass tube and extractions were repeated two more times on the remaining samples. The pooled organic solvent was evaporated completely using a steady stream of nitrogen gas. Residues were reconstituted in 1 mL of chloroform and methanol (3:1 v/v). A 100 µL aliquot of the resultant organic solution was diluted in 900 µL chloroform and methanol (3:1 v/v) for further ESI-MS analysis immediately.

2.2.3 Modified Acidification Bligh-Dyer Extraction Procedures for DSPA and DSPS after $sPLA_2$-mediated Degradation

Additional acidification procedures were developed for DSPA and DSPS using Bligh-Dyer extractions protocols. For DSPA, 5 µL of hydrochloric acid (0.3 N HCl) was added to the $sPLA_2$ buffer after enzymatic incubation. For DSPS, 5 µL of 0.3 N HCl was added to the $sPLA_2$ buffer after enzymatic incubation, and another 5 µL of 0.3 N HCl was spiked into DSPS reconstituted organic solutions, followed by mixing vigorously for 1 minute using a vortex.

2.2.4 Comparison of Extraction Efficiencies of Lipids from $sPLA_2$ Buffer Using the Conventional Bligh-Dyer and Acidified Bligh-Dyer Extraction Protocols

Six different glycerophospholipids, (DPPC 8.33 µg/mL, DSPC 5.60 µg/mL, DSPE 6.05 µg/mL, DSPA 5.74 µg/mL, DSPS 6.98 µg/mL, and DSPG 5.33 µg/mL) were mixed together in chloroform to make a stock lipids standard solution. Meanwhile, C31PC 1.75 µg/mL (for DPPC, DSPC and DSPE), DPPA 17.0 µg/mL (for DSPA), DPPS 19.8 µg/mL (for DSPS), and DPPG 12.2 µg/mL (for DSPG) were mixed as a stock internal standard solution.

Calibration curves for individual lipids were prepared by diluting lipids in organic solvents (chloroform and methanol; 3:1 v/v), in a total volume of 400 µL, and spiked with 10 µL internal standard (The concentrations of individual calibration curves and internal standards are in Supplementary Table 1.). The organic solvent was evaporated completely using a steady stream of nitrogen gas, and reconstituted with 400 µL chloroform and methanol (3:1 v/v). The reconstituted standard samples were separated into two aliquots at 200 µL each, and 2.5 µL 0.3 N HCl was spiked into one of the aliquots, which was labeled as Standard-A. Two standard curves for each lipid were constructed; acidified and non-acidified. Standard curves were constructed by

calculating the ratio of the analyte peak area to that of the internal standard, and plotting the ratio *versus* the theoretical concentration; data were fit using a weighting factor of 1/x. The standard curve was considered acceptable if greater than 90% of the standards had calculated accuracies within 15% of their theoretical value and precision had a coefficient of variation (CV) of $\leq$ 20%. The limit of quantification was determined experimentally as the minimum concentration whose response was greater than ten times the baseline value, with a CV $\leq$ 20% and accuracy ± 20%.

Control samples were prepared by spiking 10 µL of lipid and 10 µL of internal standard (IS) into a 400 µL solution of chloroform and methanol (3:1 v/v). Organic solvent was evaporated completely using a steady stream of nitrogen gas. Residues were reconstituted with 400 µL chloroform and methanol (3:1 v/v). The reconstituted control samples were separated into two aliquots at 200 µL each, and 2.5 µL 0.3N HCl was spiked into one aliquot, which was labeled as Control-A.

Conventional BD extraction samples were prepared by spiking 10 µL of lipid into 200 µL TRIS buffer (0.05 M TRIS, 2.5 µg/mL $sPLA_2$, 1 mM Ca^{2+}), which was extracted with 400 µl of chloroform and methanol (3:1 v/v). The extraction was repeated two more times. The organic layer was taken out and combined, and evaporated completely under nitrogen gas. Residues were reconstituted with 400 µL chloroform and methanol (3:1 v/v), and 10 µL of IS was added. The reconstituted BD samples were separated into two aliquots, one of which was acidified as described above, and labeled as BD-A.

The acidified BD extraction sample preparations were performed as described for the conventional BD extraction samples, except 5 µL of 0.3 N HCl was spiked into TRIS buffer before extraction. The acidified aliquot was labeled as Acidic BD-A.

The concentrations of control BD and Acidic BD samples were calculated using their

representative calibration curves. The recovery (extraction efficiency) was calculated using:

$$Recovery = (Conc._{sample}/Conc._{control}) \times 100\%.$$

2.2.5 Measurement of Lipid Composition in Liposomal Formulations Using Conventional and Acidified Bligh-Dyer Extractions

Calibration curves were prepared as described in 2.2.4 and were spiked with 10 µL of IS. Extraction was simulated by adding 200 µL of TRIS buffer. For the acidified BD extraction method, 5 µL of 0.3 N HCl was added to the TRIS buffer prior to extraction, and another 5 µL of 0.3 N HCl was spiked into the 400 µL reconstituted organic solutions. No acid was added to the formulations extracted using the convention BD extraction method.

Two liposome formulations were used. Formulation 1 consisted of DSPC, DSPE, DSPS in an 8:1:1 mole ratio; Formulation 2 consisted of DPPC, DSPG, DSPA in the same ratio. The liposomes were prepared by hydration of thin films followed by a freeze-thaw and a high-pressure extrusion process as described previously (Iverson, Lang et al. 2001). Liposome formulations were diluted to proper concentration (2 nmol/mL). An aliquot of 200 µL was taken and spiked with 10 µL of IS. Each formulation went through both acidified BD and conventional BD extraction methods as described for calibrations in this section.

2.2.6 Stability of Lipids after Acidification

Lipid samples were extracted using either the conventional or acidified BD extraction method. Extracts were then incubated at 20 or 4 ºC for 0, 1, 2, 3 or 20 hr prior to analysis by ESI-MS. Samples were triplicated.

2.2.7 Measurement of Lipids and Their Metabolites by ESI-MS

sPLA$_2$-mediated degradation analysis was performed on an Agilent 1100 HPLC-mass spectrometer (LC/MSD-Trap XCT Ultra Plus) system (Santa Clara, CA). The mobile phase consisted of acetonitrile, methanol and 0.1% ammonium formate (2:3:1 v/v/v). The flow rate was 0.15 mL/min and the injection volume was 5 µL. Nitrogen was used as a nebulizing gas at 25 psi and a drying gas at 8 psi. The drying temperature was 350°C. The capillary, capillary exit and skimmer potentials were 3500, 150.3 and 40.0 V, respectively. The *m/z* range for scanning was 200 to 2,200. The positive-ion mode was used to measure the intensity of the DPPC, DSPC, DSPE, DSPS and the corresponded LPs, whereas the negative-ion mode was used to measure the intensity of DSPA, DSPG and their LPs, and fatty acids. Signal intensity of phospholipids and their FA and LP metabolites were compared between the BD method and the ones with acidification procedures.

An Agilent 1290 UHPLC-6460 Triple Quad mass spectrometer system (Santa Clara, CA) was used to assess the extraction efficiency and determine the acidic stability of liposome formulations. The mobile phase consisted of 10% of A (10 mM ammonium formate) and 90% of B (ACN:MeOH, 2:3, v/v). The sample was introduced into the MS at a flow rate of 0.5 mL/min, and the injection volume was 1µL. Nitrogen gas was used as the drying gas (10 L/min at 300 ºC), as a nubulizer gas (45 psi), and as a collision gas. Capillary voltage was set at 4000 V for positive and 3500 V for negative. Mass spectra were acquired in the positive-ion mode for DPPC, DSPC, DSPE and DSPS; in the negative-ion mode for DSPA and DSPG. Mass transitions were monitored using multiple-reaction monitoring (MRM). The transitions, fragmentor voltage and collision energy are presented in Table 2.1.

2.2.8 Statistics

Data are presented as the mean ± the standard error of the mean (SEM) of at least 3 separate experiments (n=3/study). Differences were determined following an analysis of variance for each data set using SAS software (SAS Institute, Cary, NC) followed by a Dunnett's t-test or a Student's t-test when comparisons involved a control and single variable. Differences were considered significant if the *p*-value ≤ 0.05.

2.3 Results

2.3.1 Measurement of $sPLA_2$-mediated Phospholipid Degradation Using Conventional Bligh-Dyer Extraction Protocols and ESI-MS

$sPLA_2$ are esterases that rapidly degrade phospholipids at *sn-2* position, producing lysophospholipids and fatty acids. To investigate if the Bligh-Dyer extraction, combined with ESI-MS, can be used to track the extent of phospholipid degradation of individual phospholipids, we exposed DPPC, DSPC, DSPE, DSPA, DSPS and DSPG to Group III $sPLA_2$ (2.5 μg/mL) in TRIS buffer for 24 hr. The individual phospholipids and their metabolites were extracted by the conventional BD extraction method and their intensity measured using ESI-MS (Table 2.2). A decrease in intensity of phospholipid-ions was observed in DPPC compared to control (incubated without $sPLA_2$), while the intensity of its metabolite ions, LP and FA, increased. Similar results were observed for DSPC, DSPE and DSPG (Table 2.2). Additionally, the fold-increase in the intensity of the metabolite ions was much larger than the fold-decrease in the intensity of the phospholipid ion, which suggests that metabolite formation might be a more sensitive indicator for phospholipid degradation using ESI-MS. However, similar results were not observed for DSPA and DSPS. For DSPA, the intensity of phospholipid-ions decreased about 75%, but

significant changes were not found in the intensity of its metabolites. For DSPS, the intensities of LP and FA ions increased about 10- to 20- fold, but a corresponding decrease in the intensity of the parent-phospholipid ions was not observed.

2.3.2 Measurement of sPLA$_2$-mediated DSPA and DSPS Degradation Using Acidified Bligh-Dyer Extraction Method and ESI-MS

DSPA and DSPS are anionic lipids and exist in nature in salt forms (AOCS Lipid Library 2013). Based on this fact, we assume that the conventional (neutral) BD extraction method was not sufficient to extract these ion-formed lipids into the organic phase. We therefore hypothesized that an acidification procedure for DSPA and DSPS would enhance the extraction of these phospholipids. To test this hypothesis we added hydrochloric acid into an aqueous solution prior to extraction to increase the formation of the non-ionized lipids and increase the efficiency of extraction. The extraction efficiency of DSPA was increased after the acidification of the extraction (79.4% to 94%, Table 2.3 A). This increase was accompanied by an increase in intensity of DSPA and its metabolites (Figure 2.1 A). A similar pattern of phospholipid degradation to DPPC was observed in DSPA (Figure 2.1 A).

The effect of acidification on the extraction and MS of DSPS was quite different from that of DSPA. Acidification had no effect on the extraction efficiency of DSPS in an aqueous buffer (78.6% to 76.5%, Table 2.3 A). Yet there was a significant improvement after acidified extraction followed by acidification in reconstituted solution (89.5%, Table 2.3 B). A signal intensity increases in DSPS and its metabolites were observed as well as a DPPC-like lipid degradation pattern (Figure 2.1 B).

2.3.3 Effect of Acidification on the Extraction Efficiencies of Glycerophospholipids

We systematically examined the effect of acidified BD to further understand how acidification impacts the extraction efficiencies of phospholipids. In brief, we extracted each phospholipid using conventional BD extraction techniques, or using modified approaches including a one-step acidification (acidification in aqueous solution prior to extraction, or acidification in reconstituted solution after extraction), or two-step acidification (acidification in both prior to and after extraction, Table 2.3). These approaches did not alter the extraction efficiencies of DPPC, DSPC and DSPE. Notably, slight decreases in DPPC and DSPC were detected after all of the acidification techniques, as compared to the conventional BD extraction approach. The extraction efficiency of DSPE was increased from 93.3% to 100% after the two-step acidification. The extraction efficiency of DSPA was increased after acidification in aqueous buffer prior to extraction (from 79.4% to 94.0%), but the acidification in reconstituted solution after extraction did not improve the extraction efficiency of DSPA (77.6%). Only a slight improvement in the extraction efficiency was observed for DSPA after the two-step acidification treatment (81.7%), probably due to the hydrolysis of DSPA in low pH. However, this was greater than the extraction efficiency for DSPS after using conventional BD extraction techniques, as well as the single acidification approaches (78.6%, 76.5% and 63.4%, respectively). The extraction efficiency of DSPS was improved only when a two-step acidification approach was applied (89.5%). Similar to DSPA, DSPG's extraction efficiency was slightly improved by the acidification of the aqueous buffer prior to extraction. Further, the second step of acidification did not alter the extraction efficiency of DSPG.

Quantitative level of glycerophospholipids using ESI-MS demonstrated no difference between the conventional BD extraction and the two-step acidified BD extraction method for

DPPC, DSPC, DSPE, and DSPG (data not show). In contrast, acidification improved the quantification capacity of DSPA and DSPS significantly in terms of linearity, sensitivity and accuracy. The linearity of DSPA expanded from 71.82 – 1149.04 ng/mL to 8.98 – 1149.04 ng/mL, where the sensitivity increased almost 10-fold (LOQ from 71.82 ng/mL to 8.98 ng/mL, Figure 2.2 A and B). Similar results were seen with DSPS, whose linearity improved from 87.31 – 1397 ng/mL to 21.83 – 1397 ng/mL, while the sensitivity increased 4-fold (LOQ from 87.31 ng/mL to 21.83 ng/mL, Figure 2.2 C and D). The accuracy of DSPA increased from 67.81% to 95.80% at the concentration of 35.91 ng/mL (Figure 2.3 A and B), whereas the accuracy of DSPS improved from 135.69% to 103.07% at 43.66 ng/mL (Figure 2.3 C and D).

2.3.4 Measurement of Lipid Composition in Liposomal Formulations after Extraction Using Conventional and Acidified Bligh-Dye Methods

Two formulations were engineered for the measurement of lipid composition in more complex systems. Formulation 1 consisted of DSPC, DSPE and DSPS in the mole ratio of 8:1:1. Formulation 2 consisted of DPPC, DSPG and DSPA in the same ratio. The results (Table 2.4) showed that the observed mole ratio of three phospholipids in formulations have some differences from the theoretical ratio regardless of using conventional or acidified extraction. This difference could result from the manufacturing of the liposome formulations. Furthermore, the measurement of DSPA in the formulation using conventional BD extraction was lower than its LOQ; the measurement of DSPS was close to LOQ. In this case, a wide linear range and high sensitivity were required to simultaneously quantify these three phospholipid formulations, which might not be possible using the conventional BD extraction methods, because DSPA and DSPS have a narrow linear range and low sensitivity. With the acidified BD extraction, signal

intensities of all phospholipids tested, except DSPE, were increased compared to conventional BD extraction methods (Figure 1.2, Chapter 1), which provides a wide linear range and high sensitivity for DSPA and DSPS. It becomes possible to quantify all three phospholipids in the formulation simultaneously (Table 2.4 B), even to quantify liposome formulations with lower concentration.

2.3.5 Effect of Acidification on the Stability of Each Phospholipid after Bligh-Dyer Extraction

Phospholipids are acid sensitive (Nishihara and Koga 1987). Hydrolysis can occur at low pH conditions. To determine the effect of acidification on the stability of each phospholipid, six different phospholipids were mixed and spiked into TRIS buffer, extracted by conventional and two-step acidified BD extraction method, and allowed to incubate for 0, 1, 2, 3 and 20 hours at 4 and 20 ºC prior to analysis by ESI-MS. Temperatures were controlled by the UHPLC auto-sampler. At 20ºC, all the lipids analyzed, with the exception of DSPS, had differential grades of hydrolysis. Hydrolysis was first observed after 1 hr (data not show) for DPPC, DSPC, DSPA and DSPG, a significant decrease was observed at 3 hr (Figure 1.3 A, Chapter 1) and a 20 - 40% decrease was observed in signal intensity after 20 hr (data not show). As expected, the storage of samples at lower temperatures (4ºC) decreased hydrolysis, but there was still a significant decrease in signals for PC-containing lipids at 3 hr (Figure 1.3 B, Chapter 1).

2.4 Discussion

This study represents a systematic analysis of the extraction efficiency and accuracy of both conventional and acidified Bligh-Dyer extraction methods combined with ESI-MS to

identify and quantify individual glycerophospholipids and their degradation metabolites. Despite the fact that the BD extraction has been in use for over 50 years, surprisingly, little information on this subject could be found in the literature. Originally, the BD method was thought to be able to extract individual glycerophospholipids with high extraction efficiencies. Yet, others have reported decreased effectiveness against certain lipid species. For example, Iverson et al., reported that BD extraction methods were ineffective for extracting samples with high lipid content (>2%) (Iverson, Lang et al. 2001). Bjerve et al., also reported that that the BD method resulted in less than optimal recoveries of select LPs (Lysophospholipids) from aqueous media (Bjerve, Daae et al. 1974). No data could be found investigating the efficiency of the BD method on common glycerophospholipid classes and their metabolites.

Our data clearly showed that conventional BD methods (i.e. neutral extractions) works excellently for zwitterionic lipids PC and PE, and anionic lipid PG in showing $sPLA_2$ - mediated phospholipid degradation. However, it performed poorly for anionic lipids PA and PS. Acidification can overcome the drawback of conventional BD extraction methods and increase the signal intensity of the parent-lipid and metabolite ions. This increase in intensity could be contributed to both improvement in extraction efficiency and acid ionization enhancement. In further examination of the extraction efficiencies of conventional BD extraction and acidified protocols, our studies demonstrate that poor extraction efficiencies were found for anionic lipids PA, PS, and PG (79.4%, 78.6%, and 83.8%), and they were improved by the acidification of media (acidification in aqueous buffer prior to extraction, in addition to acidification of the reconstituted solution after extraction). One explanation that may account for the low extraction efficiencies of anionic lipids under neutral conditions are that the head groups of anionic lipids are weak acids with a lower pKa (Buckland and Wilton 2000). Ionized products of these lipids

are formed in neutral or basic conditions, which likely give these lipids poor lipophilicity, which decreases their extraction efficiency. This hypothesis is supported by the fact that acidification in aqueous buffers prior to extraction increased the extraction efficiencies of DSPA and DSPG (94.0% and 91.6%). DSPS, however, with serine as a part of the head group, gives some unique properties to the lipid. For instance, more hydrophilicity and more positive properties (positive-ion mode on MS even though DSPS has been classified in the category of anionic lipids). Additionally, in the presence of Ca^{2+} (TRIS buffer contains Ca^{2+}), DSPS has a high propensity to chelate to Ca^{2+} via the charged oxygen atoms of both the carboxyl and phosphate moieties (Figure 2.4) (AOCS Lipid Library 2013). This reaction could explain part of the signal intensity loss. Besides, the head group provides three ionizable sites, the phosphate moiety, the amino group and the carboxyl function (AOCS Lipid Library 2013). A MS scan spectrum shows that DSPS has single $[M+Na]^+$, double $[M+2Na-H]^+$ and triple $[M+3Na-2H]^+$ sodium adducts (Figure 2.5), which can reduce the signal intensity significantly of the base peak $(M+H)^+$. With these unique properties, acidification in aqueous buffers alone (76.5%) was not enough. An additional acidification step was applied when these samples were reconstituted after extraction; an extraction efficiency of 89.5% was achieved. This suggests that both steps of acidification were crucial for optimal extraction of DSPS.

Acidification increased the linear range of DSPA (8.98 – 1149.04 ng/mL) and DSPS (21.83 – 1397 ng/mL), which improved the quantification capacity (Table 2.4 B). The observed mole ratio showed some difference from the theoretical ratio regardless of conventional or acidified BD method (Table 2.4). The source of this difference could be the measurement error of each single phospholipid during liposome preparation, or the loss during membrane extrusion, or the adsorption to glassware. This measurement indicates that our formulation composition ratio

may not be exactly what we presumed, and suggest the composition of our formulation needs to be confirmed by ESI-MS. Bligh-Dyer extraction, in combination with ESI-MS, provided a way to examine the actual ratio of phospholipids in our liposome formulations. Overall, acidified BD method is more practical in measurement due to its greater linear range of DSPA and DSPS and provided better accuracy.

The phospholipid stability test results may suggest that low temperature is required for acidified BD extraction to improve its performance, especially for a large size of samples which require a longer time to analyze. Meanwhile, internal standards are crucial for an accurate quantification to prevent the errors from hydrolysis. Ideally, stable isotope internal standards are the desired choice. But, they are expensive, and most of the time they are not commercially available. The data showed that PC-containing lipids have similar stability (Figure 1.3, Chapter 1) and identical ionization enhancement (Figure 1.2, Chapter 1) in acid. This suggests that same lipid head groups could be used as an internal standard for each other. However, to have an acceptable internal standard, the difference in the length of hydrocarbon chains should not be too large in order to have similar chromatography behavior.

Acidification did not negatively impact the quantitation or extraction of the zwitterionic lipids PC and PE. In contrast, a significant improvement in the extraction efficiency was observed for DSPA and DSPS. Additionally, an increased sensitivity and enhanced accuracy was observed. This increased performance permitted the accurate measurement of the lipid composition of a liposome formulation using a single extraction protocol.

The Bligh-Dyer extraction has been used for decades. Similar extraction methods, such as the Folch procedure (Folch, Lees et al. 1957), have been commonly used, too. Many modifications of these lipid or fatty acid extraction methods, including acidification, have been

developed for specific research purposes. However, most of these modifications involved in acidification were designed for total lipid extraction or lipidomic profile research. For instance, when the water in the Bligh-Dyer solvent was replaced by 5% trichloroacetic acid, the total lipid extraction efficiency reached the maximum level from *Methanobacterium thermoautotrophicum* (Nishihara and Koga 1987). Ana Reis, et al. compared five extraction methods, including acidified Bligh-Dyer extraction, for the lipidomic study for human LDL (Reis, Rudnitskaya et al. 2013). Our data demonstrated that acidification of the Bligh-Dyer solvent is suited to quantitative extraction of individual glycerophospholipids. With this method, in combination with ESI-MS, we were able to monitor the concentration changes of single or multiple phospholipids of interest at *in vitro* or *in vivo* levels, and trace the liposome distribution in cells by quantifying probe lipids in subcellular organelles, and estimate the drug release via calculation of the extent of degradation of the lipids via quantification of both parent-lipids and their metabolites.

2.5 Conclusion

In conclusion, this study suggests that acidification in aqueous media prior to extraction, and/or acidification in reconstituted solution after extraction, can overcome some drawbacks of conventional BD extraction for analysis of some anionic lipids in biological samples. Such data are pertinent to modern pharmaceutical analysis as an increased emphasis is being placed on the identification of formulation specific excipients, such as phospholipids. Further, the increased use of lipid-based nanoparticles for drug delivery will necessitate the need for lipid-based MS methods to quantify these drug delivery devices. While the Bligh-Dyer extraction method has worked for almost half a century, data provided here further demonstrates their utility and provides for further technological uses for this method.

2.6 References

AOCS Lipid Library. (2013). "Phosphatidylserine and related lipids: structure, occurrence, biochemistry and analysis." from lipidlibrary.aocs.org.

Bjerve, K. S., L. N. Daae and J. Bremer (1974). "The selective loss of lysophospholipids in some commonly used lipid-extraction procedures." Anal Biochem **58**(1): 238-245.

Bligh, E. G. and W. J. Dyer (1959). "A rapid method of total lipid extraction and purification." Can J Biochem Physiol **37**(8): 911-917.

Broekman, M. J., J. W. Ward and A. J. Marcus (1980). "Phospholipid metabolism in stimulated human platelets. Changes in phosphatidylinositol, phosphatidic acid, and lysophospholipids." J Clin Invest **66**(2): 275-283.

Buckland, A. G. and D. C. Wilton (2000). "Anionic phospholipids, interfacial binding and the regulation of cell functions." Biochim Biophys Acta **1483**(2): 199-216.

Chaurio, R. A., C. Janko, L. E. Munoz, B. Frey, M. Herrmann and U. S. Gaipl (2009). "Phospholipids: key players in apoptosis and immune regulation." Molecules **14**(12): 4892-4914.

Daae, L. N. and J. Bremer (1970). "The acylation of glycerophosphate in rat liver. A new assay procedure for glycerophosphate acylation, studies on its subcellular and submitochondrial localization and determination of the reaction products." Biochim Biophys Acta **210**(1): 92-104.

Fadok, V. A., D. R. Voelker, P. A. Campbell, J. J. Cohen, D. L. Bratton and P. M. Henson (1992). "Exposure of phosphatidylserine on the surface of apoptotic lymphocytes triggers specific recognition and removal by macrophages." J Immunol **148**(7): 2207-2216.

Folch, J., M. Lees and G. H. Sloane Stanley (1957). "A simple method for the isolation and purification of total lipides from animal tissues." J Biol Chem **226**(1): 497-509.

Gerrard, J. M. and P. Robinson (1989). "Identification of the molecular species of lysophosphatidic acid produced when platelets are stimulated by thrombin." Biochim Biophys Acta **1001**(3): 282-285.

Iverson, S. J., S. L. Lang and M. H. Cooper (2001). "Comparison of the Bligh and Dyer and Folch methods for total lipid determination in a broad range of marine tissue." Lipids **36**(11): 1283-1287.

Kim, H. Y., T. C. Wang and Y. C. Ma (1994). "Liquid chromatography/mass spectrometry of phospholipids using electrospray ionization." Anal Chem **66**(22): 3977-3982.

Manirakiza, P., A. Covaci and P. Schepens (2001). "Comparative Study on Total Lipid Determination using Soxhlet, Roese-Gottlieb, Bligh & Dyer, and Modified Bligh & Dyer Extraction Methods." J Food Comp Anal **14**(1): 93-100.

Nishihara, M. and Y. Koga (1987). "Extraction and composition of polar lipids from the archaebacterium, Methanobacterium thermoautotrophicum: effective extraction of tetraether lipids by an acidified solvent." J Biochem **101**(4): 997-1005.

Pati, S., B. Nie, R. D. Arnold and B. S. Cummings (2016). "Extraction, chromatographic and mass spectrometric methods for lipid analysis." Biomed Chromatogr **30**(5): 695-709.

Peterson, B. L. and B. S. Cummings (2006). "A review of chromatographic methods for the assessment of phospholipids in biological samples." Biomed Chromatogr **20**(3): 227-243.

Reis, A., A. Rudnitskaya, G. J. Blackburn, N. Mohd Fauzi, A. R. Pitt and C. M. Spickett (2013). "A comparison of five lipid extraction solvent systems for lipidomic studies of human LDL." J Lipid Res **54**(7): 1812-1824.

Singh, P., R. Sinha, R. Tandon, G. Tyagi, P. Khatri, L. Chandra Shekhar Reddy, N. K. Saini, R. Pathak, M. Varma-Basil, A. K. Prasad and M. Bose (2014). "Revisiting a protocol for extraction of mycobacterial lipids." Int J Mycobacteriol **3**(3): 168-172.

Smedes, F. and T. K. Thomasen (1996). "Evaluation of the Bligh & Dyer lipid determination method." Marine Poll Bull **32**(8): 681-688.

Zhang, L., B. L. Peterson and B. S. Cummings (2005). "The effect of inhibition of Ca2+-independent phospholipase A2 on chemotherapeutic-induced death and phospholipid profiles in renal cells." Biochem Pharmacol **70**(11): 1697-1706.

Zhou, X., J. Mao, J. Ai, Y. Deng, M. R. Roth, C. Pound, J. Henegar, R. Welti and S. A. Bigler (2012). "Identification of plasma lipid biomarkers for prostate cancer by lipidomics and bioinformatics." PLoS One **7**(11): e48889.

Zhu, G., Y. Alhamhoom, B. S. Cummings and R. D. Arnold (2011). "Synthesis of lipids for development of multifunctional lipid-based drug-carriers." Bioorg Med Chem Lett **21**(21): 6370-6375.

Zhu, G., J. N. Mock, I. Aljuffali, B. S. Cummings and R. D. Arnold (2011). "Secretory phospholipase A(2) responsive liposomes." J Pharm Sci **100**(8): 3146-3159.

Table 2.1 MRM Conditions and Calibration Concentrations for Each Glycerophospholipid

Lipids	MS transition	Conc. of Calibration Curve (ng/mL)	Fragmentor voltage	Collision Energy	Polarity
DPPC	734.6 – 184.1	0.81, 1.63, 3.26, 6.51, 13.02, 26.04, 52.09 104.18, 208.35, 416.7, 833.4, 1666.8	167	28	Positive
DSPC	790.6 – 184.1	0.55, 1.09, 2.19, 4.38, 8.76, 17.51, 35.02, 70.05, 140.1, 280.19, 560.38, 1120.76	153	31	Positive
DSPE	748.5 – 607.6	0.59, 1.18, 2.36, 4.73, 9.45, 18.91, 37.81, 75.63, 151.25, 302.5, 605, 1210	174	17	Positive
C31PC (IS)	706.6 – 184.1	43.75	119	29	Positive
DSPA	703.5 – 283.5	0.56, 1.12, 2.24, 4.49, 8.98, 17.95, 35.91, 71.82, 143.63, 287.26, 574.52, 1149.04	173	38	Negative
DPPA (IS)	647.5 – 255.2	425	120	36	Negative
DSPS	792.5 – 607.6	0.68, 1.36, 2.73, 5.46, 10.91, 21.83, 43.66, 87.31, 174.63, 349.25, 698.5, 1397	145	17	Positive
DPPS (IS)	736.5 – 551.5	495	105	14	Positive
DSPG	777.5 – 283.3	0.52, 1.04, 2.08, 4.16, 8.33, 16.67, 33.33, 66.67, 133.35, 266.69, 533.38, 1066.67	181	41	Negative
DPPG (IS)	721.4 – 255.2	306.25	125	40	Negative

Table 2.2 Changes in the Signal Intensity of Parent-phospholipids and Their Metabolites after 24 hr Treatment with Group III sPLA$_2$ Followed by Conventional Bligh-Dyer Extraction (mean ± SEM, n=3)

Phospholipid	Charge	pKa	Parent-ion	LP ion	FA ion
DPPC	Zwitterionic	R-H_2PO_4 1.0	39.0 ± 0.7*	18300 ± 1040*	2670 ± 600*
DSPC	Zwitterionic	R-H_2PO_4 1.0	78.0 ± 2.7*	10500 ± 1700*	1680 ± 230*
DSPE	Zwitterionic	R-H_2PO_4 1.7 R-NH_3^+ 11.25	22.6 ± 0.6*	13400 ± 540*	2260 ± 56*
DSPG	Anionic	R-H_2PO_4 ~3.1	72.1 ± 2.2*	4210 ± 680*	3510 ± 320*
DSPA	Anionic	R-H_2PO_4 pKa1 3.0 R-H_2PO_4 pKa2 8.0	26.4 ± 11.7*	ND	114 ± 10
DSPS	Anionic	R-H_2PO_4 2.6 R-COOH 5.5 R-NH_3^+ 11.55	105.0 ± 7.0	2130 ± 510*	1330 ±260*

* Significant difference ($p < 0.05$) compared to control (incubations without sPLA$_2$)

ND: not detectable

Table 2.3 A: Comparison of Extraction Efficiencies between Conventional and One-step Acidified Bligh-Dyer Extractions (mean ± SEM, n=3)

Lipids	Control (ng/mL)	BD		Acidic BD	
		Conc. (ng/mL)	E.E. (%)	Conc. (ng/mL)	E.E. (%)
DPPC	153 ± 1.2	150 ± 0.5	98.0	141 ± 0.2	91.7
DSPC	106 ± 1.5	105 ± 0.9	98.7	100 ± 1.3	94.3
DSPE	65.2 ± 0.1	60.8 ± 0.6	93.3	62.2 ± 0.8	95.4
DSPA	97.1 ± 0.7	77.1 ± 1.6	79.4 †	91.3 ± 1.1	94.0
DSPS	128 ± 5.2	101 ± 1.3	78.6 †	98.4 ± 4.2	76.5 †
DSPG	98.2 ± 0.9	82.3 ± 1.3	83.8 †	89.9 ± 1.3	91.6

Table 2.3 B: Comparison of Extraction Efficiencies between Conventional and Two-step Acidified Bligh-Dyer Extractions (mean ± SEM, n=3)

Lipids	Control-A (ng/mL)	BD-A		Acidic BD-A	
		Conc. (ng/mL)	E.E. (%)	Conc. (ng/mL)	E.E. (%)
DPPC	164 ± 1.5	153 ± 2.2	93.4	151 ± 1.2	92.0
DSPC	111 ± 0.9	106 ± 1.4	95.2	102 ± 0.4	92.0
DSPE	60.5 ± 0.8	62.7 ± 0.7	104	60.5 ± 0.9	100
DSPA	108 ± 2.6	83.7 ± 1.2	77.6 †	88.1 ± 1.7	81.7 †
DSPS	129 ±1.8	82.1 ± 2.2	63.4 †	116 ± 0.7	89.5
DSPG	104 ± 1.1	87.7 ± 0.2	84.2 †	97.8 ± 0.4	93.9

E.E.: extraction efficiency

† E.E. < 85%

-A: followed by acidification in reconstituted solution

Table 2.4 A: Measurement of Lipid Composition in Liposome Formulation after Extraction Using Conventional Bligh-Dyer Extraction Methods (mean ± SEM, n=3)

	Conventional Bligh-Dyer Method					
	Formulation 1			Formulation 2		
	DSPC	DSPE	DSPS	DPPC	DSPG	DSPA
Molecular Weight	789.6	745.6	813.6	733.6	800.6	726.5
Mole Ratio (Theoretical)	8	1	1	8	1	1
Conc. (nmol/mL)	1.43 ± 0.021	0.15 ± 0.004	0.26 ± 0.008	1.52 ± 0.006	0.10 ± 0.002	BQL
Mole Ratio (Observe)	7.77	0.80	1.43	8.28	0.57	BQL

BQL: below quantification limit

Table 2.4 B: Measurement of Lipid Composition in Liposome Formulation after Extraction Using Acidified Bligh-Dyer Extraction Methods (mean ± SEM, n=3)

	Acidified Bligh-Dyer Method					
	Formulation 1			Formulation 2		
	DSPC	DSPE	DSPS	DPPC	DSPG	DSPA
Molecular Weight	789.6	745.6	813.6	733.6	800.6	726.5
Mole Ratio (Theoretical)	8	1	1	8	1	1
Conc. (nmol/mL)	1.52 ± 0.018	0.26 ± 0.003	0.27 ± 0.016	1.41 ± 0.008	0.12 ± 0.001	0.2 ± 0.002
Mole Ratio (Observe)	7.42	1.26	1.33	8.17	0.69	1.14

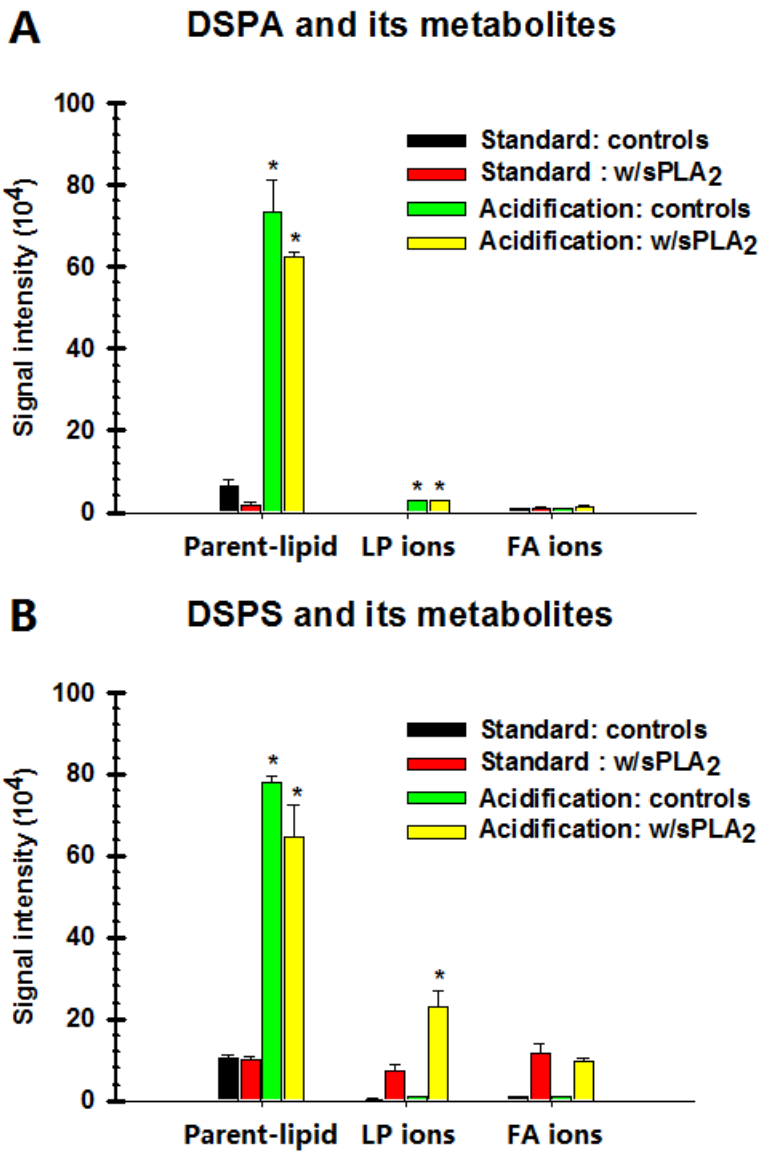

Figure 2.1 Effect of Acidification on the Signal Intensity of DSPA and DSPS and Their Metabolites after Acidified Bligh-Dyer Extraction. 1 µmol/mL of DSPA (A) and DSPS (B) were incubated in the presence and absence of 2.5µg/mL Group III $sPLA_2$ for 24 hr at 37 ºC, and were then subjected to extraction using conventional or acidification BD methods. The signal intensity for the parent phospholipids, as well as their lysophospholipid (LP) and fatty acid (FA) metabolites were then determined using electrospray ionization-mass spectrometry (ESI-MS). Data presented as mean ± SEM (n=3); * significant difference ($P < 0.05$) compare to standard.

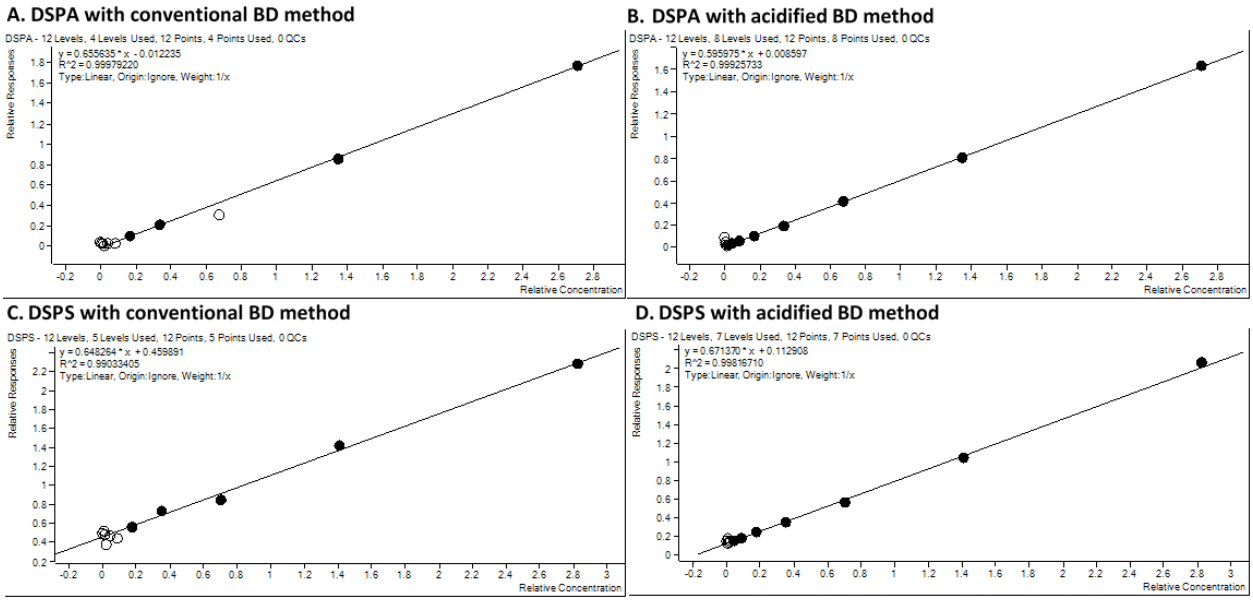

Figure 2.2 Effect of Acidification on the Standard Curves of DSPA and DSPS after Acidified Bligh-Dyer Extraction. A total of 12 concentrations of DSPA and DSPS were extracted with conventional or acidified BD extraction methods, then determined with ESI-MS. With conventional BD extraction, DSPA (A) have only 4 concentrations included in standard curve with a linear range of 71.82 – 1149.04 ng/mL; DSPS (C) have 5 concentrations used for standard curve with a linear range of 87.31 – 1397 ng/mL. With acidified BD extraction, 8 concentrations were used for DSPA (B) standard curve with a larger linear range of 8.98 – 1149.04 ng/mL; 7 concentrations were qualified for DSPS (D) standard curve, and its linear range expanded to 21.83 – 1397 ng/mL.

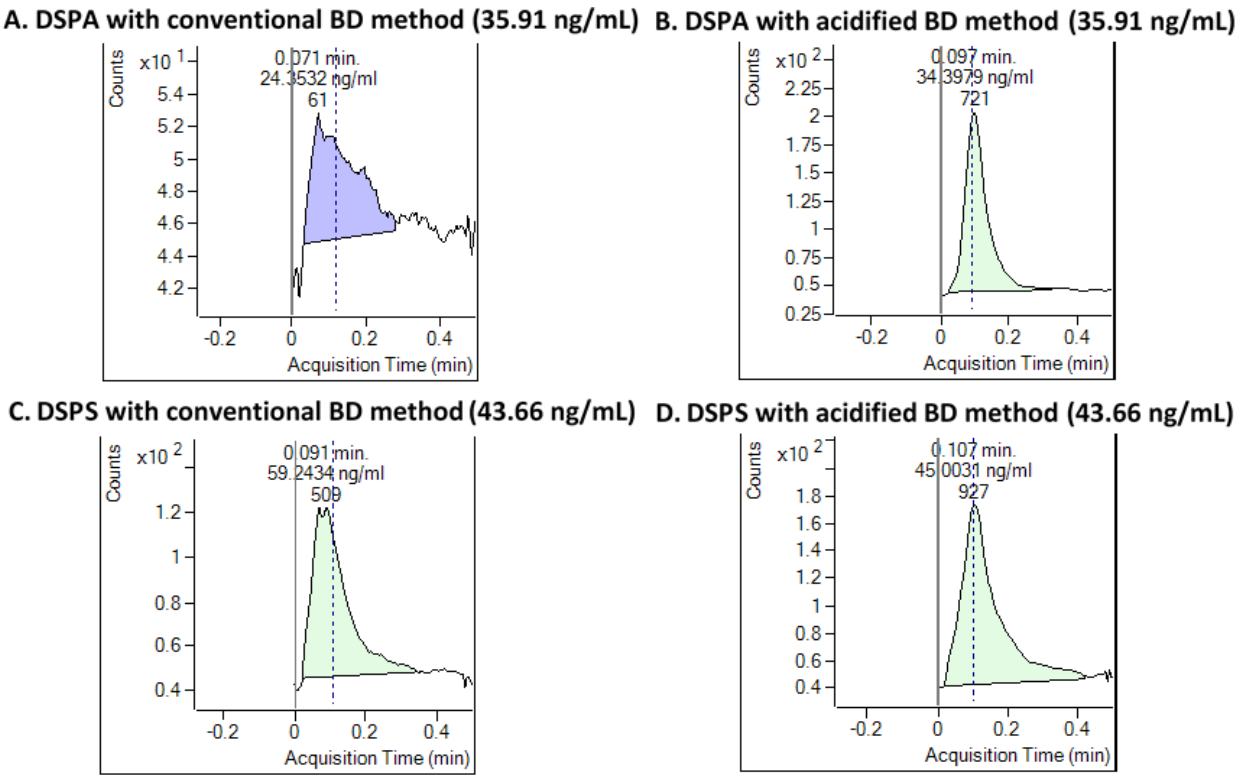

Figure 2.3 Effect of Acidification on Quantification Accuracy of DSPA and DSPS after Acidified Bligh-Dyer Extraction. Low concentration of DSPA (35.91 ng/mL) and DSPS (43.66 ng/mL) were prepared, extracted using conventional or acidified BD extraction, then determined with ESI-MS. With conventional BD extraction, DSPA (A) can hardly be detected, and its accuracy is poor (67.81%); DSPS (C) has higher signal intensity, but the accuracy is not ideal (135.69%). With acidified BD extraction, the signal intensity of DSPA (B) is significantly increased as well as the accuracy (95.80%); DSPS (D) has a similar result, increased signal intensity and increased accuracy (103.07%).

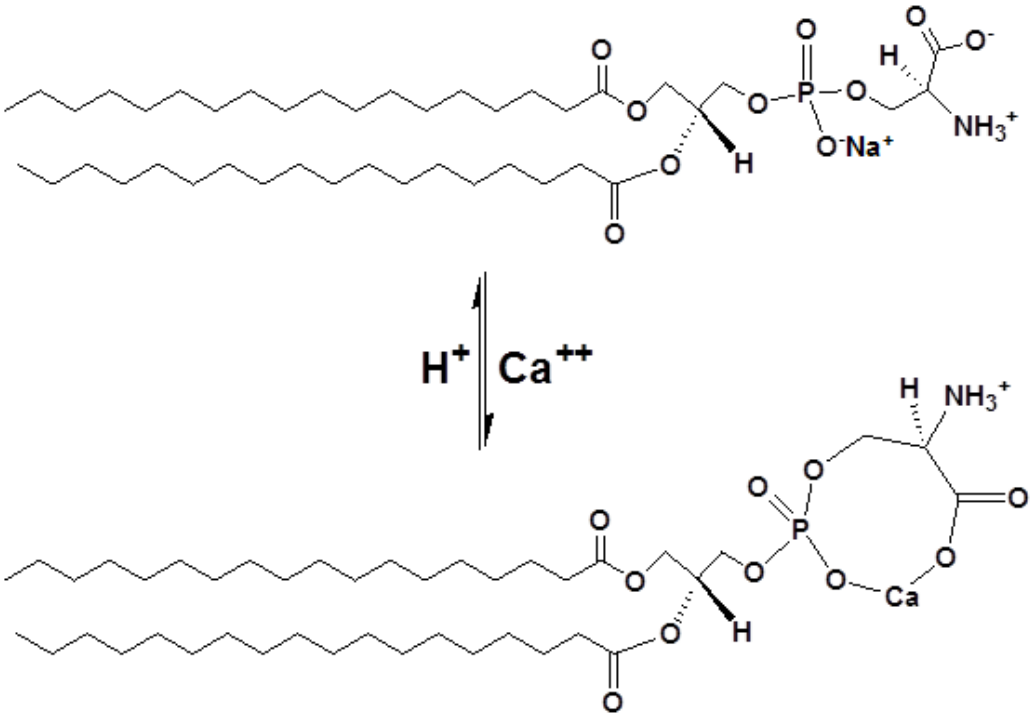

Figure 2.4 Structure of Calcium-chelated DSPS. DSPS has a high propensity to chelate to Ca^{2+} via the charged oxygen atoms of both the carboxyl and phosphate moieties.

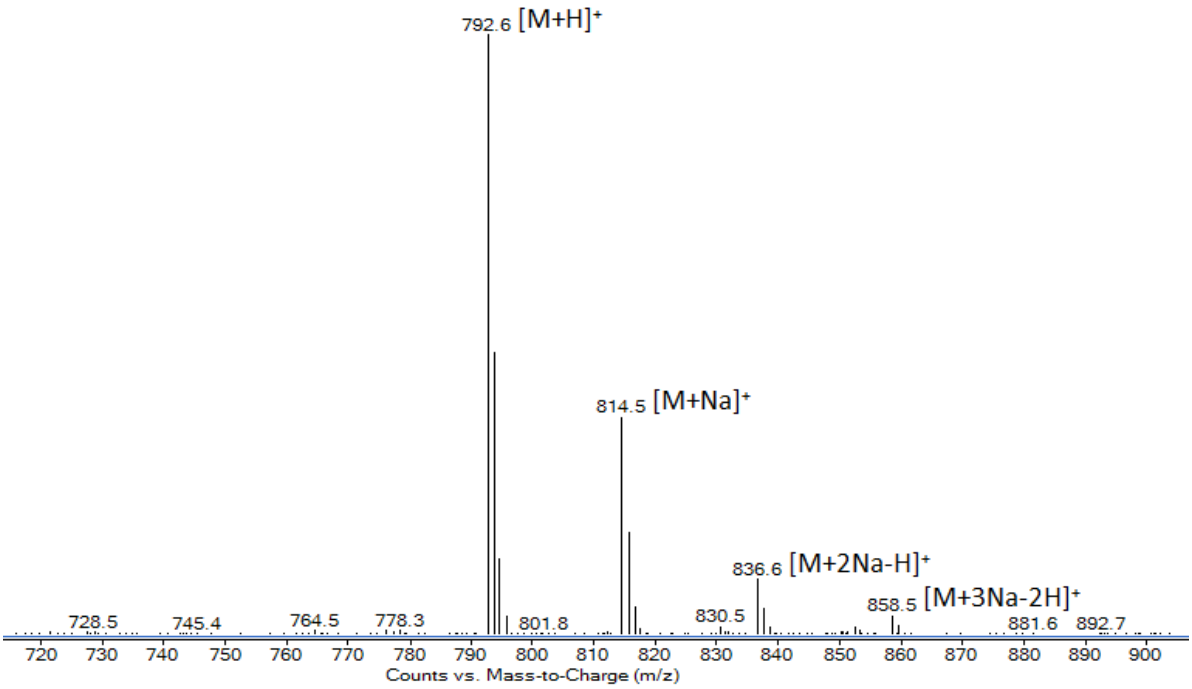

Figure 2.5 Mass Spectra of DSPS. DSPS has 3 sodium adducts. Single sodium adduct 814.5 $[M+Na]^+$, double sodium adduct 836.6 $[M+2Na-H]^+$, and triple sodium adduct $[M+3Na-2H]^+$.

Chapter 3. Development of a LC-MS/MS Method in Combination with Deuterated Phospholipids for Differentiation and Quantification of Liposomes

3.1 Introduction

The lack of sufficient quantitative analysis methods in the field of lipid-based nanomedicine has restricted our ability to optimize the formulations. The use of labels and encapsulated drugs for quantification suffered from many problems, such as premature leakage (Gabizon, Hliberty et al. 1988, Gabizon, Pappo et al. 1993), translocation (Damen, Regts et al. 1981, Moerlein and Welch 1981), altering native formulation (Huth, Wieschollek et al. 2004), interference of high background signal (Moerlein and Welch 1981, Gabizon, Hliberty et al. 1988), most importantly, unsolidified association between label signals and the lipid carriers (Moribe and Maruyama 2002, Bao, Goins et al. 2004, Medina, Zhu et al. 2004).

LC-MS/MS (triple quadrupole mass spectrometer) processes multiple dimensions of separation, partition coefficient and/or ion-exchange based chromatography and mass-to-charge (m/z) based mass detection, offers high selectivity and sensitivity. Multiple reaction monitoring (MRM) (Kondrat, McClusky et al. 1978, de Hoffmann 1996) push the selectivity and sensitivity even further by selecting paired molecule precursor ions and product ions. Thus, this technique is very suitable and widely employed for biological sample quantification. However, such a technique falls short when biological reginal isomers and isobars are present, which have similar partition coefficients, identical molecular mass-to-charge values, and the same product ions (Figure 1.4, Chapter 1).

The use of heavy isotopic phospholipids such as d70-DSPC sets formulational phospholipids apart from endogenous regional isomers or isobars. Furthermore, the synthetic heavy isotopic phospholipids share the same physiochemical and biochemical properties with their light counterpart. Thus, formulations made with heavy isotopic phospholipids are essentially the same.

In this chapter, we establish a new analytical method using LC-MS/MS in combination with d70-DSPC for *in vitro* and *in vivo* quantification of $sPLA_2$ responsive liposomes (SPRL). We replaced DSPC with d70-DSPC in our SPRL formulations (Figure 3.1), quantified d70-DSPC and its metabolite (d35-LysoPC) simultaneously in cells and tumor tissues. The method was validated for specificity, linearity, sensitivity (LOD and LLOQ), accuracy and precision. It was successfully applied for the *in vitro* and *in vivo* studies in Chapter 4.

3.2 Materials and Methods

3.2.1 Chemicals and Reagents

Deuterated phospholipids, d70-DSPC (1,2-distearoyl-d70-*sn*-glycero-3-phosphatidylcholine), d62-DPPC (1,2-dipalmitoyl-d62-*sn*-glycero-3-phosphatidylcholine), d35-Lyso PC (1-distearoyl-d35-*sn*-glycero-3-phosphatidylcholine), and d31-Lyso PC (1-dipalmitoyl-d31-*sn*-glycero-3-phosphatidylcholine) were purchased from Avanti Polar Lipids, Inc. (Alabaster, AL). Acetonitrile, isopropanol and methanol of LC-MS grade were from Sigma Aldrich (St. Louis, MO). HPLC grade ammonium acetate was from Fisher Scientific (Pittsburgh, PA). All other chemicals and solvents were of analytical grade, obtained from commercial sources and used without further purification. Ultrapure water (> 18.3 MΩ) was used and obtained from a Millipore Milli-Q synthesis system (Billerica, MA).

3.2.2 Instrumentation

An Agilent 1290 UHPLC was connected to an Agilent 6460 triple quadrupole mass spectrometer (Santa Clara, CA) with an Agilent Jet Stream ESI source controlled by Agilent Mass Hunter Acquisition software (B.06.00). Positive-ion scan mode was applied based on a better ionization efficiency for zwitterionic phospholipids. Nitrogen gas was used as a desolvation and collision gas. Ion source acquisition parameters were optimized according to the deuterated phospholipids: desolvation gas temperature and shealth gas temperature were set at 350 ºC and 400 ºC, respectively; desolvation gas flow and shealth gas flow were optimized to 10 L/min and 12 L/min, respectively; the nebulizer was set at 45 psi; capillary voltage was + 4000 V. Multiple reaction monitoring (MRM) scan mode was used for the quantification. MRM mass transitions for each deuterated phospholipid and their parameters are summarized in Table 3.1.

3.2.3 Column and Mobile Phase Selection

Three different columns along with the mobile phases chosen according to the stationary phases were tested for their suitability for best separation of deuterated phospholipids. A ZORBAX SB C8 (2.1 × 50 mm, 1.8 µm) column was purchased from Agilent Technologies (Santa Clara, CA). The two-phase mobile phase for this column consists of (A) 10mM Ammonium Acetate (pH 5.0) / Acetonitrile (60/40, v/v), and (B) Isopropanol/Acetonitrile (90/10, v/v). The ACQUITY UPLC BEH HILIC (2.1 × 100 mm, 1.7 µm) column was from Waters Corporation (Milford, MA). The mobile phase for this column consists of (A) 10mM Ammonium Acetate, and (B) Acetonitrile. The third column was also from Waters, ACQUITY UPLC HSS T3 (2.1 × 100 mm, 1.8 µm). Its mobile phase was the same as ZORBAX SB C8. The samples that were used for column selection were prepared by spiking deuterated phospholipids

into homogenized xenograft tumor tissue of human prostate adenocarcinoma (PC-3, ATCC, Manasses, VA). The suitable column and mobile phases were selected based on the separation of deuterated phospholipids, peak width, peak symmetry, linearity and LLOQ.

3.2.4 Method Validation

3.2.4.1 Specificity

Deuterated $sPLA_2$ responsive liposomes (d70-SPRL) were prepared by replacing DSPC with d70-DSPC in the formulation as indicated in Figure 3.1. DSPE, d70-DSPC, DSPE-PEG and cholesterol (1:8:1:5, mole ratio) were mixed together, and the formulation was prepared according to our previously published procedure (Zhu, Mock et al. 2011). Once the liposome was ready, 0.5 mM of d70-SPRL was incubated with human prostate cancer cells (PC-3) in a 6-well plate with a seeding density of 100,000 cells for 48 hr. After 48 hr, PC-3 cells were collected and washed with PBS 3 times to remove excessive d70-SPRL. Total lipids were extracted using the Bligh-Dye extraction, and detected using LC-MS/MS. Method specificity was determined by comparing d70-SPRL incubated cells, blank cells and deuterated phospholipid standards (d70-DSPC and d35-LysoPC).

3.2.4.2 Linearity, LOD and LLOQ

The linearity of the LC-MS/MS method was evaluated by analyzing serial dilution of the mixture of d70-DSPC and its metabolite d35-LysoPC. A mixture of d62-DPPC and its metabolite d31-LysoPC, indecently prepared, were used as internal standards. d70-DSPC and d35-LysoPC were mixed together at a concentration of 1.1 mg/mL in chloroform as the standard stock solution. The standard application solution was prepared by diluting from the stock solution to a

concentration of 2.2 µg/mL in chloroform. A 1:2 ratio serial dilution was applied to obtain a serial of concentrations started at 2.2 µg/mL for evaluation of the method linearity. Internal standard stock solution was prepared in the same manner at a concentration of 2.5 mg/mL. The internal standard application solution was prepared by dilution to a concentration of 1.25 µg/mL. An aliquot of 5 µL internal standard was added into an aliquot of 400 µL standard solution. An aliquot of 100 µL methanol and 150 µL of homogenized (sonication) cell suspension was added to mimic Bligh-Dye extraction process. The chloroform layer was collected and dried under ultrapure nitrogen gas. The standards were reconstituted with 100 µL of chloroform/methanol (50/50, v/v), then analyzed using LC-MS/MS. Calibration curves were constructed by calculating the ratio of the analyte peak area to that of the internal standard, and plotting the ratio *versus* the theoretical concentration; data were fit using quadratic regression with a weighting factor of $1/x^2$ (Singtoroj, Tarning et al. 2006). The standard curve was considered acceptable if greater than 90% of the standards had calculated accuracies within 15% of their theoretical value, and precision had a coefficient of variation (CV) of $\leq$ 20%.

Limit of detection (LOD) and lower limit of quantification (LLOQ) were defined as the lowest concentration with a signal to noise ratio (S/N) of 3 and 10, respectively. LOD and LLOQ were estimated by analyzing the lower concentrations of the serial standard concentrations. LLOQ were consider acceptable with an accuracy ± 20%.

3.2.4.3 Accuracy and Precision

Accuracy was determined by analyzing 4 known concentrations of d70-DSPC and d35-LysoPC samples in triplicates. LLOQ, low, medium and high level of the calibration curve were

used for accuracy examination. An acceptable accuracy should fall within 80 - 120%. The formula for accuracy calculation:

$$Accuracy = (Measurements / Theoretical\ Concentrations) \times 100\%.$$

The precision was evaluated by determining the intra-day and inter-day coefficient of variation (CV %) of the measurements. Same concentrations as in accuracy determination were used. Each concentration was injected 3 times the same day (n=3 per day) and on three consecutive days (n=9 for inter-day). An acceptable precision should have a CV $\leq$ 20% and accuracy ± 20%.

3.3 Results

3.3.1 Deuterated Phospholipids

Deuterated phospholipids, d70-DSPC, d35-LysoPC, and their internal standards d62-DPPC and d31-LysoPC were detected under MS2 full scan mode for confirmation of molecular weight and selection of precursor ions (Figures 3.2 and 3.3). A serial of deuterated ions were detected for each deuterated phospholipid, which indicated a unified deuterium labeling in conflict with the manufacturer's claim of purity (> 99%). Take d70-DSPC as an example, a spread of $[M+1]^+$ ions were observed from 855 to 863 (Figure 3.2 A). The exact mass of d70-DSPC is 860.064. If the labeling is complete and unified, we should see a sole peak of 861. The same happened to other deuterated phospholipids as well. The possible explanation for this phenomenon is deuterium and hydrogen (D-H) back-exchange (Wu, Kaveti et al. 2006, Walters, Ricciuti et al. 2012) occurred after the synthesis was finished. A few deuterium atoms on the phospholipid molecule exchanged with the hydrogen on the solvent molecules. In the case of

d70-DSPC, base peak of 859 was observed which means d68-DSPC is predominately present in the product. For this reason, 859 was chosen as the precursor ion for d70-DSPC.

3.3.2 Column and Mobile Phase Selection

The columns tested were reverse column and HILIC column. We used two different reverse column: C8 (Agilent) and T3 (Waters). The separation obtained on C8 column (Figure 3.4 A) was sufficient, however, the sensitivity (LLOQ > 10 pg on column) suffered due to the over-strong retention of phospholipids on reverse columns, which leads to a broadened and asymmetric peak. HILIC (Hydrophilic Interaction Chromatography) column (Hemström and Irgum 2006) is very commonly used for lipidomics and lipid analysis. The over-strong retention of lipids can be overcome in its normal phase chromatography mode. In our studies, the separation was not ideal for d70-DSPC (Figure 3.4 B), and the sensitivity wasn't great either (LLOQ > 20 pg on column). Waters T3 column outperformed the other two columns (Figure 3.4 C) due to its unique T3 bonding that promotes polar compound retention and reduces lipid retention. Even after a longer elution, the target peak remained narrow and symmetric with a high sensitivity (LLOQ 2-4 pg on column). Based on these results, the T3 column was chosen for our studies.

3.3.3 LC-MS/MS Method Validation

PC-3 cells was incubated with d70-SPRL. Total lipids were extracted using BD extraction method and detected using LC-MS/MS. Chromatograms showed that d70-DSPC (Figure 3.5) and its metabolite (Figure 3.7, enzymolysis of $sPLA_2$) were able to be separated. The results were confirmed by comparing the retention time and mass transitions with standards. Blank

controls (PC-3 cells) showed no interference from endogenous molecules that verified the differential ability and specificity of the method. The internal standards were checked by the LC-MS/MS method in the same manner. d62-DPPC (Figure 3.6) and d31-LysoPC (Figure 3.8) were spiked in PC-3 cells and extracted using the BD extraction method. The LC-MS/MS results were compared with standards and blank controls and affirmed the specificities for those compounds. Based on the specificity results, the LC-MS/MS method is able to differentiate d70-DSPC and d35-LysoPC from endogenous phospholipids.

The method was linear from 4.3 ng/mL to 1100 ng/mL with an injection volume of 1 µL, corresponding to the tested concentrations with correlation coefficients (R^2) greater than 0.99. Quadratic regression analysis was applied instead of straight linear regression due to the fact that variability increase along with the increase of concentrations in biological samples (Singtoroj, Tarning et al. 2006). LOD and LLOQ for both d70-DSPC and d35-LysoPC were 1.0 ng/mL and 4.3 ng/mL, respectively. The results are summarized in Table 3.2.

Four levels of concentration, LLOQ, low, median and high, were used for accuracy and precision test. The accuracy for both d70-DSPC and d35-LysoPC at all 4 levels of concentration were within 80-120 %; the intraday and interday variation were < 20%. The results are summarized in Table 3.3.

3.4 Discussion

We were not the first to use d70-DSPC for differentiation of liposome from endogenous molecules. Matthaus et al (Matthaus, Kale et al. 2008) use d70-DSPC combined with Raman microspectroscopy for visual localization of liposome uptake in cells. They also attempted a quantitative comparison by counting optical density. They admitted that it was not a perfect

quantification. We used d70-DSPC combined with LC-MS/MS to quantify not only the parent phospholipids but also their metabolite to assess the enzymatic metabolism of liposomes in cells. The deuterated phospholipids we purchased from Avanti were not uniformly labeled with deuterium, probably due to back-exchange of deuterium and hydrogen (other labs had the same problem with Avanti deuterated phospholipids). This is problematic for us because it reduced the amount of detectable target by choosing only one variation of deuterated phospholipids, thus the sensitivity of the assay was decreased. Fortunately, the D-H exchange follows patterns. In the case with d70-DSPC, distearoyl chains were labeled with 35 deuterium in each chain (Figure 3.5 C). Predominate variation was d68-DSPC, which means each chain had one deuterium exchanged with hydrogen. Its metabolite, d35-LysoPC, 35 deuterium was labeled on the stearoyl chain. The Mass scan result showed d34-LysoPC was predominately present, which means one deuterium exchanged with hydrogen. With this observed pattern, we were still be able to use these deuterated phospholipids to assess lipid cellular metabolism. Avanti should increase the quality control of their products, minimize the D-H back-exchange.

Phospholipids have over-strong retention on reverse phase columns. Usually an aggressive mobile phase (incorporate isopropanol) (Patterson, Ducrocq et al. 2015) will be paired with lipids elution on reverse columns. Even with such a mobile phase, the over-strong retention broadened the peak width on C8 column and caused a reduced sensitivity. HILIC column is also commonly used for lipid research with its normal phase mode to overcome the over-strong retention of lipids. However, due to the high percentage of organic phase (acetonitrile, which is not a proton donator) needed to activate the normal phase mode, the ionization of the phospholipids was decreased and resulted in a low sensitivity. T3 column was classified in reverse column, but with the T3 bounding that utilizes a trifunctional C18 alkyl phase bonded at

a ligand density that promotes polar compound retention and aqueous mobile phase compatibility. Therefore, the retention of phospholipids were reduced. Also, T3 column endcapping process is more effective than traditional trimethyl silane (TMS) endcapping, enhancing the column performance, peak shape and stability.

Analytical scientists have been using different regression approaches for biological analysis due to the complexity of biological samples that the variation of measurement increases with the concentration of target compounds where a straight linear model become insufficient and inaccurate. Singtoroj et al (Singtoroj, Tarning et al. 2006) determined different models with different weighting factors. The results showed that quaduatic regression is one of the more suitable regression modles for bioanlytical study. The straight linear approches ranked last of all models. We used the quadratic model with a weighting factor of $1/x^2$. The corelation coefficients were greater than 0.99. The accuracy of each tested calibration concentration was within 80-120%.

3.5 Conclusion

We have established a validated LC-MS/MS method that is able to differentiate the deuterated phospholipids in liposomal formulations and quantify them and their metabolites. It is a powerful tool to enhance our ability to optimize formulations based on valuable *in vitro* and *in vivo* quantitative data of the lipid-carriers. Combined with the well-established doxorubicin LC-MS/MS quantification method (Arnold, Slack et al. 2004), we can understand the uptake mechanism from both encapsulated drug and the lipid-carriers. The use of different isotopic (deuterium, ^{13}C, ^{15}N) lipids can be employed based on specific lipid-based nanomedicine

formulations in combination with LC-MS/MS to explore uptake mechanisms and optimize formulations.

3.6 References

Arnold, R. D., J. E. Slack and R. M. Straubinger (2004). "Quantification of Doxorubicin and metabolites in rat plasma and small volume tissue samples by liquid chromatography/electrospray tandem mass spectroscopy." J Chromatogr B Analyt Technol Biomed Life Sci **808**(2): 141-152.

Bao, A., B. Goins, R. Klipper, G. Negrete and W. T. Phillips (2004). "Direct 99mTc labeling of pegylated liposomal doxorubicin (Doxil) for pharmacokinetic and non-invasive imaging studies." J Pharmacol Exp Ther **308**(2): 419-425.

Damen, J., J. Regts and G. Scherphof (1981). "Transfer and exchange of phospholipid between small unilamellar liposomes and rat plasma high density lipoproteins. Dependence on cholesterol content and phospholipid composition." Biochim Biophys Acta **665**(3): 538-545.

de Hoffmann, E. (1996). "Tandem mass spectrometry: A primer." J Mass Spectrom **31**(2): 129-137.

Gabizon, A., J. Hliberty, R. M. Straubinger, D. C. Price and D. Papahadjopoulos (1988). "An Improved Method for in Vivo Tracing and Imaging of Liposomes Using a Gallium 67-Deferoxamine Complex." J Liposome Res **1**(1): 123-135.

Gabizon, A. A., O. Pappo, D. Goren, M. Chemla, D. Tzemach and A. T. Horowitz (1993). "Preclinical Studies with Doxorubicin Encapsulated in Polyethyleneglycol-Coated Liposomes." J Liposome Res **3**(3): 517-528.

Hemström, P. and K. Irgum (2006). "Hydrophilic interaction chromatography." J Sep Sci **29**(12): 1784-1821.

Huth, U., A. Wieschollek, Y. Garini, R. Schubert and R. Peschka-Suss (2004). "Fourier transformed spectral bio-imaging for studying the intracellular fate of liposomes." Cytometry A **57**(1): 10-21.

Kondrat, R. W., G. A. McClusky and R. G. Cooks (1978). "Multiple reaction monitoring in mass spectrometry/mass spectrometry for direct analysis of complex mixtures." Anal Chem **50**(14): 2017-2021.

Matthaus, C., A. Kale, T. Chernenko, V. Torchilin and M. Diem (2008). "New ways of imaging uptake and intracellular fate of liposomal drug carrier systems inside individual cells, based on Raman microscopy." Mol Pharm **5**(2): 287-293.

Medina, O. P., Y. Zhu and K. Kairemo (2004). "Targeted liposomal drug delivery in cancer." Curr Pharm Des **10**(24): 2981-2989.

Moerlein, S. M. and M. J. Welch (1981). "The chemistry of gallium and indium as related to radiopharmaceutical production." Int J Nucl Med Biol **8**(4): 277-287.

Moribe, K. and K. Maruyama (2002). "Pharmaceutical design of the liposomal antimicrobial agents for infectious disease." Curr Pharm Des **8**(6): 441-454.

Patterson, R. E., A. J. Ducrocq, D. J. McDougall, T. J. Garrett and R. A. Yost (2015). "Comparison of blood plasma sample preparation methods for combined LC–MS lipidomics and metabolomics." J Chromatogr B **1002**: 260-266.

Singtoroj, T., J. Tarning, A. Annerberg, M. Ashton, Y. Bergqvist, N. J. White, N. Lindegardh and N. P. Day (2006). "A new approach to evaluate regression models during validation of bioanalytical assays." J Pharm Biomed Anal **41**(1): 219-227.

Walters, B. T., A. Ricciuti, L. Mayne and S. W. Englander (2012). "Minimizing back exchange in the hydrogen exchange-mass spectrometry experiment." J Am Soc Mass Spectrom **23**(12): 2132-2139.

Wu, Y., S. Kaveti and J. R. Engen (2006). "Extensive Deuterium Back-Exchange in Certain Immobilized Pepsin Columns Used for H/D Exchange Mass Spectrometry." Anal Chem **78**(5): 1719-1723.

Zhu, G., J. N. Mock, I. Aljuffali, B. S. Cummings and R. D. Arnold (2011). "Secretory phospholipase A(2) responsive liposomes." J Pharm Sci **100**(8): 3146-3159.

Table 3.1 Mass Transitions of Deuterated Phospholipids

Deuterated Phospholipids	Precursor Ion (m/z)	Product Ion (m/z)	Fragmentor (V)	Collision Energy (V)
D70-DSPC	859.0	184.0	170	37
D62-DPPC (IS)	794.9	184.0	180	33
D35-LysoPC	558.6	104.0	150	27
D31-Lyso PC (IS)	526.6	104.0	100	27

Table 3.2 Linearity, LOD and LLOQ of d70-DSPC and d35-LysoPC

Deuterated Phospholipids	Type	Weight	Equation	R^2	Linear Range (ng/mL)	LOD (ng/mL)	LLOQ (ng/mL)
d70-DSPC	Quadratic	$1/x^2$	$y = 0.846x^2 + 0.0784x + 0.000752$	0.99	4.3-1100	1.0	4.3
d35-LysoPC	Quadratic	$1/x^2$	$y = 0.131x^2 + 0.0625x + 0.00135$	0.99	4.3-1100	1.0	4.3

Table 3.3 A: Accuracy and Precision of d70-DSPC

d70-DSPC	Measurement (Mean ± SD, n=3)	Accuracy (%)	Precision (CV %)			
			Intra-day (n=3)			Inter-day (n=9)
			Day 1	Day 2	Day 3	
LLOQ (4.30 ng/mL)	4.09 ± 0.34	95.0	8.2	16.8	12.4	13.1
Low (8.59 ng/mL)	7.93 ± 0.43	92.4	5.4	8.0	2.6	13.2
Medium (68.75 ng/mL)	72.87 ± 2.11	106.0	2.9	2.7	0.8	3.6
High (550 ng/mL)	553.98 ± 2.78	100.7	0.5	2.1	7.4	4.9

Table 3.3 B: Accuracy and Precision of d35-LysoPC

d35-LysoPC	Measurement (Mean ± SD, n=3)	Accuracy (%)	Precision (CV %)			
			Intra-day (n=3)			Inter-day (n=9)
			Day 1	Day 2	Day 3	
LLOQ (4.30 ng/mL)	4.01 ± 0.02	93.3	0.4	3.6	1.8	4.9
Low (8.59 ng/mL)	7.26 ± 0.12	84.5	1.6	4.2	0.9	2.4
Medium (68.75 ng/mL)	66.03 ± 0.04	96.0	0.6	0.4	0.3	1.1
High (550 ng/mL)	531.11 ± 2.47	96.6	0.5	0.1	11.0	7.3

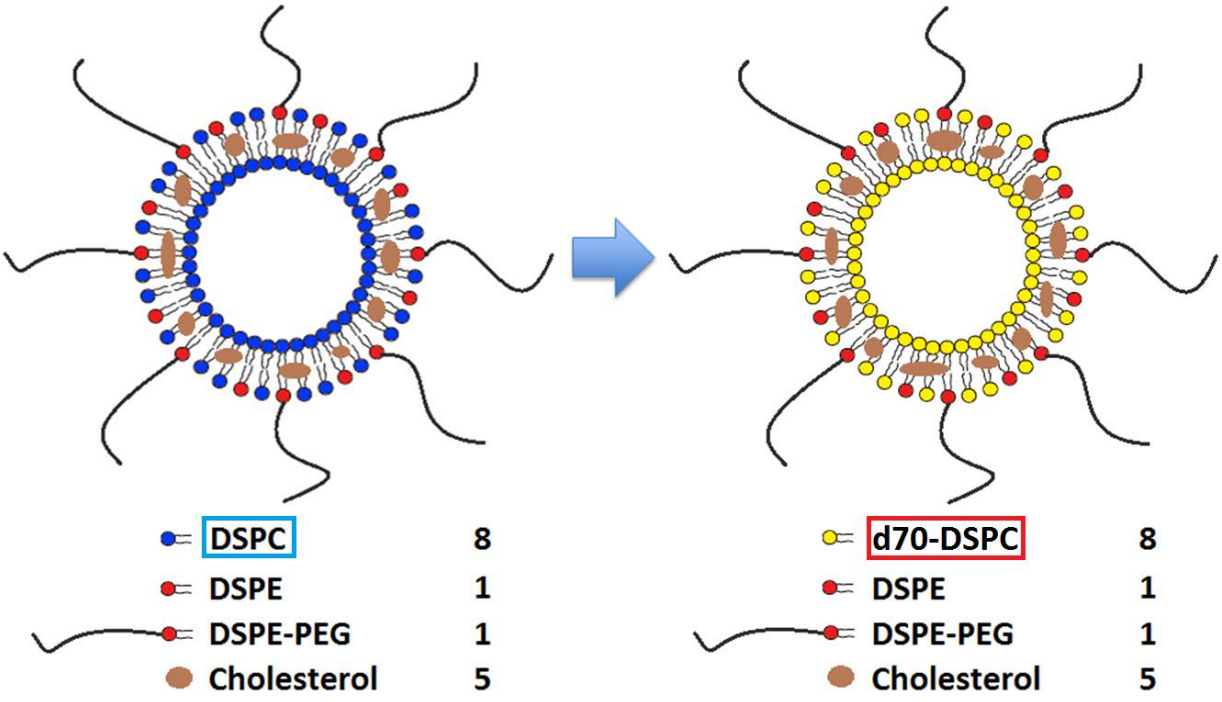

Figure 3.1 Illustration of Deuterated SPRL formulation. DSPC was completely replaced by d70-DSPC.

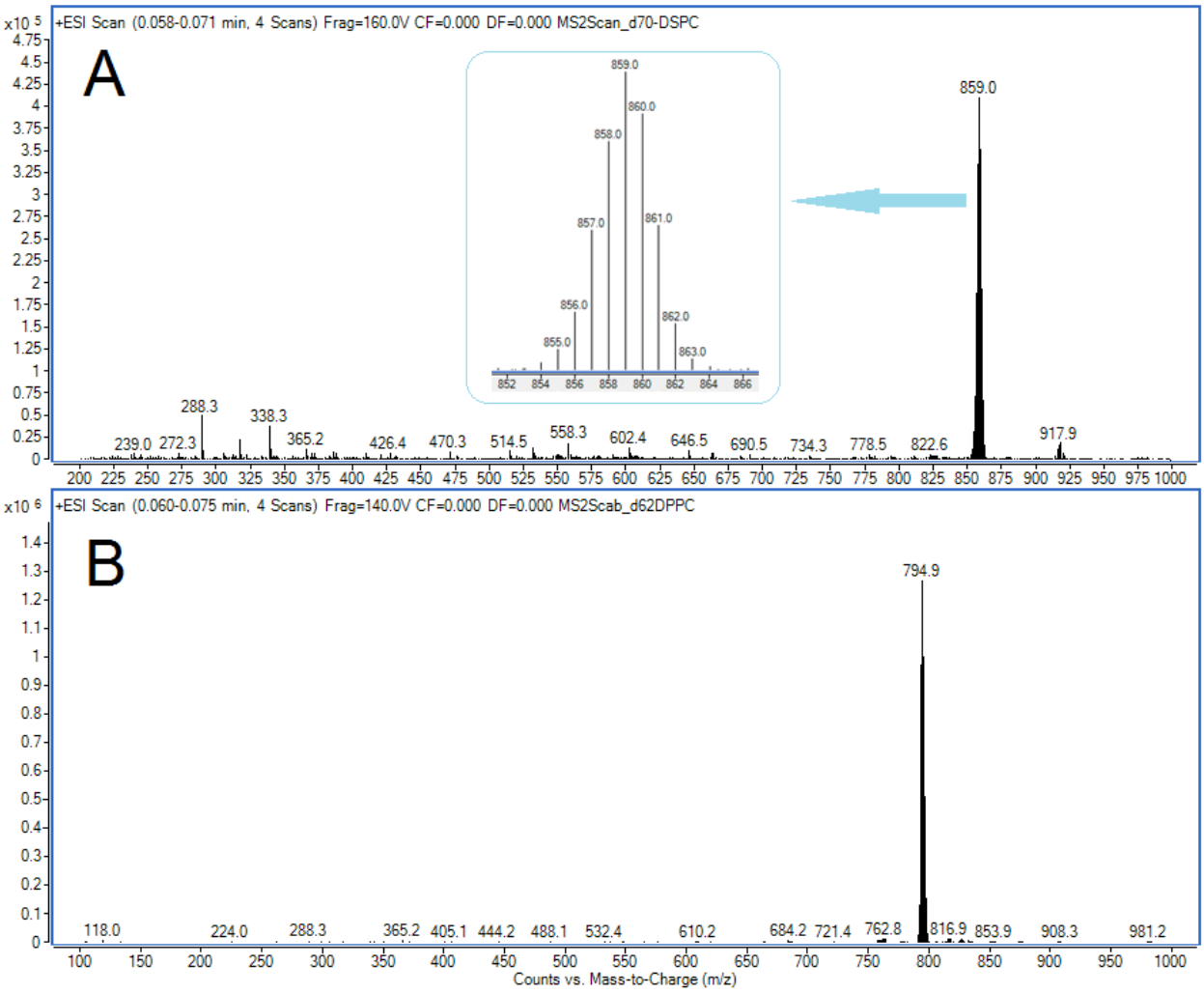

Figure 3.2 Mass Spectra of d70-DSPC and Its Internal Standard d62-DPPC. Both spectra indicated a unified deuterium labeling. D70-DSPC spectra (A) showed base peak of 859, d68-DSPC is predominately present; d62-DPPC spectra (B) showed base peak of 794.9, d60-DPPC is predominately present.

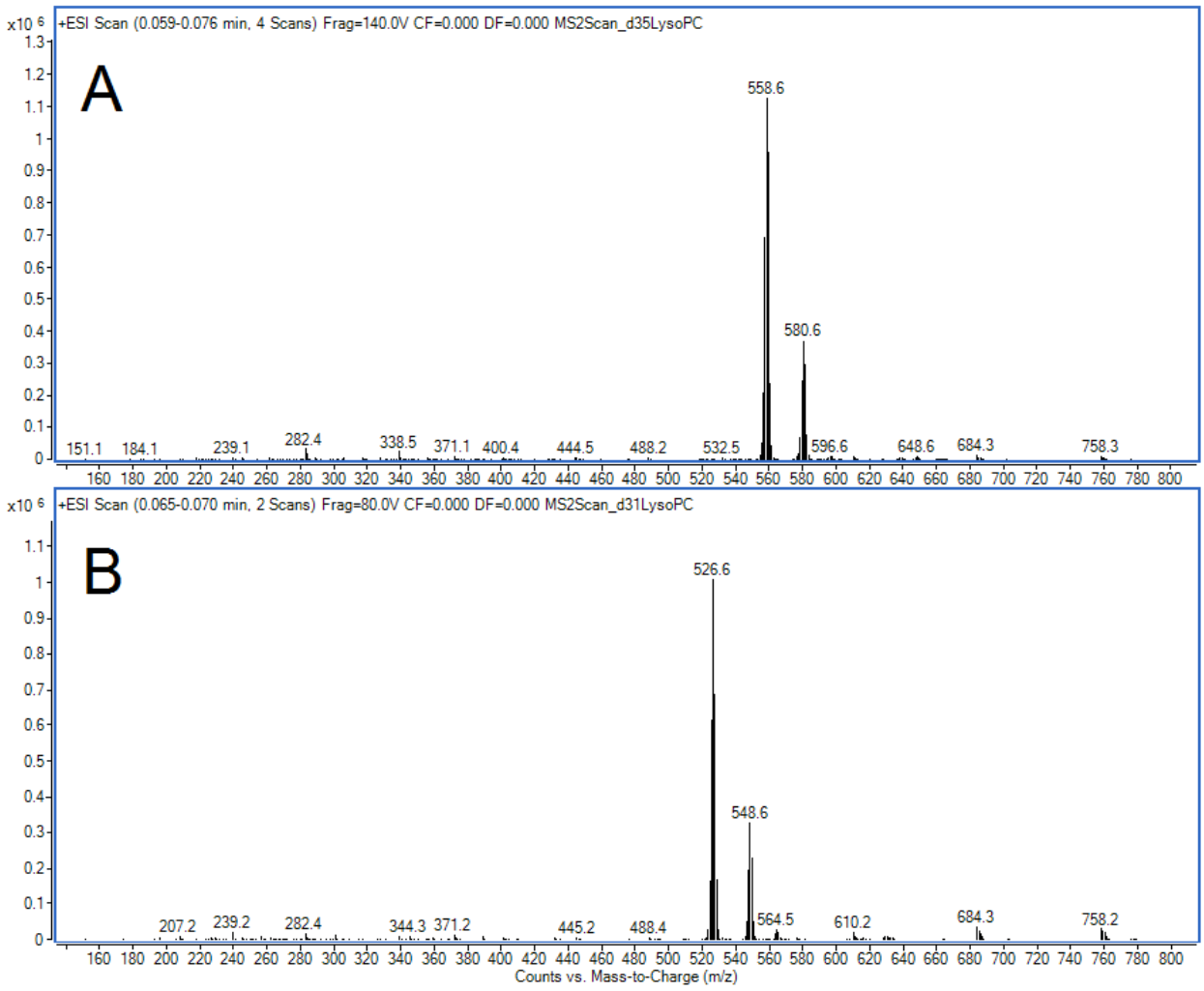

Figure 3.3 Mass Spectra of d35-LysoPC and Its Internal Standard d31-LysoPC. Both spectra indicated a unified deuterium labeling. D35-LysoPC spectra (A) showed base peak of 558.6, d34-LysoPC is predominately present; d31-LysoPC spectra (B) showed base peak of 526.6, d30-LysoPC is predominately present. Sodium adducts were showed in spectra as well.

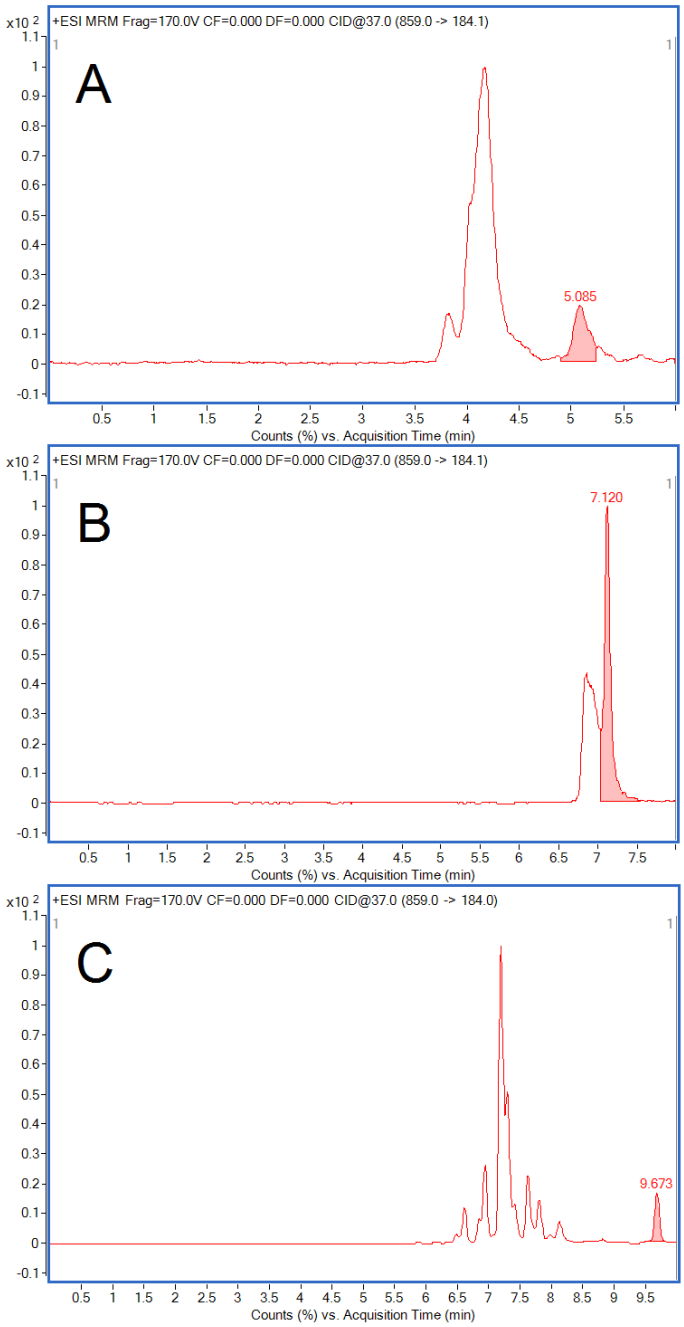

Figure 3.4 LC-MS/MS Chromatography of d70-DSPC Separation Performed on Three Different Columns. Separation on C8 column (A) showed a broadened and asymmetric peak with lower sensitivity (LLOQ > 10 pg on column); Separation on HILIC column (B) wasn't sufficient; a high sensitivity (LLOQ 2-4 pg on column) and ideal separation was achieved on T3 column (C).

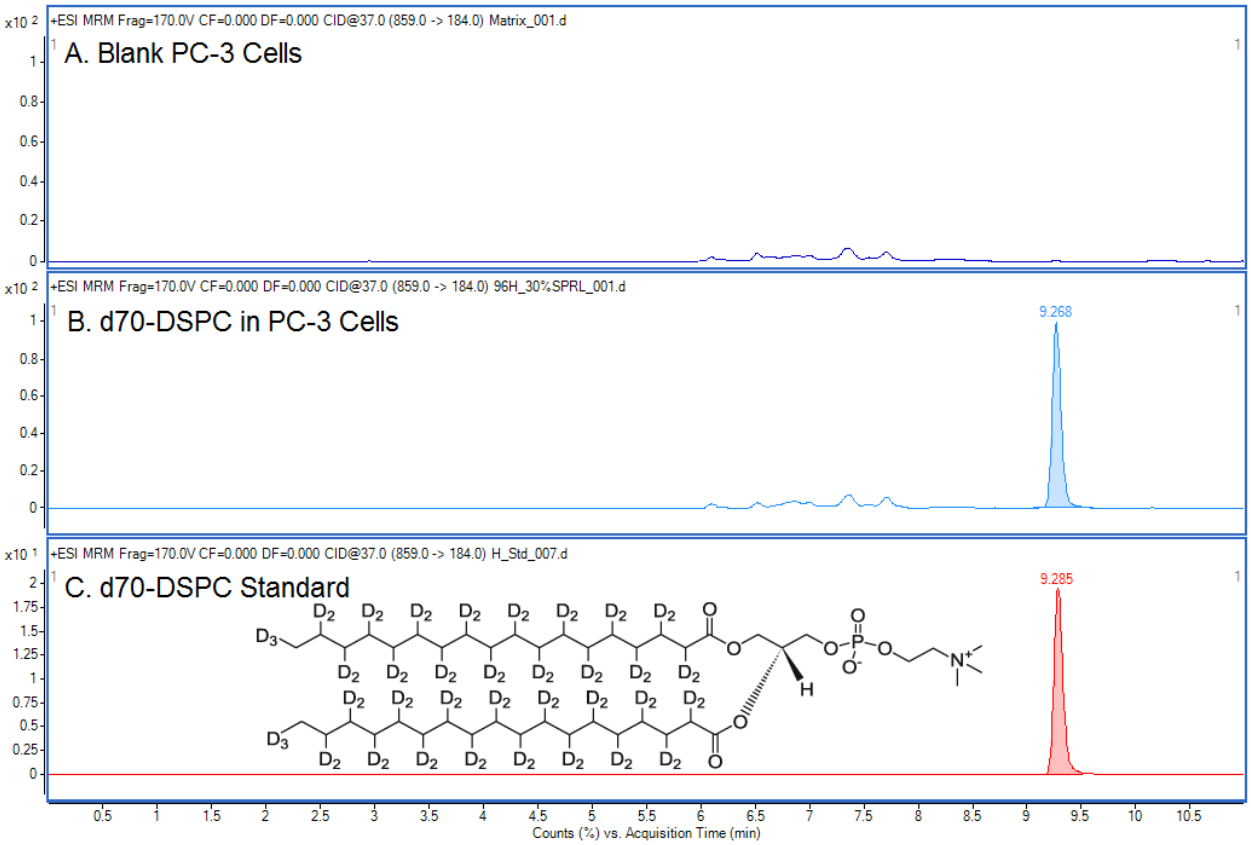

Figure 3.5 Comparison of LC-MS/MS Chromatography of d70-DSPC Standard, Sample and Background. The retention time of d70-DSPC was indicated by standard at 9.285 min (C), PC-3 cells that incubated with d70-SPRL showed a peak at same retention time at 9.268 min (B) using the same mass transition (859.0-184.0). Little or no interference was observed from blank control PC-3 cells (A).

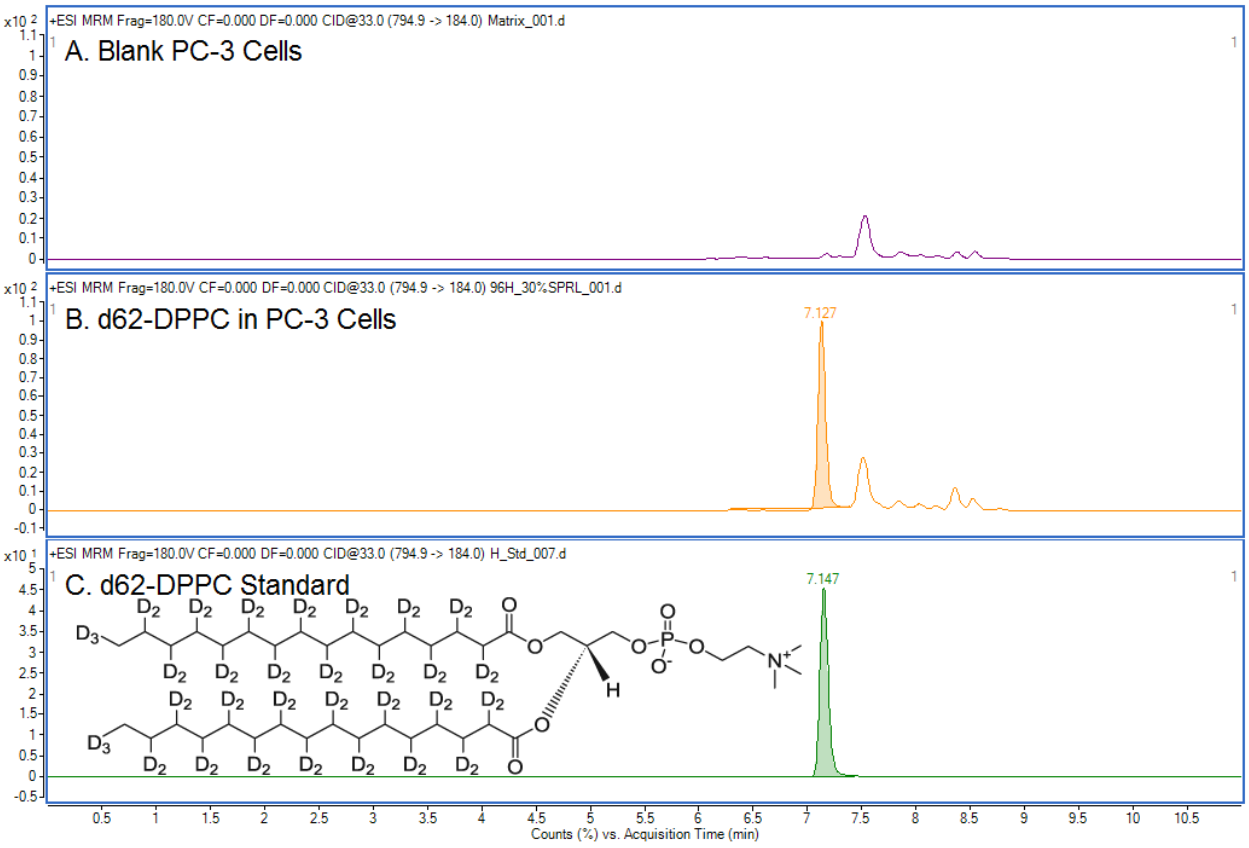

Figure 3.6 Comparison of LC-MS/MS Chromatography of d62-DPPC Standard, Sample and Background. The retention time of d62-DPPC was indicated by standard at 7.147 min (C), PC-3 cells that spiked with d62-DPPC showed a peak at same retention time at 7.127 min (B) using the same mass transition (794.9-184.0). Little or no interference was observed from blank control PC-3 cells (A).

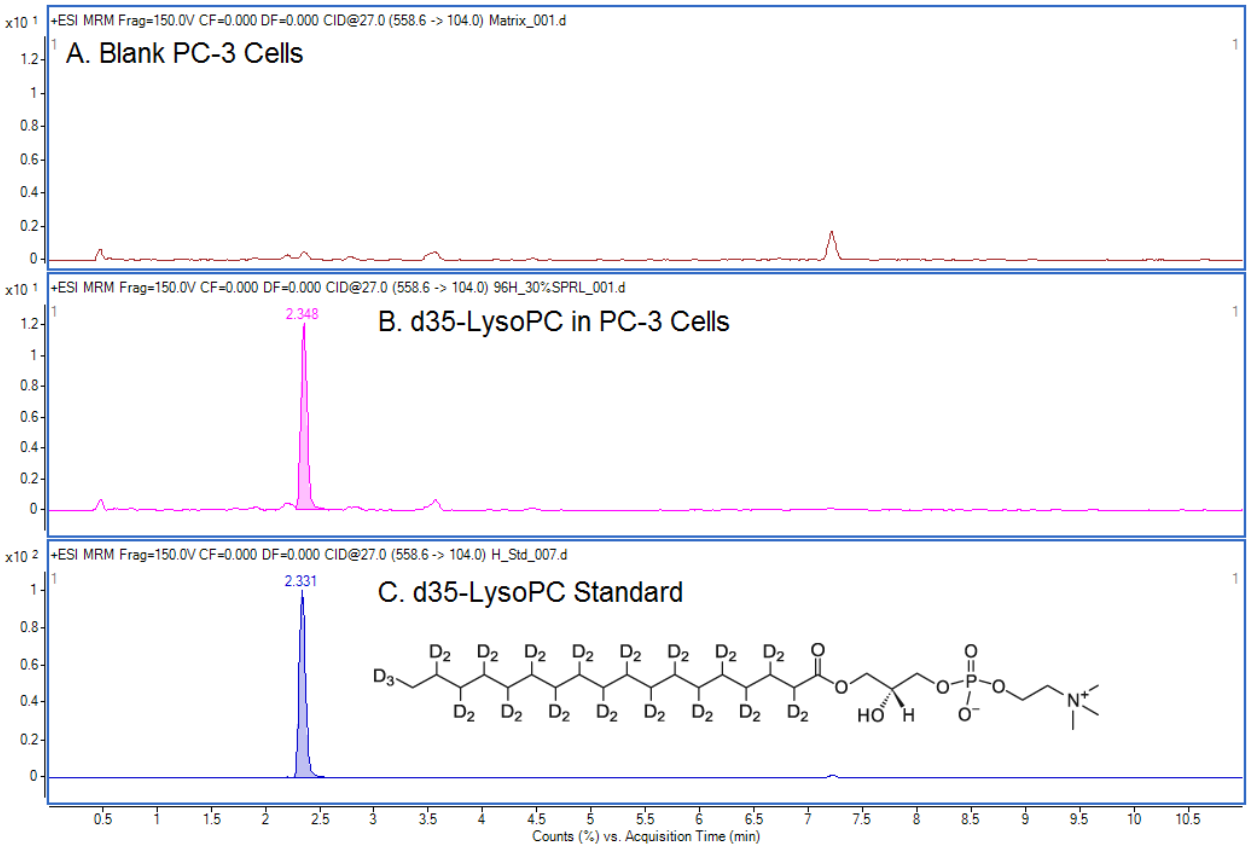

Figure 3.7 Comparison of LC-MS/MS Chromatography of d35-LysoPC Standard, Sample and Background. The retention time of d35-LysoPC was indicated by standard at 2.331 min (C), PC-3 cells that incubated with d70-SPRL showed a peak at same retention time at 2.348 min (B) using the same mass transition (558.6-104.0). Little or no interference was observed from blank control PC-3 cells (A).

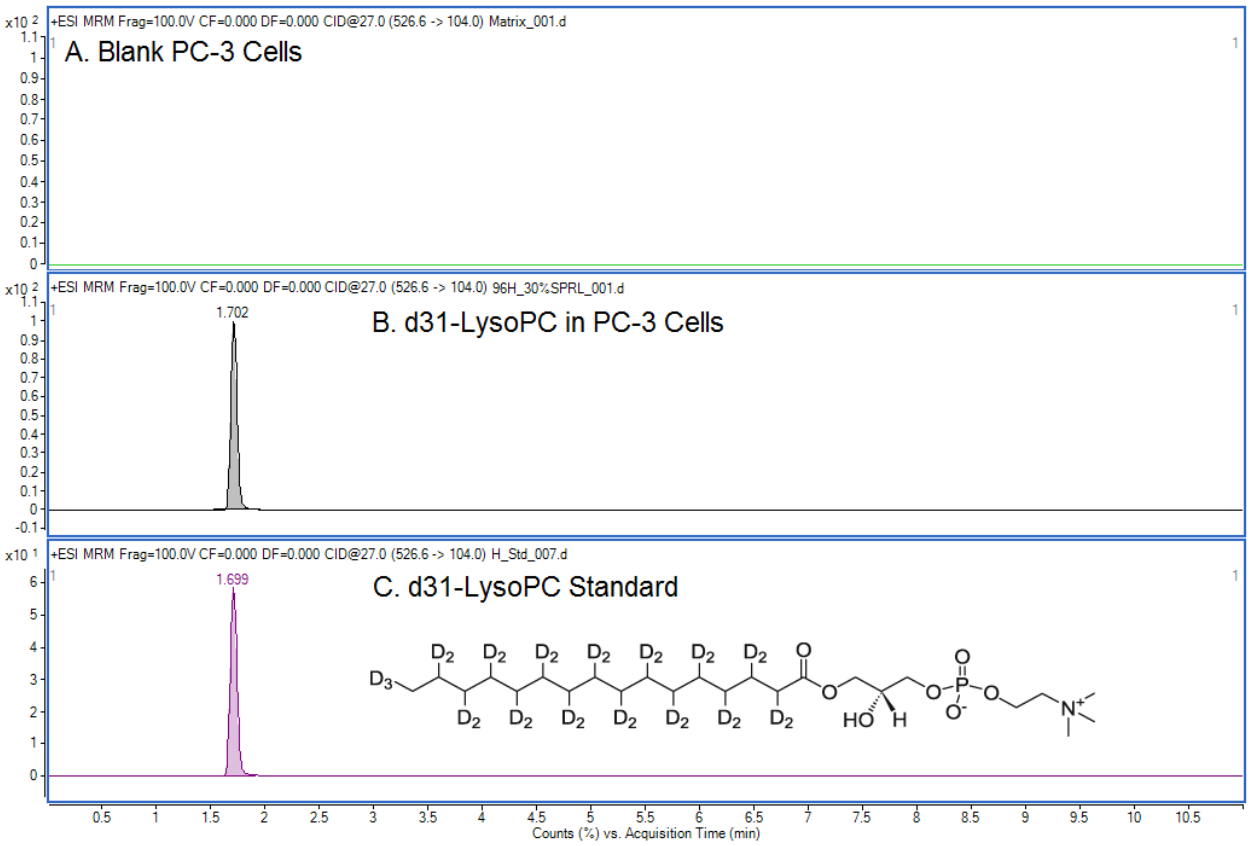

Figure 3.8 Comparison of LC-MS/MS Chromatography of d31-LysoPC Standard, Sample and Background. The retention time of d31-LysoPC was indicated by standard at 1.699 min (C), PC-3 cells that spiked with d31-LysoPC showed a peak at same retention time at 1.702 min (B) using the same mass transition (526.6-104.0). Little or no interference was observed from blank control PC-3 cells (A).

Chapter 4. Evaluation of *In vitro* and *In vivo* Intracellular Uptake, Disposition and Degradation of $sPLA_2$ Responsive Liposome in Prostate Cancer by LC-MS/MS

4.1 Introduction

Secretory phospholipase A_2 ($sPLA_2$) is a calcium-dependent (Hsu, Burke et al. 2009) enzyme important for cellular phospholipid metabolism (Burke and Dennis 2009). They degrade phospholipids by cleavage of the sn-2 acyl chain and generated one molecule of lysophospholid and one molecule of fatty acid (Burke and Dennis 2009, Quach, Arnold et al. 2014). In cancer, $sPLA_2$ served as both enzyme and ligand promoting tumor growth by triggering bioactive lipid signaling and receptror-mediated signaling (Brglez, Lambeau et al. 2014). The increased concentration of $sPLA_2$ found in various cancers including breast, liver, skin, stomach, pancreatic and prostate cancers has proven the expression of $sPLA_2$ is associated with tumor pathologies (Abe, Sakamoto et al. 1997). In a particular example, $sPLA_2$-IIA mRNA is significantly increased (22-folder) in prostate cancer compared to normal prostate (Dong, Patel et al. 2006). While the increased concentration of $sPLA_2$ was detected in tumor throughout many studies, the serum level of $sPLA_2$ is very low (< 10 ng/mL) (Nevalainen, Graham et al. 2008), which may indicate a cellular mechanism of $sPLA_2$ internalization, such as receptor-mediated internalization (Silliman, Moore et al. 2002).

Based on the pathological characteristics of $sPLA_2$ in cancer, we hypothesize that the lipid specificity and reactivity of $sPAL_2$ and its ability to interact with PLA_2 receptor (PLA2R) are potential targets for development of an enzymatic liposome drug delivery system. An

Illustration of this hypothesis is summarized in Figure 4.1. In brief, liposomes that can be recognized by $sPLA_2$ will form a liposome-enzyme complex. The complex will then partially be transferred into cells mediated by PLA2R, and partially be destabilized and release the drug outside of cells. The transferred complex will shortly release the drug intracellularly. Thus, the intercellular and intracellular drug accumulation can be increased.

We have developed a prototype $sPLA_2$ responsive liposome (SPRL) via *in vitro* enzymatic evaluation of selectivity and reactivity of $sPLA_2$ toward liposomal formulations (Zhu, Mock et al. 2011). Now, with our newly developed LC-MS/MS method, we are able to test SPRL intracellular performance through *in vitro* and *in vivo* studies, further optimize SPRL formulations, and understand the intracellular uptake mechanism.

The studies in this chapter were carried out on human prostate cancer cells (PC-3), and tumor xenografts model of PC-3 cells. The intracellular performance of SPRL were evaluated by comparing to the classic sterically stabilized liposome (SSL) (Woodle 1995, Arnold, Mager et al. 2005).

4.2 Materials and Methods

4.2.1 Chemicals and Reagents

Phospholipids and deuterated phospholipids, DSPE (1,2-distearoyl-*sn*-glycero-3-phosphatidylethanolamine), DSPE-PEG (1,2-distearoyl-*sn*-glycero-3-phosphatidylethanolamine-N-[methoxy(polyethylene glycol)-2000], d70-DSPC (1,2-distearoyl-d70-*sn*-glycero-3-phosphatidylcholine), d62-DPPC (1,2-dipalmitoyl-d62-*sn*-glycero-3-phosphatidylcholine), d35-Lyso PC (1-distearoyl-d35-*sn*-glycero-3-phosphatidylcholine), and d31-Lyso PC (1-dipalmitoyl-d31-*sn*-glycero-3-phosphatidylcholine) were purchased from Avanti Polar Lipids Inc (Alabaster,

AL). Doxorubicin and Daunorubicin were purchased from Sigma Aldrich (St. Louis, MO). Acetonitrile, isopropanol and methanol of LC-MS grade were also from Sigma Aldrich. HPLC grade ammonium acetate was from Fisher Scientific (Pittsburgh, PA). All other chemicals and solvents were of analytical grade, obtained from commercial sources and used without further purification. Ultrapure water (> 18.3 MΩ) was obtained from a Millipore Milli-Q synthesis system (Billerica, MA).

4.2.2 LC-MS/MS Conditions

4.2.2.1 Deuterated Phospholipids

An Agilent 1290 UHPLC was connected to an Agilent 6460 triple quadrupole mass spectrometer (Santa Clara, CA) with Agilent Jet Stream ESI source controlled by Agilent Mass Hunter Acquisition software (B.06.00). The column used was ACQUITY UPLC HSS T3 (2.1 x 100 mm, 1.8 μm) obtained from Waters (Milford, MA). The mobile phase consisted of two phases: phase (A) 10mM Ammonium Acetate (pH 5.0) / Acetonitrile (60/40, v/v), and phase (B) Isopropanol/Acetonitrile (90/10, v/v). The flow rate was 0.5 mL/min, and the column temperature was 60℃. Injection volume was 1 μL. Separation was performed using a gradient from 40% of B to 55% over 2 min, then to 75% over 8 min, maintained at 75% of B for another 1 min. The total sample run was 11 min.

Mass spectra were acquired in positive-ion mode, and mass transitions were monitored using multiple reaction monitoring (MRM). For the mass transitions of deuterated phospholipids see Table 3.1. Nitrogen gas was used as desolvation gas and collision gas. Desolvation gas temperature and shealth gas tempterature were set at 350 ºC and 400 ºC, respectively.

Desolvation gas flow and shealth gas flow were optimized to 10 L/min and 12 L/min, respectively. Nebulizer was set at 45 psi. Capillary voltage was + 4000 V.

4.2.2.2 Doxorubicin

Same hardware and software setting as deuterated phospholipid quantification were used for Doxorubicin quantification. The separation was carried out on an ACQUITY UPLC HSS T3 (2.1 x 100 mm, 1.8 μm) column with a mobile phase of (A) 5 mM Ammonium Acetate (pH 3.5) and (B) Acetonitrile. The gradient started with 30% of B changed to 50% over 0.5 min, then to 100% of B over 0.3 min, maintained at 100% for another 0.7 min. Total sample run was 1.5 min. Flow rate was 0.5 mL/min, and column temperature was 40℃. Injection volume was 1 μL.

Positive scan mode was applied for doxorubicin. Multiple reaction monitoring (MRM) was used for quantification. Mass transitions of doxorubicin and daunorubicin were summarized in Table 4.1. ESI ion source parameter settings were similar to deuterated phospholipids except desolvation gas temperature here was 200 ºC due to the molecule fragility of doxorubicin.

4.2.3 Deuterated Liposome Formulation Preparation

Deuterated liposomes were prepared by hydration of thin films followed by a freeze-thaw and a high-pressure extrusion process as previously published (Zhu, Mock et al. 2011). In brifef, deuterated phospholipids, phospholipids, cholesterol and DSPE-PEG were mixed in chloroform, dried under vacuum at 65℃ water bath for 10-20 min using a Buchi Rotavapor r-200 (Postlfach, Switzerland) and the thin film was hydrated using 0.9% saline or 250 mM ammonium sulfate at pH 5.5 (for Doxorubicin remote loading) for 20 min to achieve a final lipid concentration of 10 mM. The formulation then underwent seven liquid nitrogen freeze-thaw cycles above the phase

transition temperature of the primary lipid prior to extrusion (n=7) through double-stacked polycarbonate membranes (80 nm) from GE Osmonics (Trevose, PA) using a Lipex extruder from Northern Lipids Inc. (Burnaby, BC, Cannada) at 65℃. Liposome formulations had a mean particle diameter of 100-110 nm (Figure 4.2) as determined using Zetasizer Nano range from Malvern (Malvern, UK). Deuterated liposomes were sterilized by filtration (0.2 μm filter) and stored in glass container under a nitrogen atmosphere at 4℃, protected from light, and used within 48 hr of preparation. Total phospholipid concentration of each formulation was quantified using a colorimetric phosphorus assay (Bartlett 1959).

4.2.4 Remote Loading of Doxorubicin

Remote loading uses combined pH and electrochemical gradients and increases encapsulation efficiency for doxorubicin dramatically (Madden, Harrigan et al. 1990, Lasic, Martin et al. 1991, Gabizon 1992). The procedure followed was described (Arnold, Mager et al. 2005). The deuterated lipid thin film was hydrated using 250 mM ammonium sulfate at pH 5.5 and extruded as in 4.2.3. The unencapsulated ammonium sulfate was removed by dialysis against hypertonic sucrose (500 mOsmol) at 4℃. A 10 mg/mL doxorubicin solution in 10% (w/v) sucrose was prepared, warmed to 65℃, and incubated with the preformed deuterated vesicles for 60 min at 65℃ with intermittent vortex mixing. Unencapsulated doxorubicin was removed by dialysis and the formulation was sterilized by filtration through 0.2 μm filters. Doxorubicin concentrations were determined from absorbance at 490 nm using SpectraMax from Molecular Devices (Sunnyvale, CA). Total phospholipid concentration were measured with phosphorus assay. The final drug/lipid ration was typically 0.22:1.0 (mol:mol).

4.2.5 Cells, Animals and Tumor Model

All animal studies were performed under a protocol approved by the Institutional Animal Care and Use Committee and with Public Health Science Policy on Humane Care and Use of Laboratory Animal (2015 report). Tumor xenografts of human prostate cancer cells (PC-3 ATCC, Manasses, VA) were established subcutaneously in the left flank of athymic NCr (*nu*/*nu*), 6-8 week-old, male mice (Taconic Biosciences Inc., Albany, NY). In brief, PC-3 cells, maintained in F-12K medium (Mediatech Inc., Manassas, VA) supplemented with 10% (v/v) fetal bovine serum (Hyclone Laboratories Inc., Logan, UT), were harvested at sub-confluence using 0.25% (v/v) trypsin (Mediatech Inc.) and collected as a suspension with complete medium. Total cells were counted, pelleted by centrifuging at 250 × g for five minutes, had media removed by aspiration, and were re-suspended in phenol-free, serum-free F-12K media to a final concentration of 1×10^7 cells per mL. Prior to injection, the cell suspension was mixed (1:1, v/v) with ice-cold, Matrigel (BD Biosciences, San Jose, CA). While providing 1-3% isoflurane gas (Henry-Schien, Melville, NY) with oxygen to the mice to induce and maintain anesthesia, a 1.0 mL syringe with 26-gauge needle (BD Biosciences) was used to implant 200 µL of cell mixture ($1x10^6$ prostate cancer cells) subcutaneously into the left flank of each mouse. Implants were allowed to set for 5-10 min before allowing the mice to recover from anesthesia. Vitals and tumor growth were assessed biweekly by recording mouse weight and by obtaining digital caliper measurements of observable length and width dimensions of the subcutaneous tumor to determine volume. Volumes were calculated using a standard formula, derived from the volume of an ellipsoid:

$$\textit{Caliper Tumor Volume} = (\pi/6)\ (\textit{larger diameter})\ (\textit{smaller diameter})^2$$

Humane endpoints generally were defined as tumors that approached or exceeded 1500mm^3 or if total mouse weight (corrected for tumor volume, assuming a density of 1 g/cm^3) declined greater than 20% from peak during treatment regimen.

4.2.6 *In vitro* Evaluation

4.2.6.1 Formulation Selection

Six deuterated liposome formulations were prepared, SSL and five SPRL. The formulations are listed in Table 4.2. The deuterated liposomes were spiked into F-12K medium with 10% (v/v) fetal bovine serum at the final total lipid concentration of 0.5 mM. An aliquot of 2.5 mL medium was added to PC-3 cells seeded 6-well plates with a seeding density of 100,000 per well. Each formulation was triplicated. The 6-well plates were incubated at 37℃ for 24, 48, 72 and 96 hr. At each end point of incubation, cells were collected using 0.25% (v/v) trypsin, and rinsed using PBS solution with a centrifuge force of 800 × g for 5 min 3 times to remove excessive and loose binding formulations. Cells then homogenized using a probe sonic dismembrator (Fisher Scientific, Pittsburgh, PA) in PBS solution.

An aliquot of 150 µL cell homogenized solution was taken for Bligh-Dye extraction. Briefly, 5 µL of deuterated phospholipid internal standard (d62-DPPC and d31-LysoPC) prepared as in **Chapter 3** was added, followed by addition of 200 µL of methanol and 400 µL of chloroform. Extraction was performed twice with addition of another 300 µL chloroform the second time. The chloroform layer was collected and dried under ultrapure nitrogen, and reconstituted using a mixture of methanol and chloroform (50:50, v:v). Samples were then transfered to HPLC injection vial for LC-MS/MS quantification.

Another aliquot of 25 µL cell homogenized solution was taken for BCA total protein quantification using Pierce BCA Protein Assay Kit purchased from Thermo Scientific (Waltham, MA). The total protein of each sample was used for deuterated phospholipids normalization.

4.2.6.2 Evaluation of the Role of PLA2R in SPRL Intracellular Uptake

The selected SPRL formulation along with SSL formulation were prepared using deuterated phospholipid (d70-DSPC). Formulations were incubated with PC-3 cells and PLA2R knock-down PC-3 cells (PC-3 KD) at 37℃ for 48 hr. The incubation, cell collection, total lipid extraction and protein quantification followed the procedures described in 4.2.6.1.

4.2.7 *In vivo* Evaluation

4.2.7.1 Single Dose Experiment

A cohort of 24 mice were implanted with PC-3 cells. Tumors were allowed to grow to approximately 650 mm^3 ± 180 mm^3 before injecting a single treatment in bolus via tail vein. The mice were split equally into treatment groups of SSL and SPRL. Mice received 125 µL injections of deuterated liposome formulation loaded with doxorubicin in 10% sucrose at 10 µmol/mL of lipid concentration and 0.2:1 DXR:Lipid (mole ratio). Following treatment, four mice from each group were euthanized at time points of 24, 48 and 72hr, perfused of blood with heparinized saline, and tumors were harvested and flash frozen to analyze and quantify disposition of deuterated liposomes and Doxorubicin by LC-MS/MS.

4.2.7.2 Multiple Dose Experiment

In one cohort of 10 mice, after tumors had established at 200mm^3 two weeks following implant of PC-3 cells, mice were treated five times over an eight week period with doxorubicin-loaded liposomes. Half the cohort (five mice) were treated with SSL formulation, and the other half (five mice) were administered SPRL formulation via tail vein injection. Injections consisted of 120uL of formulation, at 10 µmol/mL (lipid basis) and 0.2:1 DXR:Lipid ratio, in 10% sucrose. Treatment time points occurred on weeks 2, 3, 6, 7, and 9. For the final treatment, liposomes prepared with deuterated lipids were administered. At 48 hours, mice were euthanized, perfused of blood with heparinized saline, and tumor tissue was excised and flash frozen to analyze by LC-MS/MS for concentrations of deuterated lipid and doxorubicin.

4.2.7.3 Doxorubicin Quantification

Doxorubicin quantification was performed using LC-MS/MS modified from a previously published procedure (Arnold, Slack et al. 2004) to suit our current instrument settings. In brief, tumor tissues were homogenized in ultrapure water at a concentration of 5% (5 g of tissue/100 mL of water). A standard curve was prepared by making a serial dilution of Doxorubicin (1.5 - 1550 ng/mL) and blank homogenized tumor tissue. An aliquot of 100 µL of Daunorubicin (IS, 900 ng/mL) in methanol was added into an aliquot of 200 µL of standard, blank and sample, followed by adding 700 µL of ice cold acetonitrile for deproteinization. 500 µL of supernatant was acquired for LC-MS/MS quantification after centrifuging at 14,000 × g for 20 min.

4.2.8 Statistics

Data are presented as the mean ± standard deviation (SD). Differences were determined following an analysis of variance for each data set using SAS software (SAS Institute, Cary, NC) followed by a One-way ANOVA test. Differences were considered significant if the *p*-value $\leq$ 0.05.

4.3 Results

4.3.1 *In vitro* Evaluation

4.3.1.1 Formulation Selection

The Prototype SPRL formulation was formulated based on the enzymatic releasing results in an earlier study (Zhu, Mock et al. 2011). It contains 10% DSPE of total lipids. In this experiment, we generated 5 different formulations of SPRL (10-50% SPRL) using d70-DSPC. Their intracellular uptake was evaluated on PC-3 cells compared to SSL formulation. Both d70-DSPC and its metabolite were measured using LC-MS/MS. The results showed a time-dependent uptake on all formulations. However, no significant differences compared to SSL were observed except for 50% SPRL at 24 and 48 hrs (Figure 4.3 A). In the case of metabolites, a time-dependent increase was observed as well according to the quantification results of d35-LysoPC by LC-MS/MS. Interestingly, metabolite increases were with the increased percentage of DSPE in the formulations at all time points. 40% SPRL showed a consistent significance (Figure 4.3 B). This may suggest that formulations with a higher DSPE percentage are better substrates to $sPLA_2$. Liposome uptake results were plotted in Figure 4.3 C, converted using: Liposome = Parent lipids + Metabolites. Metabolites are very small fractions compare to the parent lipids, the liposome uptake showed a similar pattern as the parent lipids (Figure 4.3 A). A metabolism plot

was also summarized in Figure 4.3 D, metabolism (metabolism = metabolites/liposomes) decreased after 48 hr for all formulations. This result might indicate that $sPLA_2$ were saturated by liposomal formulations.

Due to the fact that no significant differences between all SPRL formulations and SSL formulation exist, especially at the longer time point, we used the well characterized 10% SPRL formulation for our later experiments later sections.

4.3.1.2 Comparison of SPRL Intracellular Uptake between Wild and PLA2R Knock-down PC-3 Cell lines

PLA2R receptor was knocked down on PC-3 cells in order to study the function of PLA2R in SPRL intracellular uptake. Both SSL and SPRL formulations were incubated with both wild and PLA2R know-down PC-3 cells. This set of data showed a higher uptake of SPRL compare to SSL in both wild and knock-down PC-3 cells (Figure 4.4 A and B). A time dependent increase of SPRL uptake was also observed in PC-3 cells (Figure 4.4 A). PLA2R knock-down resulted in a decrease in the uptake of SPRL (Figure 4.4 C), however, a similar decrease was not observe for SSL (Figure 4.4 D). This decrease suggests PLA2R is involved in the intracellular uptake of SPRL, but may not be in the intracellular uptake of SSL. More degradation was observed in the knock-down cells based on the metabolite (d35-LysoPC).

4.3.2 In vivo Evaluation

4.3.2.1 Single Dose Time Course Disposition

A single dose of doxorubicin encapsulated deuterated SPRL and SSL were injected in PC-3 tumor bearing mice. Tumors were harvested at 24, 48 and 72 hr after injection and

analyzed using LC-MS/MS. The liposome uptake were calculated by combining both d70-DSPC and d35-LysoPC measurements (Figure 4.5 C). The average area under the curve (AUC) of SSL is 559, while AUC of SPRL is 537. The results showed no significant difference between SSL and SPRL. However, SPRL (24 hr) showed a faster peak of concentration in tumor than SSL (48 hr). This might suggest that DSPE content in the formulation accelerated tumor accumulation due to being a substrate to $sPLA_2$ as *in vitro* date suggested. Both metabolite and metabolism plots (Figure 4.5 B and D) contradict *in vitro* data probably because the *in vivo* environment is dynamic where liposomes are cleared during circulation rather than staying at constant concentration in a static *in vitro* environment. The metabolites were a small fractions of total lipids, therefore, the parent lipids disposition pattern (Figure 4.5 A) is similar to liposome.

The accumulation of doxorubicin in tumor were also quantified using LC-MS/MS. The mass spectra of doxorubicin and its internal standard daunorubicn are shown in Figure 4.6. The target compound and internal standard were well separated and no endogenous interference (Figure 4.7). Doxorubicin disposition patterns were matched to its carriers, which indicates that doxorubicin accumulation is directly associated with liposome. Therefore, no significant difference between doxorubicin carried by the two formulations was observed; but doxorubicin carried by SPRL showed a faster accumulation (Figure 4.8 A). Drug/lipid ratios (mol/mol) were also calculated (Figure 4.8 B). The drug/lipid ratio in tumor was about 0.03-0.04/1.0, while the formulation prepared for injection was 0.2/1.0. This may indicate significant leakage in circulation before reaching the tumor.

4.3.2.2 Multiple Dose Accumulation

Tumor mice were treated 5 times with doxorubicin encapsulated SPRL and SSL. At the last treatment, drug was carried by deuterated liposomal formulations. Tumor were collected 48 hr after the last injection and analyzed using LC-MS/MS. Consistent results (Figure 4.9) showed that SSL had higher uptake than SPRL at 48 hr as previous *in vivo* data (Figure 4.5 A). Doxorubicin repetitive dosing accumulation can be indicated by comparing 5 dose doxorubicin to single dose deuterated liposome where the drug/lipid ratio is about 1.6-1.8/1.0 for 5 doses (v.s. 0.03-0.04/1.0 for single does).

4.4 Discussion

It was no surprise that SPRL didn't outperform SSL in terms of AUC and peak concentration in tumors. After all, the two formulations had very little difference (10% DSPE). But a noticeable phenomenon is that SPRL's peak concentration in tumors showed up faster than SSL (24 hr vs 48 hr, Figure 4.5 C). The peak concentration of its carried drug (DXR) was faster as well (Figure 4.8 A). Typical PEGylated liposomes have a maximum accumulation in tumors at around 48 hr (Gabizon, Pappo et al. 1993, Gabizon, Goren et al. 1997). The adding of DSPE to the formulation increased the rate of tumor disposition by making the liposomes more of a substrate to $sPLA_2$. This assumption could be backed up by the *in vitro* metabolites data (Figure 4.3 B), where the yield of metabolites increased along with the increase of the DSPE percentages. The altered accumulation profile suggests that $sPLA_2$ is involved in the intracellular uptake of SPRL, but not significantly for SSL. It is reasonable to predict that liposomal formulations that contain a higher amount of DSPE may result an even faster accumulation in tumor. A multiple dose strategy based on these results may increase chemotherapy efficacy by

the fast acting SPRL formulations, but further investigation is required. The information provided by metabolites are valuable to the development of an enzymatic targeted and triggered liposomal formulation. The newly developed LC-MS/MS method in combination with deuterated phospholipids is superior to other methods because it can not only quantify the parent phospholipids but also their metabolites. The measurements of metabolites can be used to evaluate the effectiveness of enzymatic targeting as well as enzymatic triggered release.

PLA2R knock-down resulted in a decrease of SPRL uptake but had less or no effect on SSL formulations, which suggested the function of PLA2R in the intracellular uptake of SPRL (or SPRL-sPLA$_2$ complex). Although the difference didn't show any significance, the tendency was well observed. PLA2R knock-down reduced the expression of PLA2R, but didn't eliminate it. The remaining PLA2R were still able to function normally. A better choice for a future study might be using a knock-out cell line for a further confirmation of the role that PLA2R played.

Previous studies showed significant increased accumulation of doxorubicin in tumor carried by PEGylated liposomes (Gabizon, Pappo et al. 1993, Gabizon, Catane et al. 1994, Gabizon and Martin 1997, Arnold, Mager et al. 2005). However, no studies were able to report the uptake of the drug carrier in the same tissue. Therefore, the drug/lipid ratio was not able to be determined. Without this vital information, the optimization of liposomes were limited. Our data obtained using LC-MS/MS method showed that the drug/lipid ratio were only 0.03-0.04/1.0 in tumor, significantly lower than the original formulation for injection. Drug metabolism and lipid metabolism could be partially responsible for this reduction, but the leaking of drug during the circulation was undeniable. This might be universal even for the liposomal formulations clinically approved. A further formulation optimization is needed to achieve a better efficacy of therapy and reduced drug accumulation in vital organs such as the heart.

4.5 Conclusion

The *in vitro* formulation comparison and *in vivo* accumulation determination in the level of parent phospholipids, lipid metabolites and encapsulated drug simultaneously performed in this study could not be accomplished using pre-exiting labeling methods. The LC-MS/MS method we developed is able to obtain more detailed information of the performance of liposomal formulations *in vitro* and *in vivo*. That information is critical for understanding the mechanism of liposome intracellular uptake and to further optimize their therapeutic purpose.

4.6 References

Abe, T., K. Sakamoto, H. Kamohara, Y. Hirano, N. Kuwahara and M. Ogawa (1997). "Group II phospholipase A2 is increased in peritoneal and pleural effusions in patients with various types of cancer." Int J Cancer **74**(3): 245-250.

Arnold, R. D., D. E. Mager, J. E. Slack and R. M. Straubinger (2005). "Effect of repetitive administration of Doxorubicin-containing liposomes on plasma pharmacokinetics and drug biodistribution in a rat brain tumor model." Clin Cancer Res **11**(24 Pt 1): 8856-8865.

Arnold, R. D., J. E. Slack and R. M. Straubinger (2004). "Quantification of Doxorubicin and metabolites in rat plasma and small volume tissue samples by liquid chromatography/electrospray tandem mass spectroscopy." J Chromatogr B Analyt Technol Biomed Life Sci **808**(2): 141-152.

Bartlett, G. R. (1959). "Phosphorus assay in column chromatography." J Biol Chem **234**(3): 466-468.

Brglez, V., G. Lambeau and T. Petan (2014). "Secreted phospholipases A2 in cancer: diverse mechanisms of action." Biochimie **107 Pt A**: 114-123.

Burke, J. E. and E. A. Dennis (2009). "Phospholipase A2 biochemistry." Cardiovasc Drugs Ther **23**(1): 49-59.

Burke, J. E. and E. A. Dennis (2009). "Phospholipase A2 structure/function, mechanism, and signaling." J Lipid Res **50 Suppl**: S237-242.

Dong, Q., M. Patel, K. F. Scott, G. G. Graham, P. J. Russell and P. Sved (2006). "Oncogenic action of phospholipase A2 in prostate cancer." Cancer Lett **240**(1): 9-16.

Gabizon, A., R. Catane, B. Uziely, B. Kaufman, T. Safra, R. Cohen, F. Martin, A. Huang and Y. Barenholz (1994). "Prolonged circulation time and enhanced accumulation in malignant exudates of doxorubicin encapsulated in polyethylene-glycol coated liposomes." Cancer Res **54**(4): 987-992.

Gabizon, A., D. Goren, A. T. Horowitz, D. Tzemach, A. Lossos and T. Siegal (1997). "Long-circulating liposomes for drug delivery in cancer therapy: a review of biodistribution studies in tumor-bearing animals." Adv Drug Deliv Rev **24**(2): 337-344.

Gabizon, A. and F. Martin (1997). "Polyethylene glycol-coated (pegylated) liposomal doxorubicin. Rationale for use in solid tumours." Drugs **54 Suppl 4**: 15-21.

Gabizon, A. A. (1992). "Selective Tumor Localization and Improved Therapeutic Index of Anthracyclines Encapsulated in Long-Circulating Liposomes." Cancer Res **52**(4): 891-896.

Gabizon, A. A., O. Pappo, D. Goren, M. Chemla, D. Tzemach and A. T. Horowitz (1993). "Preclinical Studies with Doxorubicin Encapsulated in Polyethyleneglycol-Coated Liposomes." J Liposome Res **3**(3): 517-528.

Hsu, Y. H., J. E. Burke, S. Li, V. L. Woods, Jr. and E. A. Dennis (2009). "Localizing the membrane binding region of Group VIA Ca2+-independent phospholipase A2 using peptide amide hydrogen/deuterium exchange mass spectrometry." J Biol Chem **284**(35): 23652-23661.

Lasic, D. D., F. J. Martin, A. Gabizon, S. K. Huang and D. Papahadjopoulos (1991). "Sterically stabilized liposomes: a hypothesis on the molecular origin of the extended circulation times." Biochim Biophys Acta **1070**(1): 187-192.

Madden, T. D., P. R. Harrigan, L. C. Tai, M. B. Bally, L. D. Mayer, T. E. Redelmeier, H. C. Loughrey, C. P. Tilcock, L. W. Reinish and P. R. Cullis (1990). "The accumulation of drugs

within large unilamellar vesicles exhibiting a proton gradient: a survey." Chem Phys Lipids **53**(1): 37-46.

Nevalainen, T. J., G. G. Graham and K. F. Scott (2008). "Antibacterial actions of secreted phospholipases A2. Review." Biochim Biophys Acta **1781**(1-2): 1-9.

Quach, N. D., R. D. Arnold and B. S. Cummings (2014). "Secretory phospholipase A2 enzymes as pharmacological targets for treatment of disease." Biochem Pharmacol **90**(4): 338-348.

Silliman, C. C., E. E. Moore, G. Zallen, R. Gonzalez, J. L. Johnson, D. J. Elzi, X. Meng, K. Hanasaki, J. Ishizaki, H. Arita, L. Ao, K. M. England and A. Banerjee (2002). "Presence of the M-type sPLA(2) receptor on neutrophils and its role in elastase release and adhesion." Am J Physiol Cell Physiol **283**(4): C1102-1113.

Woodle, M. C. (1995). "Sterically stabilized liposome therapeutics." Adv Drug Deliv Rev **16**(2): 249-265.

Zhu, G., J. N. Mock, I. Aljuffali, B. S. Cummings and R. D. Arnold (2011). "Secretory phospholipase A(2) responsive liposomes." J Pharm Sci **100**(8): 3146-3159.

Table 4.1 Mass Transitions of Doxorubicin and Daunorubicin

Compound Name	Ion Type	Precursor Ion (m/z)	Product Ion (m/z)	Fragmentor (V)	Collision Energy (V)
Doxorubicin	Quantifier ion	544.2	397.3	103	6
	Qualifier ion	544.2	361.4	103	23
Daunorubicin	Quantifier ion	528.1	321.2	115	23
	Qualifier ion	528.1	363.1	115	9

Table 4.2 Deuterated Liposome Formulations

Name	Formulation	Lipid Mole Ratio
SSL	d70-DSPC:DSPE-PEG:Chol	9:1:5 *
10% SPRL	d70-DSPC:DSPE:DSPE-PEG:Chol	8:1:1:5
20% SPRL	d70-DSPC:DSPE:DSPE-PEG:Chol	7:2:1:5
30% SPRL	d70-DSPC:DSPE:DSPE-PEG:Chol	6:3:1:5
40% SPRL	d70-DSPC:DSPE:DSPE-PEG:Chol	5:4:1:5
50% SPRL	d70-DSPC:DSPE:DSPE-PEG:Chol	4:5:1:5

%: the percentage of DSPE in total lipid content of the formulation

* Similar formulation to clinically applied liposomes Doxil® (FDA approved)

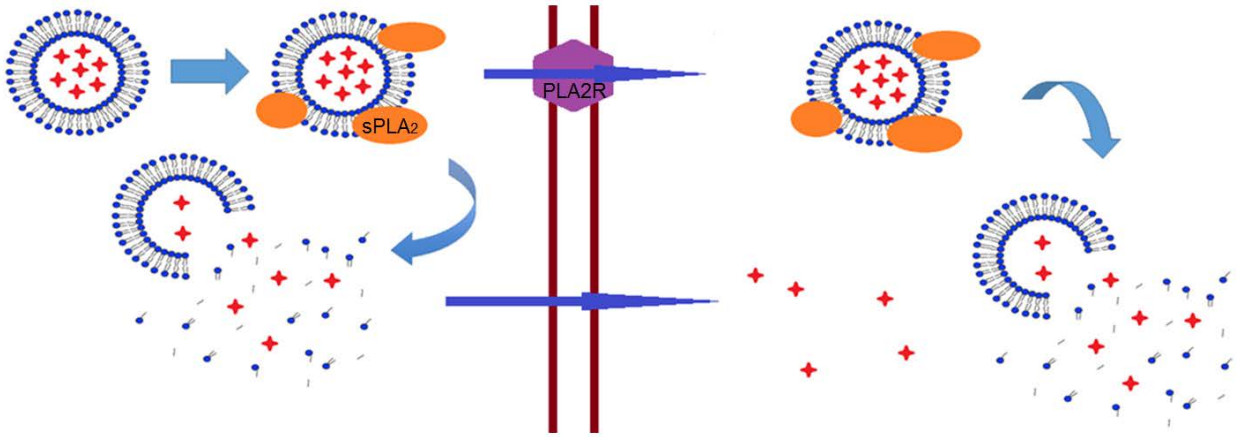

Figure 4.1 Interaction among SPRL, $sPLA_2$ and PLA2R, and the hypothesis of Using This Interaction as a Target for Drug Delivery Development.

Results

		Size (d.nm):	% Intensity:	St Dev (d.n...
Z-Average (d.nm): 103.2	Peak 1:	104.4	100.0	10.34
PdI: 0.011	Peak 2:	0.000	0.0	0.000
Intercept: 0.973	Peak 3:	0.000	0.0	0.000
Result quality : Good				

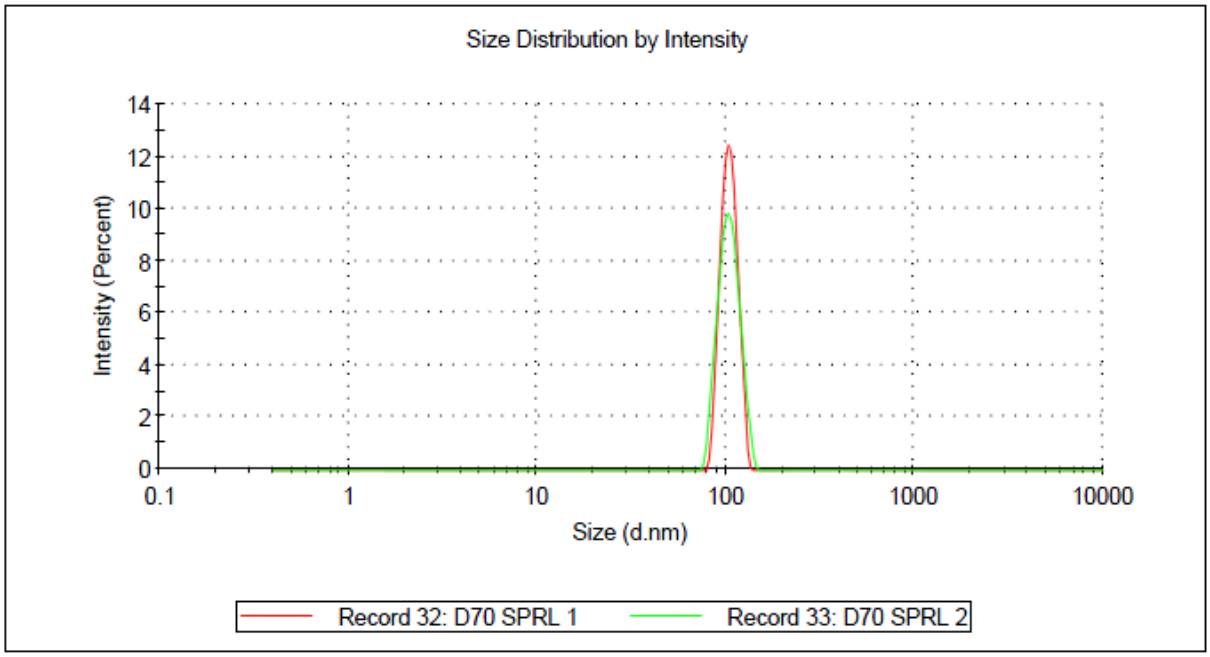

Figure 4.2 Light Scattering Sizing Analysis of d70-SPRL Formulation. The d70-SPRL typically has a mean diameter of 100-110 nm.

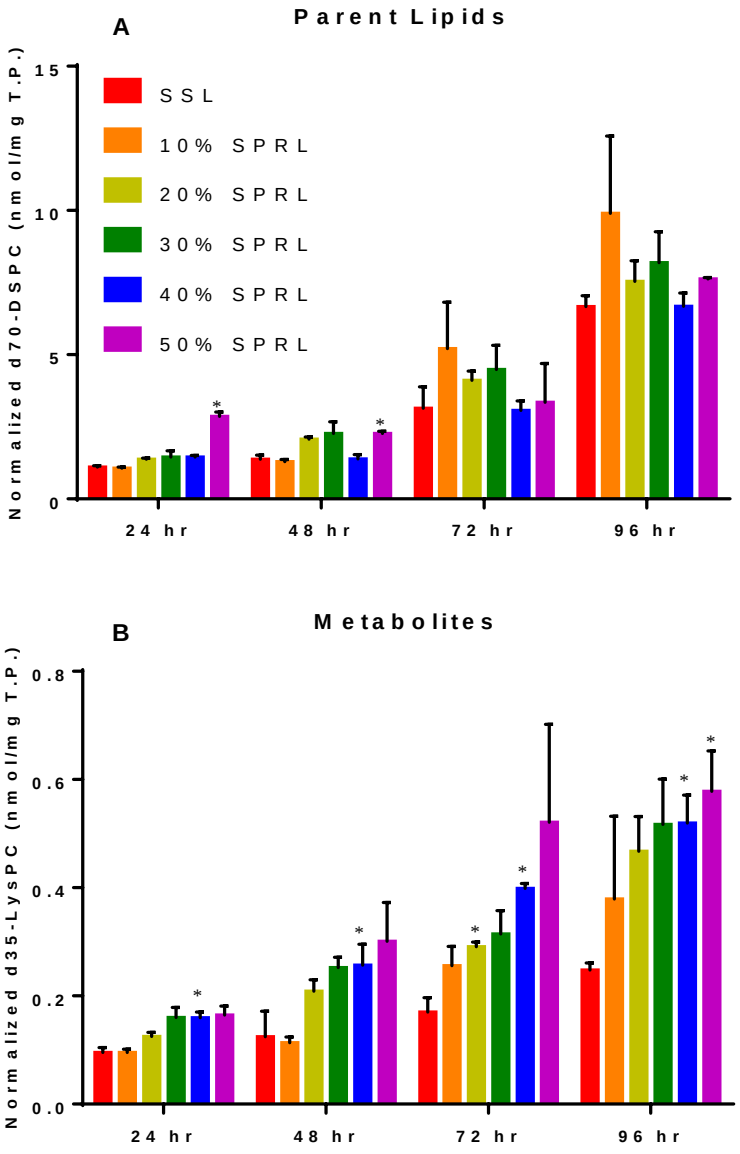
A
Parent Lipids
Normalized d70-DSPC (nmol/mg T.P.)
15
10
5
0
SSL
10% SPRL
20% SPRL
30% SPRL
40% SPRL
50% SPRL
*
*
24 hr
48 hr
72 hr
96 hr
B
Metabolites
Normalized d35-LysPC (nmol/mg T.P.)
0.8
0.6
0.4
0.2
0.0
*
*
*
*
*
24 hr
48 hr
72 hr
96 hr

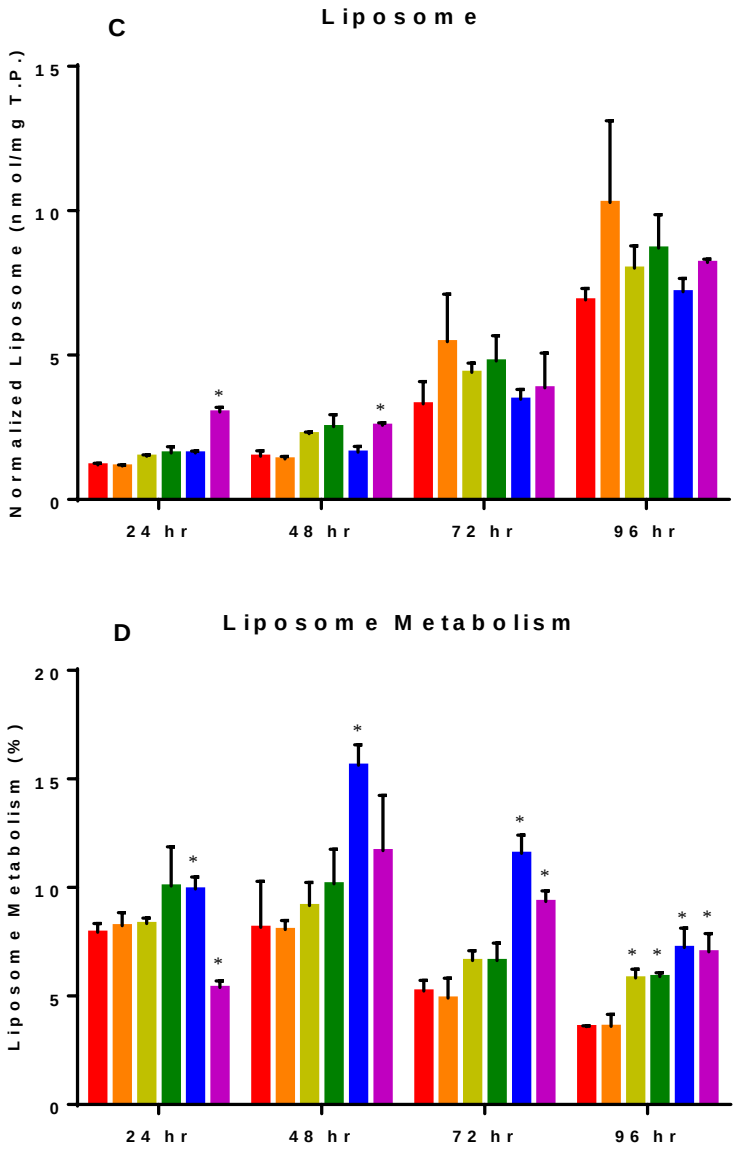

Figure 4.3 Intracellular Uptake of SSL and 5 different SPRL Formulations in PC-3 Cells. (A) Uptake of SSL and SPRLs indicated using sole parent lipids by quantifying d70-DSPC; (B) The yield of metabolites indicated by quantifying d35-LysoPC; (C) Uptake of SSL and SPRLs indicated using the combination of d70-DSPC and d35-LysoPC; (D) Metabolism plotted by calculating the fraction of metabolites in the total lipids. Mean ± SD, n=3. * $P < 0.05$.

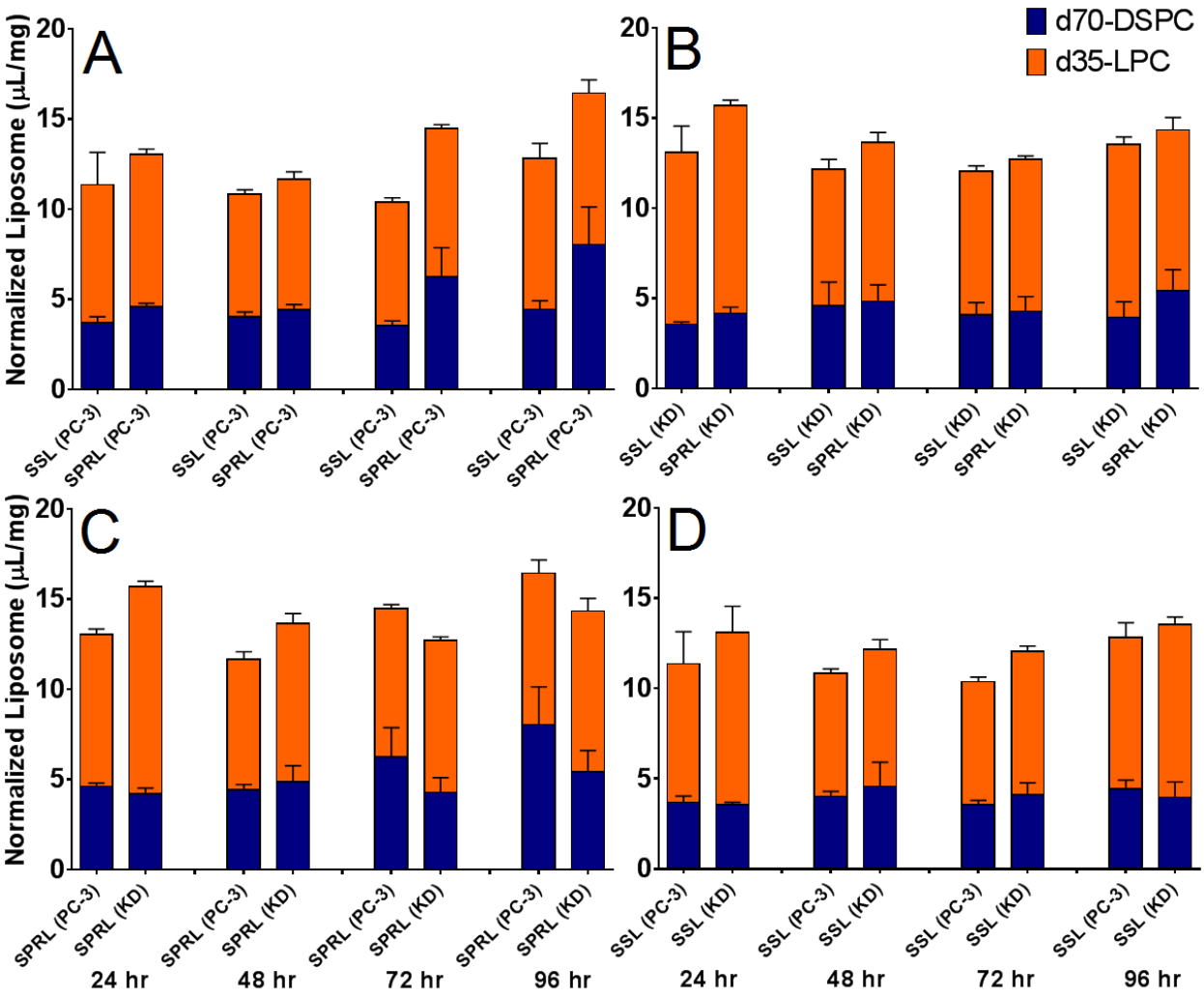

Figure 4.4 Comparison of SPRL and SSL Uptake in Wild and PLA2R knock-down PC-3 cells over 96 hr based on LC-MS/MS quantification of d70-DSPC and its metabolite d35-LysoPC. (A) Comparison of SPRL and SSL uptake in wild PC-3 cells; (B) Comparison of SPRL and SSL uptake in PLA2R knock-down PC-3 cells. (C) Comparison of SPRL uptake in both wild and PLA2R knock-down PC-3 cells; (D) Comparison of SSL uptake in both wild and PLA2R knock-down PC-3 cells. Mean ± SD, n=3.

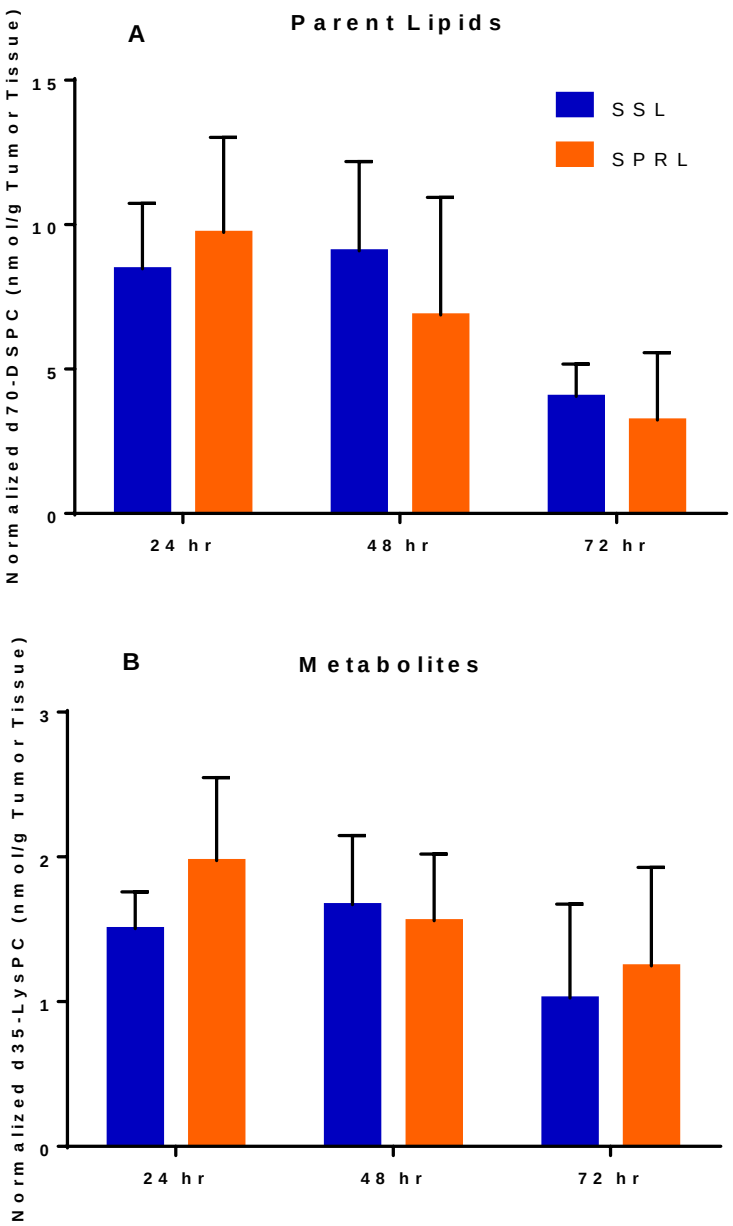
A
Parent Lipids
Normalized d70-DSPC (nmol/g Tumor Tissue)
15
10
5
0
SSL
SPRL
24 hr
48 hr
72 hr
B
Metabolites
Normalized d35-LysPC (nmol/g Tumor Tissue)
3
2
1
0
24 hr
48 hr
72 hr

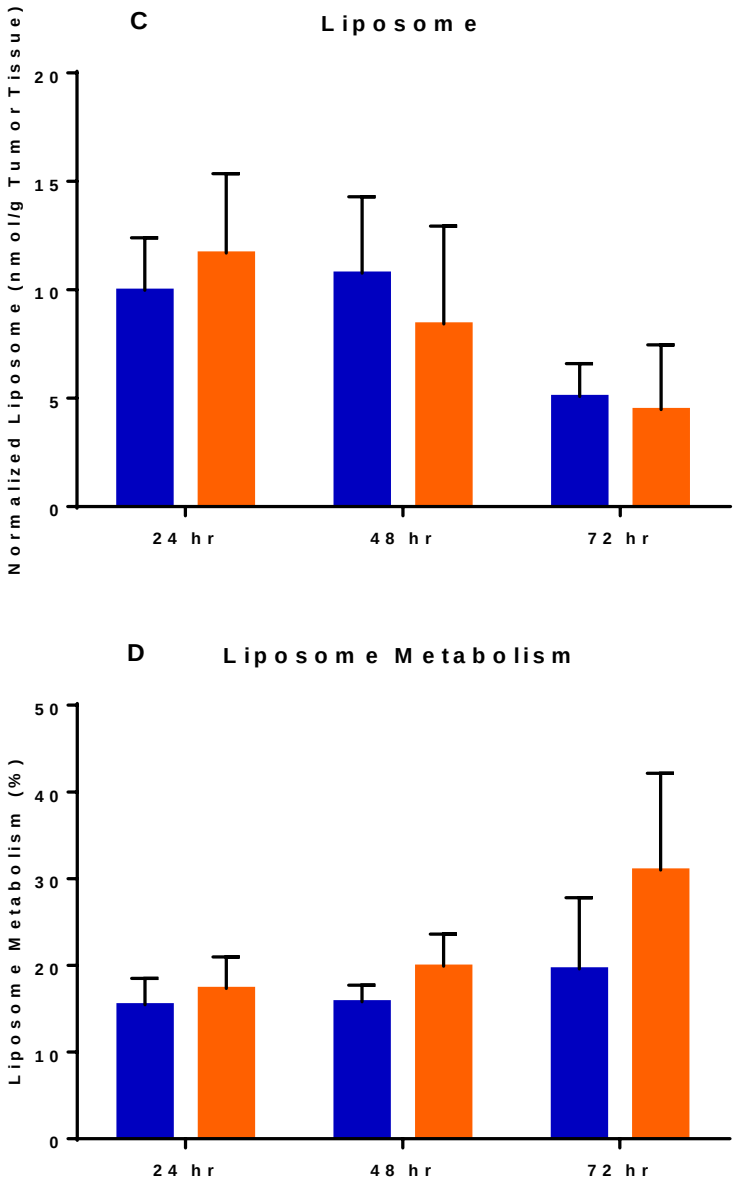

Figure 4.5 *In vivo* Disposition of SSL and SPRL in Xenograft Mouse Tumor Model of PC-3 Cells. (A) Uptake of SSL and SPRL indicated using sole parent lipids by quantifying d70-DSPC; (B) The yield of metabolites indicated by quantifying d35-LysoPC; (C) Uptake of SSL and SPRL indicated using the combination of d70-DSPC and d35-LysoPC; (D) Metabolism plotted by calculating the fraction of metabolites in the total lipids. Mean ± SD, n=4.

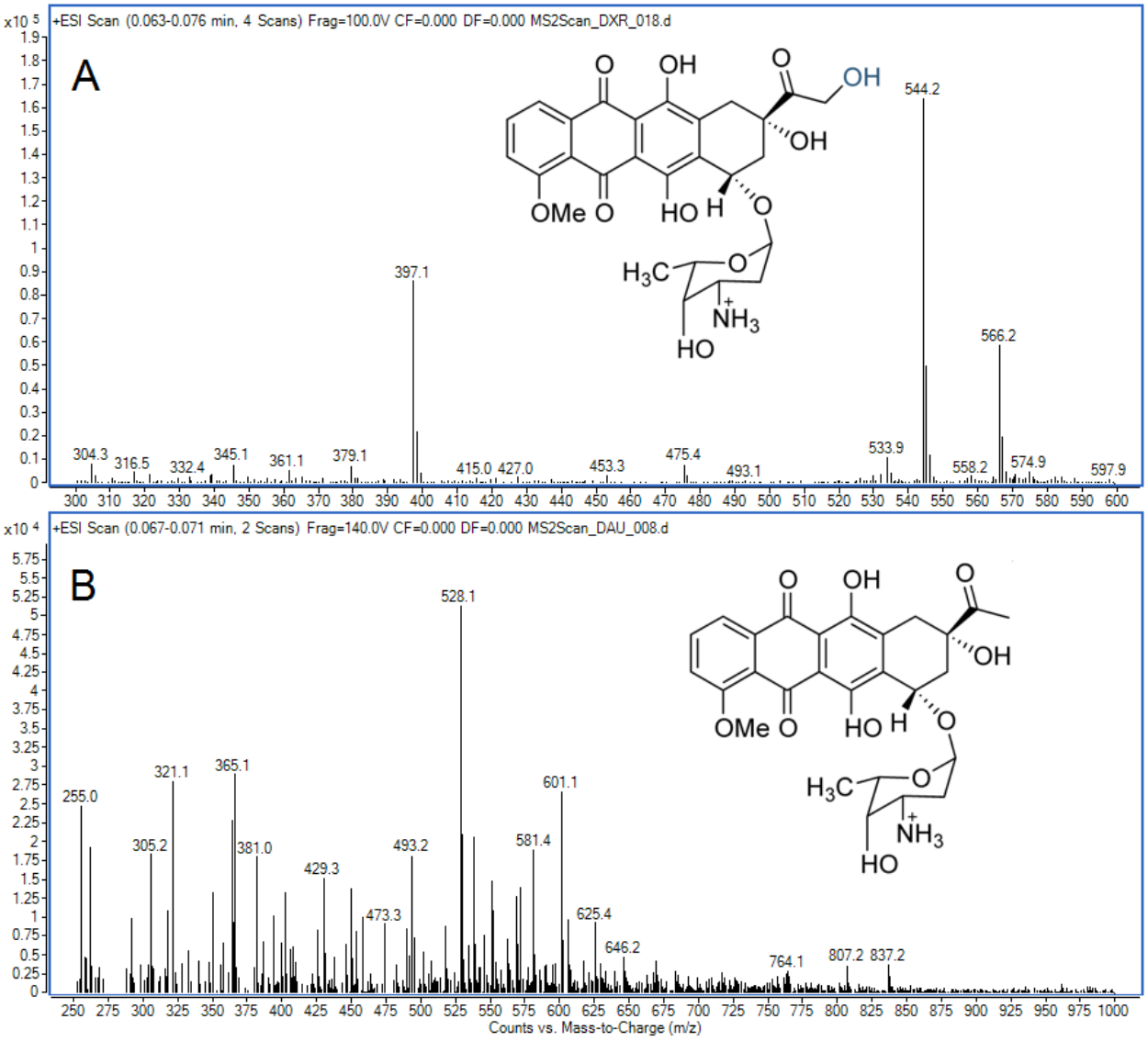

Figure 4.6 Mass Spectra of Doxorubicin and Daunorubicin. (A) Doxorubicin mass spectra, molecular ion $[M+1]^+$ 544.2, a product ion 397.1 showed up in MS2 full scan indicated the fragileness of doxorubicin molecule. Sodium adduct occurred, $[M+22]^+$ 566.2; (B) Daunorubicin mass spectra, molecular ion $[M+1]^+$ 528.1.

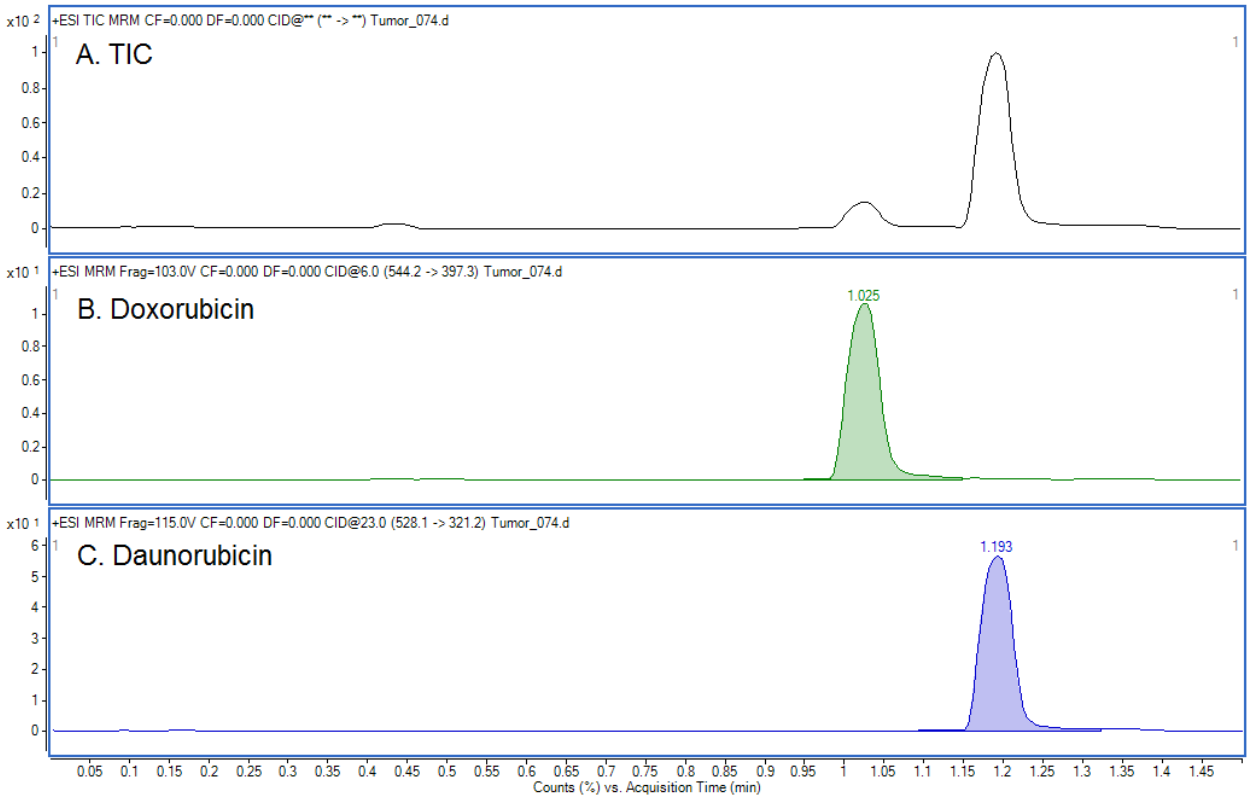

Figure 4.7 LC-MS/MS Chromatography of Doxorubicin and Daunorubicin in Tumor Tissue. (A) Total ion chromatography; (B) MRM chromatography of doxorubicin; (C) MRM chromatography of daunorubicin.

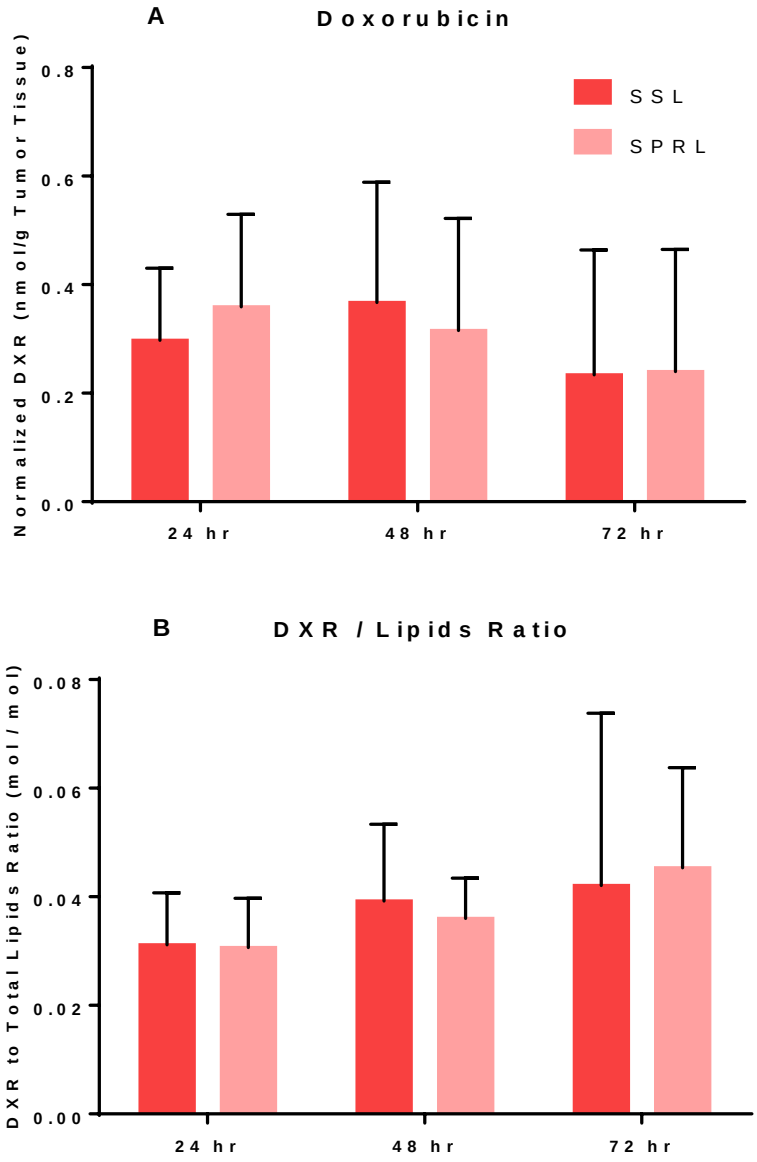

Figure 4.8 Doxorubicin Accumulation of Single Dose Treatment. (A) Doxorubicin accumulation in tumor carried by SPRL and SSL; (B) Drug/lipids ratio in tumor. Mean ± SD, n=4.

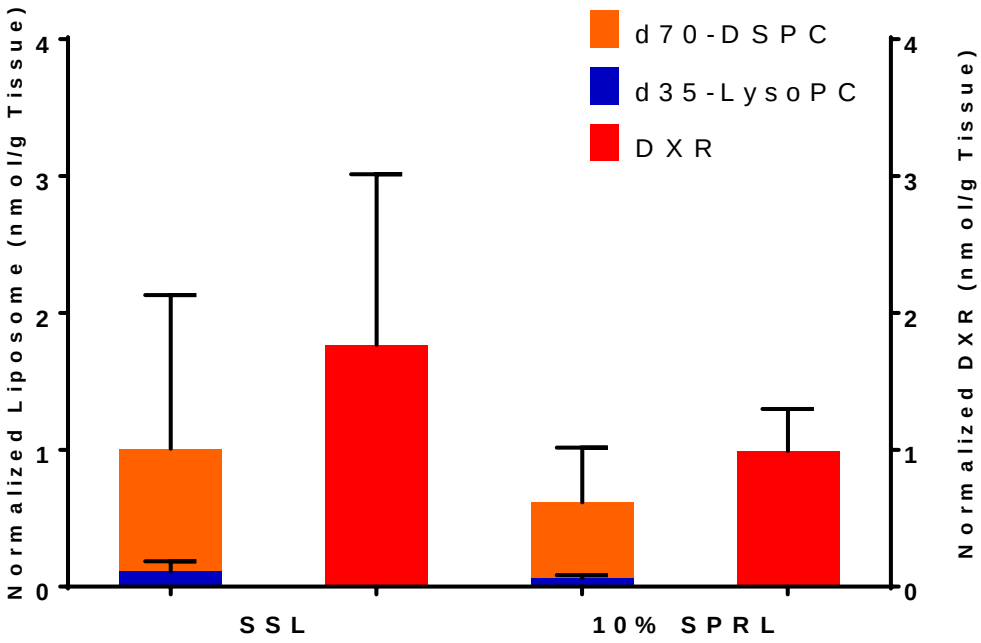

Figure 4.9 Doxorubicin Accumulation of Multiple Dose Treatment. A repetitive accumulation of doxorubicin was indicated by comparing to a single dose of deuterated liposome. Mean ± SD, n=5.

Appendix: Journal Publications

Two papers directly related to my PhD dissertation work are in preparation for publication. The manuscripts will be submitted shortly. In addition to my PhD work, I have also participated in multiple collaborative projects. In these projects, I developed LC-MS/MS methods for *in vivo* drug quantification, performed data analysis (non-compartmental analysis, compartmental modeling and dosing regimen simulation) and contributed to paper writing. The experiences I gained from these projects improved my skills for bioanalytical method development and pharmacokinetic data analysis as well as helped me gain insights for my own research work.

All my publications during my PhD study in Auburn University are listed.

Publication in Preparation

1. **Nie, B.**, Zhu, G., Cummings, B.S. and Arnold, R.D., Acidification procedure improved extraction and analysis of phospholipids using ESI-MS, (in preparation for Journal of Pharmaceutical Sciences).

2. **Nie, B.**, Cummings, B.S. and Arnold, R.D., Assessment of Drug Delivery Function of sPLA2 and Its Receptor PLA2R, and Quantification of Disposition, Intracellular Uptake and Degradation of Lipid-Based Nano-Medicines by LC-MS/MS, (in preparation for Journal of Lipid research).

Publication

1. Brown, J.C., Brainard, B.M., Fletcher, D.J., **Nie, B.**, Arnold, R.D. and Schmidt, C.W., Effect of Aminocaproic acid on clot strength and clot lysis of canine blood determined by use of an in vitro model of hyperfibrinolysis, American Journal of Veterinary Research (2016),77(11): 1258-1265 (impact factor 1.35)

Abstract:

Objective: To determine pharmacodynamic and pharmacokinetic profiles of aminocaproic acid (ACA) by use of a thromboelastography (TEG)-based in vitro model of hyperfibrinolysis and high-performance liquid chromatography–mass spectrometry.

ANIMALS 5 healthy adult dogs.

Procedures: A single dose of injectable ACA (20, 50, or 100 mg/kg) or an ACA tablet (approximately 100 mg/kg) was administered orally. Blood samples were collected at 0, 15, 30, 45, 60, 90, 120, and 240 minutes after ACA administration for pharmacokinetic analysis. Samples were obtained at 0, 60, and 240 minutes for pharmacodynamic analysis by use of a TEG model of hyperfibrinolysis.

Results: No adverse effects were detected. In the hyperfibrinolysis model, after all doses, a significantly higher TEG maximum amplitude (clot strength), compared with baseline, was detected at 60 and 240 minutes. Additionally, the percentage of fibrinolysis was reduced from the baseline value at 60 and 240 minutes, with the greatest reduction at 60 minutes. At 240 minutes, there was significantly less fibrinolysis for the 100 mg/kg dose than the 20 mg/kg dose. Maximum plasma ACA concentration was dose dependent. There was no significant difference in pharmacokinetic parameters between 100 mg/kg formulations.

Conclusion and Clinical Relevance: In an in vitro model of hyperfibrinolysis, ACA inhibited fibrinolysis at all doses tested. At 240 minutes after administration, the 100 mg/kg dose inhibited fibrinolysis more effectively than did the 20 mg/kg dose. Thus, ACA may be useful for in vivo prevention of fibrinolysis in dogs.

Impact for Human Medicine: These data may improve research models of hyperfibrinolytic diseases.

Contribution:

Pharmacokinetic analysis: Non-compartmental analysis, one-compartmental modeling, dosing regimen simulation.

2. Kaye, S., Johnson, S., Arnold, R.D., **Nie, B.**, Davis, J.T., Gulland, F., Abou-Madi, N. and Fletcher, D.J., Pharmacokinetic study of oral ε-Aminocaproic acid in the northern elephant seal (Mirounga Angustirostris), Journal of Zoo and Wildlife Medicine (2016), 47(2): 438-446 (impact factor: 0.421)

Abstract:

ε-Aminocaproic acid (EACA) is a lysine analogue antifibrinolytic drug used to treat bleeding disorders in humans and domestic animals. Its use in zoological medicine is rare, and dosage is anecdotal. One possible application of EACA is to treat bleeding associated with prepatent Otostrongylus arteritis in Northern elephant seals (Mirounga angustirostris) presenting to wildlife rehabilitation centers. This study used an in vitro model of hyperfibrinolysis and a thromboelastograph-based assay to estimate the therapeutic plasma

concentration of EACA in elephant seals (85 μg/ml, 95% confidence interval = 73.8–96.8 μg/ml). A concurrent pharmacokinetic study of orally administered, single-dose EACA found that doses of 75 and 100 mg/kg achieved therapeutic plasma concentrations (>85 μg/ml), but the drug was rapidly eliminated and remained in the therapeutic range for only 0.4 and 1.5 hr, respectively. Models of repeated oral dosing at 100 mg/kg every 6 hr predict that therapeutic plasma concentration will be maintained for 31.7% (7.6 hr) of a 24-hr period. More frequent dosing would be required to maintain continuous therapeutic concentrations but would be impractical in a wildlife rehabilitation setting. Further pharmacodynamic studies to evaluate the duration of action of EACA in elephant seals and a prospective, placebo-controlled study are needed to determine if EACA is effective in decreasing bleeding associated with prepatent Otostrongylus arteritis and other bleeding disorders in this species.

Contribution:

Pharmacokinetic analysis: Non-compartmental analysis, Two-compartmental modeling, dosing regimen simulation.

3. Dixon-Jimenez, A.C., Brainard, B.M., Brooks, M.B., Abrams J.C. **Nie, B.**, Arnold, R.D. and Rapoport, G.S., Pharmacokinetic and pharmacodynamic evaluation of oral rivaroxaban in healthy adult cats, Journal of Veterinary Emergency and Critical Care (2016), 26(5): 619-629 (impact factor: 1.052)

Abstract:

Objectives: To determine the pharmacodynamics and pharmacokinetics of rivaroxaban (RVX), in healthy cats and to evaluate the clinicopathologic effects of various plasma RVX

concentrations within target therapeutic ranges established for people.

Design: Prospective randomized cross-over study performed between July 2013 and November 2014.

Setting: Veterinary university teaching hospital.

Animals: Six healthy adult domestic shorthair cats (3 males, 3 females).

Interventions: Cats were treated with oral RVX at single, fixed doses (1.25, 2.5, 5 mg PO), q 12 h for 3 days (1.25 mg); q 24 h for 7 days (2.5 mg); and q 24 h for 28 days (1.25 mg). Blood samples were collected for complete blood count, blood chemistry, and RVX anticoagulant activity based on prolongation of dilute prothrombin time, activated partial thromboplastin time (aPTT), activated Factor X (FXa) inhibition (anti-Xa activity [aXa]) and high-pressure liquid chromatography tandem mass spectrometry determination of drug concentration.

Measurements and Main Results: Treated cats had no signs of hemorrhage or clinicopathologic off-target adverse effects. There were dose-dependent prolongations of coagulation times and increase in aXa, with peak effect at 3 hours postadministration. There was a direct correlation between plasma RVX concentration and dilute prothrombin time and aXa. Coagulation parameters returned to baseline by 24 hours after the last dose.

Conclusions: Oral RVX was well tolerated by healthy cats with predictable pharmacokinetics and anticoagulant effects. Clinical studies of RVX are warranted in cats with heart disease.

Contribution:

Established LC-MS/MS method for quantification of rivaroxaban in cat blood plasma; Pharmacokinetic analysis: Non-compartmental analysis.

4. Epstein, K.L., Bergren, A., **Nie, B.**, Arnold, R.D. and Brainard, B., Comparison of the pharmacokinetics of two formulations of hydroxyethyl starch in healthy horses, Journal of Vet Pharmacology and Therapeutics (2016), DOI: 10.1111/jvp.12359 (impact factor 1.323)

Abstract:

A lower molecular weight and molar substitution formulation (130/0.4) of hydroxyethyl starch solution has been shown to have a more sustained effect on COP and similar hemodynamic effects as a higher molecular weight and molar substitution formulation (600/0.75) in healthy horses. In humans, these pharmacodynamic characteristics are coupled with more rapid clearance and decreased adverse coagulation effects and accumulation. The objective of this study was to determine and compare the pharmacokinetics of these two formulations in horses. Eight healthy horses were given a 10 mL/kg bolus of each formulation (600/0.75 and 130/0.4) of hydroxyethyl starch solution in a randomized crossover design. Blood was collected, and plasma was harvested for plasma levels over 24 h. Pharmacokinetic parameters for each horse were estimated from a noncompartmental analysis. Treatment with 600/0.75 resulted in a higher initial plasma concentration (C_0), systemic half-life ($t_{1/2}$), and overall drug exposure ($AUC_{0–inf}$) in addition to decreased elimination rate (β), volume of distribution (Vd), and clearance (CL), compared to treatment with 130/0.4 ($P < 0.001$). The pharmacokinetic findings combined with previous pharmacodynamics findings suggest that 130/0.4 can provide similar benefits to 600/0.75 with a lower risk of accumulation in the circulation.

Contribution:

Developed hydrolysis method for hydroxyethyl starch digestion and quantification; Pharmacokinetic analysis: Non-compartmental analysis.

5. Pati, S., **Nie, B.**, Arnold, R.D. and Cummings, B.S., Extraction, chromatographic and mass spectrometric methods for lipid analysis (Invited Review), Biochemical Chromatography (2016), 30(5): 695-709 (impact factor 1.723)

Abstract:

Lipids make up a diverse subset of biomolecules that are responsible for mediating a variety of structural and functional properties as well as modulating cellular functions such as trafficking, regulation of membrane proteins and subcellular compartmentalization. In particular, phospholipids are the main constituents of biological membranes and play major roles in cellular processes like transmembrane signaling and structural dynamics. The chemical and structural variety of lipids makes analysis using a single experimental approach quite challenging. Research in the field relies on the use of multiple techniques to detect and quantify components of cellular lipidomes as well as determine structural features and cellular organization. Understanding these features can allow researchers to elucidate the biochemical mechanisms by which lipid–lipid and/or lipid–protein interactions take place within the conditions of study. Herein, we provide an overview of essential methods for the examination of lipids, including extraction methods, chromatographic techniques and approaches for mass spectrometric analysis.

Contribution:

Review writing of lipid extraction methods.

6. Kephart, W.C., Wachs, T.D., Thompson, R.M., Mobley, C.B., Fox, C.D., McDonald, J.R., Ferguson, B.S., Young, K.C., **Nie, B.**, Martin, J.S., Company, J.M., Pascoe, D.D., Arnold, R.D., Moon, J.R. and Roberts, M.D., Ten weeks of branched chain amino acid supplementation improves select performance and immunological variables in trained cyclists, Amino Acids (2016), 48(3): 779-789 (impact factor 3.293)

Abstract:

We examined if supplementing trained cyclists (32 ± 2 year, 77.8 ± 2.6 kg, and 7.4 ± 1.2 year training) with 12 g/day (6 g/day l-Leucine, 2 g/day l-Isoleucine and 4 g/day l-Valine) of either branched-chain amino acids (BCAAs, $n = 9$) or a maltodextrin placebo (PLA, $n = 9$) over a 10-week training season affected select body composition, performance, and/or immune variables. Before and after the 10-week study, the following was assessed: (1) 4-h fasting blood draws; (2) dual X-ray absorptiometry body composition; (3) Wingate peak power tests; and (4) 4 km time-trials. No group × time interactions existed for total lean mass ($P = 0.27$) or dual-leg lean mass ($P = 0.96$). A significant interaction existed for body mass-normalized relative peak power (19 % increase in the BCAA group pre- to post-study, $P = 0.01$), and relative mean power (4 % increase in the BCAA group pre- to post-study, $P = 0.01$). 4 km time-trial time to completion approached a significant interaction ($P = 0.08$), as the BCAA group improved in this measure by 11 % pre- to post-study, though this was not significant ($P = 0.15$). There was a tendency for the BCAA group to present a greater post-study serum

BCAA: l-Tryptophan ratio compared to the PLA group (P = 0.08). A significant interaction for neutrophil number existed (P = 0.04), as there was a significant 18 % increase within the PLA group from the pre- to post-study time point (P = 0.01). Chronic BCAA supplementation improves sprint performance variables in endurance cyclists. Additionally, given that BCAA supplementation blunted the neutrophil response to intense cycling training, BCAAs may benefit immune function during a prolonged cycling season.

Contribution:

Established LC-MS/MS method for simultaneous quantification for Leucine, Isoleucine, Valine and Tryptophan in human plasma.

7. Mouli, S., Nanaykkara, G., Fu, R., AlAsmari, A., Haitham, E., Berlin, A., Lohani, M., **Nie, B.**, Navazis, N.A., Smith, F., Arnold, R.D., Beyers, R., Denney, T., Dhanasekaran, M., Quindry, J., Zhong, J. and Amin, R., B.S., The role of frataxin in doxorubicin mediated cardiac hypertrophy, American Journal Physiological, Heart and Circulatory Physiology (2015), 309(5): H844-H859 (impact factor: 3.838)

Abstract:

Doxorubicin (DOX) is a highly effective anti-neoplastic agent; however, its cumulative dosing schedules are clinically limited by the development of cardiotoxicity. Previous studies have attributed the cause of DOX-mediated cardiotoxicity to mitochondrial iron accumulation and the ensuing reactive oxygen species (ROS) formation. The present study investigates the role of frataxin (FXN), a mitochondrial iron-sulfur biogenesis protein, and its role in

development of DOX-mediated mitochondrial dysfunction. Athymic mice treated with DOX (5 mg/kg, 1 dose/wk with treatments, followed by 2-wk recovery) displayed left ventricular hypertrophy, as observed by impaired cardiac hemodynamic performance parameters. Furthermore, we also observed significant reduction in FXN expression in DOX-treated animals and H9C2 cardiomyoblast cell lines, resulting in increased mitochondrial iron accumulation and the ensuing ROS formation. This observation was paralleled in DOX-treated H9C2 cells by a significant reduction in the mitochondrial bioenergetics, as observed by the reduction of myocardial energy regulation. Surprisingly, similar results were observed in our FXN knockdown stable cell lines constructed by lentiviral technology using short hairpin RNA. To better understand the cardioprotective role of FXN against DOX, we constructed FXN overexpressing cardiomyoblasts, which displayed cardioprotection against mitochondrial iron accumulation, ROS formation, and reduction of mitochondrial bioenergetics. Lastly, our FXN overexpressing cardiomyoblasts were protected from DOX-mediated cardiac hypertrophy. Together, our findings reveal novel insights into the development of DOX-mediated cardiomyopathy.

Contribution:

Doxorubicin quantification using LC-MS/MS.

8. Boozer, L.B., Platt, S.R., Haley, A.C., Linville, A., Kent, M., Barron, L., and **Nie, B.** and Arnold, R.D., Pharmacokinetic evaluation of immediate- and extended-release formulations of Levetiracetam in dogs, American Journal of Veterinary Research (2015), 76(8): 719-723 (impact factor: 1.35)

Abstract:

Objective: To compare the pharmacokinetics of various formulations of levetiracetam after oral administration of a single dose to healthy dogs.

Animal: 6 neurologically normal mixed-breed dogs.

Procedures: A crossover study design was used. Blood samples for serum harvest were collected from each dog before and at various points after oral administration of one 500-mg tablet of each of 2 generic extended-release (ER) formulations, 1 brand-name ER formulation, or 1 brand-name immediate-release (IR) formulation of levetiracetam. Serum samples were analyzed to determine pharmacokinetic properties of each formulation by means of ultra–high-performance liquid chromatography with tandem mass spectrometry.

Results: No dogs had clinically important adverse effects for any formulation of levetiracetam. All ER formulations had a significantly lower maximum serum drug concentration and longer time to achieve that concentration than did the IR formulation. Half-lives and elimination rate constants did not differ significantly among formulations. Values for area under the drug concentration-versus-time curve did not differ significantly between ER formulations and the IR formulation; however, 1 generic ER formulation had a significantly lower area under the curve than did other ER formulations.

Conclusion and Clinical Relevance: All ER formulations of levetiracetam had similar pharmacokinetic properties in healthy dogs, with some exceptions. Studies will be needed to evaluate the clinical efficacy of the various formulations; however, findings suggested that twice-daily administration of ER formulations may be efficacious in the treatment of seizures in dogs.

Contribution:

Established LC-MS/MS method for quantification of Levetiracetam in dog serum; Pharmacokinetic analysis: Non-compartmental analysis.

9. Kang, JY., Eggert, M., Mouli, S., Aljuffali, I., Fu, X., **Nie, B.**, Sheil, A.,Waddey, K., Oldham, C.D., May, S.W., Amin, R. and Arnold, R.D., Pharmacokinetics, antitumor and cardioprotective effects of liposome-encapsulated phenylaminoethyl selenide in human prostate cancer rodent models, Pharmaceutical Research (2015), 32(3): 852-862 (impact factor: 3.952)

Abstract:

Purpose: Cardiotoxicity associated with the use of doxorubicin (DOX), and other chemotherapeutics, limits their clinical potential. This study determined the pharmacokinetics and antitumor and cardioprotective activity of free and liposome encapsulated phenyl-2-aminoethyl-selenide (PAESe).

Methods: The pharmacokinetics of free PAESe and PAESe encapsulated in liposomes (SSL-PAESe) were determined in rats using liquid chromatography tandem mass-spectrometry. The antitumor and cardioprotective effects were determined in a mouse xenograft model of human prostate (PC-3) cancer and cardiomyocytes (H9C2).

Results: The encapsulation of PAESe in liposomes increased the circulation half-life and area under the drug concentration time profile, and decreased total systemic clearance significantly compared to free PAESe. Free- and SSL-PAESe improved survival, decreased weight-loss and prevented cardiac hypertrophy significantly in tumor bearing and healthy mice following

treatment with DOX at 5 and 12.5 mg/kg. *In vitro* studies revealed PAESe treatment altered formation of reactive oxygen species (ROS), cardiac hypertrophy and gene expression, *i.e.*, atrial natriuretic peptide and myosin heavy chain complex beta, in H9C2 cells.

Conclusions: Treatment with free and SSL-PAESe exhibited antitumor activity in a prostate xenograft model and mitigated DOX-mediated cardiotoxicity.

Contribution:

Histological data processing;

Pharmacokinetic data processing.